Simulation and Validation of a Single Tank Heat Pump Assisted Solar Domestic Water Heating System

by

William Robert Wagar

A thesis

presented to the University of Waterloo

in fulfillment of the

thesis requirement for the degree of

Master of Applied Science

in

Mechanical Engineering

Waterloo, Ontario, Canada, 2013

Author's Declaration

I hereby declare that I am the sole author of this thesis. This is a true copy of the thesis, including any required final revisions, as accepted by my examiners. I understand that my thesis may be made electronically available to the public.

Abstract

This thesis is a study of an indirect heat pump assisted solar domestic hot water (I-HPASDHW) system, where the investigated configuration is called the Dual Side I-HPASDHW system. The study outlines the development of an Experimental Test Unit (ETU), and focuses on the experimental validation of TRNSYS models. Shortcomings of the system design realized throughout the validation process, as well as weaknesses in the control schemes used to operate the system are also provided.

A description of the Dual Side I-HPASDHW system is provided along with the design intent of the system. The corresponding ETU is presented in detail to provide a comprehensive understanding of the ETU's simulation capabilities. Components of the ETU, such as the heat pump, heat exchanger, and domestic hot water (DHW) tank are characterized in order to provide input data for built-in TRNSYS models, and to develop custom TRNSYS models for the heat pump and heat exchanger. Heat exchanger performance is modelled with a linear correlation, while the heat pump performance is mapped by applying experimental data to three-dimensional surface fitting software.

For the purpose of validation, the ETU is used to simulate the performance of the Dual Side I-HPASDHW system under a realistic control scheme. Four full day tests are conducted using data from a fall, winter, and summer day. The full day summer test is repeated with and without electrical backup heating. The TRNSYS model of the Dual Side system is tuned in order to provide the closest match possible between the computer simulation and the measured performance of the ETU.

Experimental tests were compared with TRNSYS simulations to reveal some disparity in the results. The majority of simulation error was attributed to inaccuracy in modeling DHW tank temperatures and water circulation patterns. The disparity created by the DHW tank model only resulted in substantial performance deviation when inaccurate DHW temperatures were used directly for vital control decisions.

Conclusions were drawn suggesting that the TRNSYS model of the ETU was valid for a majority of operating conditions, often matching experimental tests well within experimental uncertainty. Caution was recommended towards the use of the developed TRNSYS model, where techniques were recommended for tracking and minimizing substantial simulation errors. Several key performance issues affecting the Dual Side I-HPASDHW system were targeted with recommendations for design and control alterations, along with future improvement and optimization studies.

Acknowledgements

My time at the University of Waterloo would not have been possible without support, encouragement, and guidance from a great number of individuals and organizations to whom I am indebted.

To my long-standing girlfriend Katie for your continuing love and support, and for remaining by my side in my pursuit of knowledge.

To family members whose love, support, and values have been vital to my success. Your giving spirit will never be forgotten.

To my supervisor Dr. Michael Collins for providing an environment for continued learning and self-improvement, for helping me round out my engineering background, and for disseminating your wealth of knowledge to all of your students.

Thank you to my readers Dr. Zhongchao Tan and Dr. Fue-Sang Lien. Thank you for taking the time to review my thesis and providing your recommendations.

To Dr. John Wright, Mr. Dave Mather, Carsen, Ivan, Scott, Andrew, Ned, Alex, Ken and Bart. I thank you all for your wonderful companionship and for sharing your knowledge and experiences.

To Neil Griffett, Jim Merli, and Andy Barber for their technical assistance in developing the Experimental Test Unit, as well as Martha Morales for tackling my IT challenges.

Lastly, I would like to acknowledge the financial support of The Natural Sciences and Engineering Research Council of Canada (NSERC), the Government of Ontario, and the University of Waterloo through their graduate scholarships.

Table of Contents

List of Figures

List of Tables

Nomenclature

$a \to k$	coefficients used in high order three dimensional curve fitting for the HP	$W/K^{0,1,2,3,4}$
a	solar collector efficiency constant	$W/m^2K^{0,1,2}$
	pump power correlation constant	dimensionless
A_c	solar collector area	m^2
b	solar collector incident angle modification constant	dimensionless
C	heat capacity rate	W/K
C_p	fluid specific heat	J/kgK
$f\{\dots\}$	high order three dimensional curve fit for energy transfer rates	W
F_R	solar collector heat removal factor	dimensionless
G	incident radiation	W/m^2
I	electrical current	A
$\dot{m}$	mass flow rate	kg/s
M	mass of a DHW tank volume element	kg
N	total number of equal temperature nodes	dimensionless
	number of pump power coefficients	dimensionless
$\dot{Q}$	heat transfer rate	W
R	R-value for thermal resistance rating of insulation	m^2K/W
R^2	coefficient of determination	dimensionless
S	radiation reaching the solar collector's absorber surface	W/m^2
t	time	s, hr
T	temperature	℃
$u, \Delta u$	DHW tank thermal loss coefficient and incremental loss coefficient	W/m^2K
U_L	solar collector thermal loss coefficient	W/m^2K
V	voltage	V
$\dot{V}$	volume flow rate	m^3/s
$\dot{W}$	electrical energy transfer rate	W
x	inlet source temperature supplied to the heat pump	℃
y	inlet load temperature supplied to the heat pump	℃

Greek Symbols

α	plate absorptivity	dimensionless
δ	uncertainty	dimensionless
Δ	difference	dimensionless
ε	effectiveness	dimensionless
γ	variable speed pump control signal	dimensionless
η	efficiency	dimensionless
ρ	density	kg/m^3
τ	glazing transmissivity	dimensionless
$\tau\alpha$	solar collector optical efficiency	dimensionless
θ	angle of incidence for beam radiation	rad

Subscripts and Superscripts

$'$	theoretical value
0	solar collector efficiency intercept
	first order IAM
	pump power correlation constant
1	solar collector efficiency slope
	second order IAM
	first order pump power correlation constant
2	solar collector efficiency curvature
a	ambient
avg	average of source and load inlet temperatures
b	beam
c	heat pump compressor
	cold side of heat exchanger
d	derating
f, i	fluid inlet
h	hot side of heat exchanger
i	numeric indicator for tank model volume elements
	inlet

j	numeric indicator for pipe model volume elements
$L, load$	parameter for the load side of the system
m	mean value
max	maximum value
min	minimum value
n	normal angle of incidence
p	process
	pump
r	rated value
$S, source$	source side of the system
T	total value on a tilted surface
u	solar collector useful energy gain

Abbreviations

AC	alternating current
Bot	bottom of the DHW tank
COP	coefficient of performance
DAQ	data acquisition unit
DC	direct current
DHW	domestic hot water
DLL	dynamic link library
$DTank$	domestic hot water tank
DX	direct expansion
ETU	Experimental Test Unit
FIT	feed-in tariff
GHG	greenhouse gasses
GS	ground source
HP	heat pump, or in reference to heat pump operation
HPA	heat pump assisted
$HVAC$	heating, ventilation and air conditioning
HWB	Hottel, Whillier, Bliss correlation

HX	heat exchanger, or in reference to heat exchanger operation
I	indirect
IAM	incident angle modifier
Mid	middle of the DHW tank
SA	solar assisted
$Scale$	scaling factor for nominal equipment size
$SDHW$	solar domestic hot water
SIM	computer simulation
SLE	special limits of error
$SubVI$	lower level virtual instrument
Top	top of the DHW tank
$T\&P$	temperature and pressure
TTL	transistor–transistor logic
VI	virtual instrument
VSP	variable speed pump

Chapter 1 Introduction

1.1 Motivation

Population growth and human development are putting pressure on energy resources and their exploitation. According to the International Energy Agency (IEA) [1], the world's total final energy consumption in 2008 was $8428\ Mtoe$ with fossil fuels (oil, gas and coal) accounting for 67% of the total. As human activities continue to rely on fossil fuels, the supply and demand of fossil fuels remains a prominent issue in global politics. Though combustible fuels are widely available today, it is clear that production cannot increase indefinitely. While the supply of fossil fuels diminishes, global energy consumption continues to increase. This forms an unsustainable trend which must be curbed both by the use of renewable resources in addition to a vast reduction in energy consumption. In Bentley [2], the author concludes that peak oil production without intervention from the Organization of the Petroleum Exporting Countries (OPEC) has been reached, and the global conventional oil peak will have occurred between the years of 2002 and 2012. Such demands on oil production are evident as reserves such as Alberta's Oil Sands become economically viable. These demands are also evident in deep sea oil drilling operations, where the risks and challenges have recently been brought to light with the 2010 British Petroleum oil spill; called the "worst environmental disaster America has ever faced" [3] .

In addition to implications of fossil fuel resource depletion, the consumption of oil, gas and coal leads to an immense release of greenhouse gasses (GHG) and further to climate change. Atmospheric levels of CO_2, CH_4, and N_2O have increased noticeably with human activity from 1750 to the present [4]. As of 2005, greenhouse gas levels have by far exceeded the natural fluctuations observed over the past 650000 years [4]. Increased concentrations of GHG and aerosols, along with altered use of land, has disrupted the planet's balance of energy with solar radiation and results in climate change [4].

In order to manage the impacts of climate change, a document has been released by Natural Resources Canada (NRCan) describing measures that should be taken by municipalities. The predicted impacts of climate change in Canada [5] include, among others:

- Drought
- Extreme weather
- Reduced surface water quality
- Increased frequency of vector-borne diseases
- Frequent heat waves reducing air quality
- Increased flooding in coastal regions

According to the Intergovernmental Panel on Climate Change (IPCC) [4], without alleviating the causes of climate change, it is doubtful that natural or man-made systems will be able to adjust. At this point in time, renewable energy development has to compete with the low cost of fossil fuels. In order to bolster support, many governments have implemented green energy programs. In particular, Feed-in Tariff (FIT) programs such as that implemented in Ontario have become popular. Though renewables have not yet captured a major portion of the energy market, they have several advantages over fossil fuels. Not only is renewable energy utilization more environmentally benign, but it provides a virtually inexhaustible supply of energy. The principle cost of systems to harvest renewable energy is often high compared to other competing systems. This has made it difficult to convince consumers to invest in such technologies. However, with a free supply of energy, many renewable energy systems provide a financial payback period well within the system lifetime. Renewable resources and energy efficient technologies are necessities for the planet's future energy supply and demand.

1.2 Energy and Buildings

Annually, approximately 40% of the total world energy consumption can be attributed to building energy end use [6].The building stock is highly represented in the Residential and Commercial/Institutional sectors of energy use. In Figure 1.1, the breakdown of Canada's 2007 energy end-use is shown by sector.

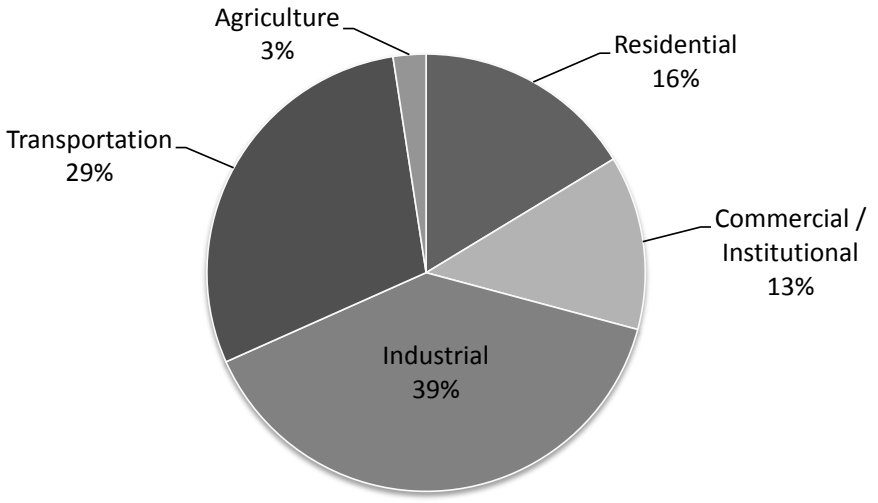

Figure 1.1 2007 Canadian total end-uses by sector [7]

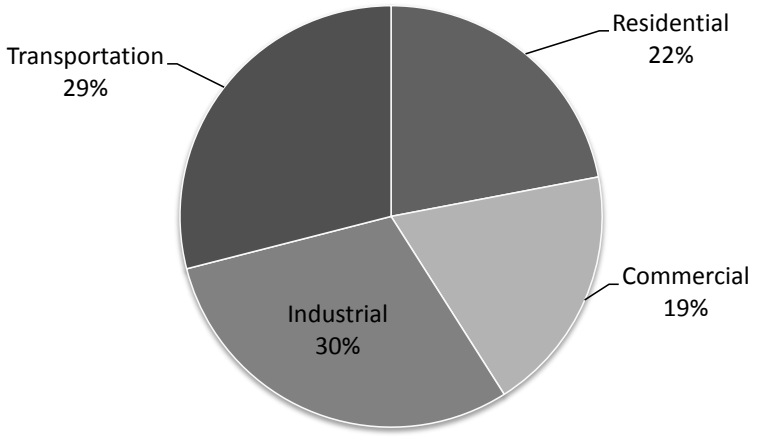

Figure 1.2 2009 United States total end-uses by sector [8]

As can be seen by comparing Figure 1.1 and Figure 1.2, Canada's energy use in the Residential and Commercial sectors is slightly less than that of the United States, as a percentage of the total. The difference in these sectors is made up for in the Industrial sector and the definition of an Agricultural sector in Canada. By observing Figure 1.2, Building Energy use would be expected to be approximately 40%, near the total percentage found in the Residential and Commercial sectors. This is reinforced by the U.S. Department of Energy (DOE) [9], which shows that buildings accounted for 39.3% of the total U.S. primary energy consumption in 2005 and are projected to remain around 40% to the year 2035.

Within the domain of non-concentrating solar thermal energy technology, building heating applications are especially important. As shown in Figure 1.3, within the Canadian Residential sector, space heating accounts for 63% of total site energy use, while water heating represents 18%. Figure 1.4 demonstrates that U.S. space heating is less significant at 46%, while U.S. water heating has a similar importance to Canada's at 18%.

It is important to note that use of the site energy value will tend to lower the apparent portion of electrical energy consumption with respect to the total source energy required. This is due to the nature of electrical production, and is of particular importance in areas with a high fraction of fossil fuel based power generation. In fact, for the U.S. Residential and Commercial building sector in 2008, the conversion factor for site-to-source electricity consumption was $\frac{3.16\ J\ source}{1.00\ J\ site}$ [9]. Other factors that may somewhat cloud the end-use split of data within and between countries include: climatic variation both

between countries and year, differences in the building stock, and the regional availability of energy resources.

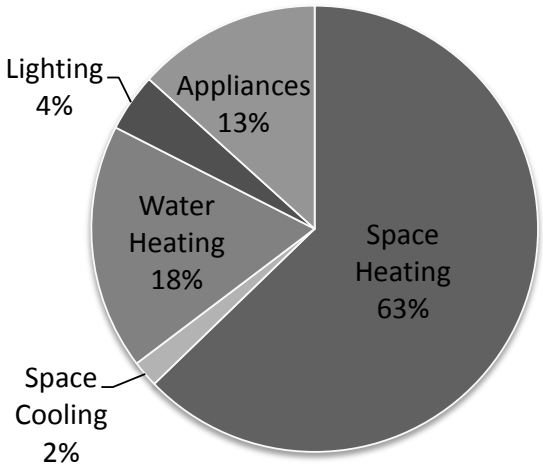

Figure 1.3 2007 Canadian Residential sector site energy splits by end-use: adapted from [7]

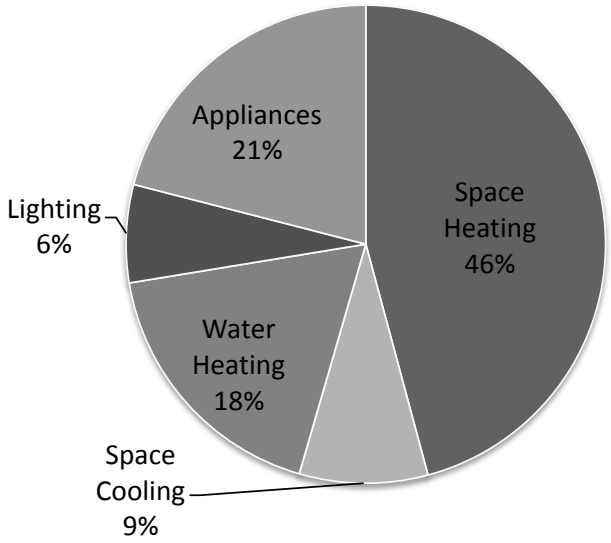

Figure 1.4 2008 United States Residential sector site energy splits by end-use: adapted from [9]

In the United States, a breakdown of end-use splits is also available for the Building sector as a whole. The Residential sector and the Building sector have very similar overall figures when it comes to space and water heating while lighting and space cooling represent an increased share within the Building sector.

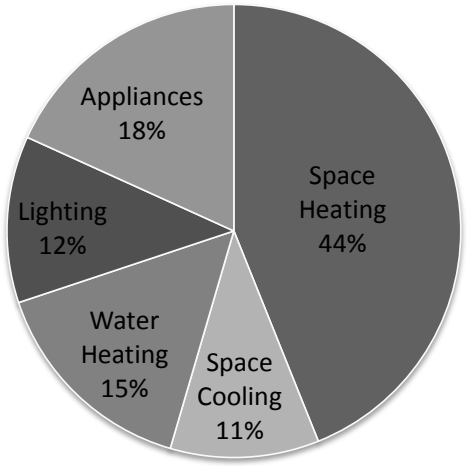

Figure 1.5 2008 United States Building sector site energy splits by end-use: adapted from [9]

In both Canada and the United States, heating applications account for a significant portion of the total building energy usage in both the Residential and Commercial sectors. Therefore, energy efficient heating technologies and renewable heat sources have a significant market to fulfill and will be an important part of the future energy landscape. Further, as buildings become more efficient, water heating will make up a larger share of the total building energy consumption.

1.3 Domestic Water Heating

A water heater is a device that is able to increase the temperature of a building's cold water supply, providing hot water to a number of end-uses such as sinks and dishwashers [10]. The increase in temperature is achieved by the addition of energy from a fuel supply. In Canada and the United States, water heating accounts for approximately 18% of residential site energy use [7, 9]. In Canada, this is the second highest household energy consumption next to space heating. There are a number of domestic water heating options available, including storage tank, tankless, solar, and integrated space/water heaters [10].

1.3.1 Storage Tank Water Heaters

Despite the availability of tankless on-demand water heaters, storage tank water heaters are the most common residential hot water systems in Canada [10]. Within the category of storage tank water heaters, several choices are available, depending on fuel type. The main choices include electric, natural gas, liquid propane and heating oil, where the fuel source used is often dependent on its availability in a

particular location [11]. As of 2007, 50% of all Canadian households used electric water heaters while 43% used natural gas for water heating, forming a combined 93% of the market [12]. With 50% of all Canadian households relying on electric hot water, there is clear potential for improved methods of water heating in Canada.

Electric storage tank water heaters rely on electrical heating elements to add energy to the water. These tanks often have an upper and lower element contained within the tank, as shown in Figure 1.6. Thermostats are used to control each element to maintain a sufficient water temperature at the thermostat location in order to adequately supply the heating load. Thermostats work by setting a minimum allowed temperature at the measured point, and electrical elements are turned on when the temperature drops sufficiently below this point [11]. For typical electric water heaters, a relatively large tank volume is necessary to allow for sufficient recovery time after hot water is used [11]. During use, hot water is drawn from the top of the tank, while cold makeup water is provided to the bottom, often through a tube mounted at the top of the tank. These tanks are insulated to impede heat loss to the environment that is often referred to as standby loss.

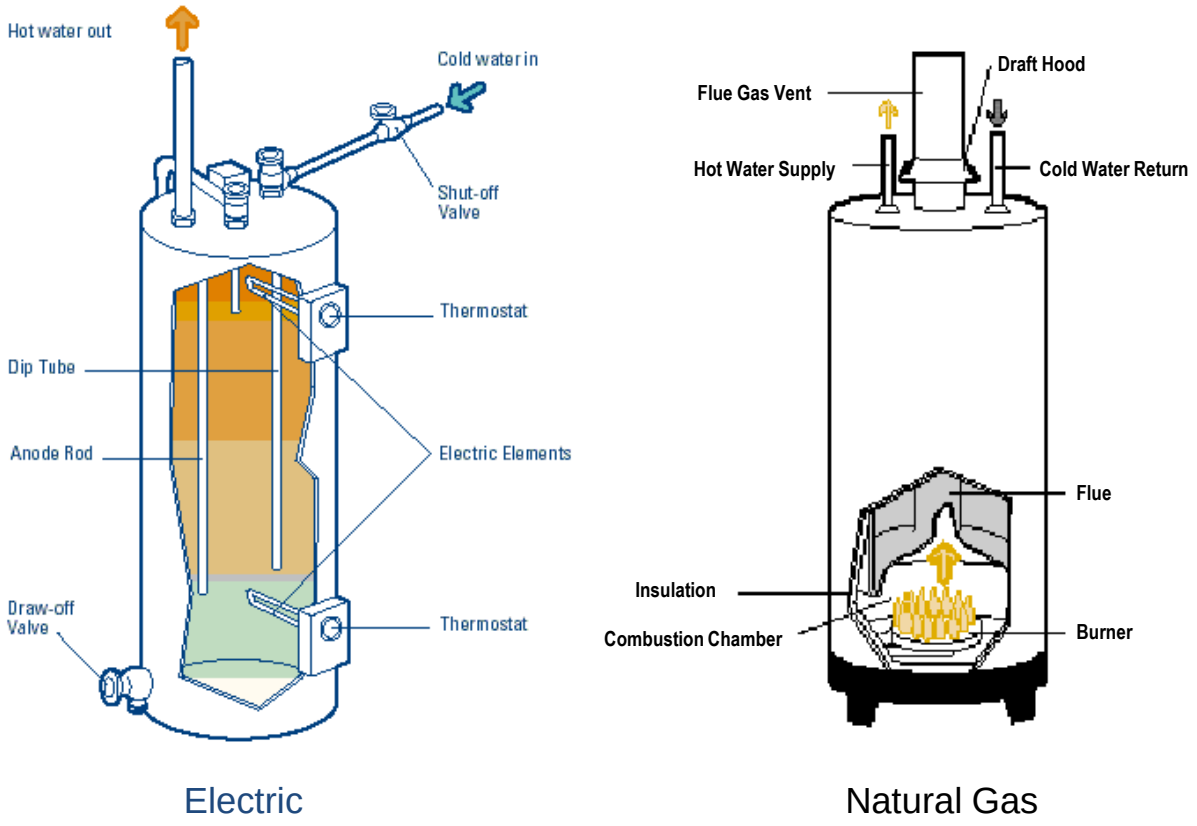

Figure 1.6 Electric [11] and natural gas [13] storage tank water heaters

Natural gas storage tank water heaters rely on a gas burner to add energy to the water. As shown in Figure 1.6, the flue carries hot exhaust gasses upward towards the exhaust vent while also exchanging heat with the water. The temperature of the water within the tank is monitored by a combined thermostat and gas valve that controls the flow of gas to the burner [13]. Since Natural gas water heaters are able to heat water at a faster rate, they do not require tank volumes as large as electric water heaters, and therefore recover quickly [11]. Hot water draws occur in a similar manner to those of the electric tanks. Also similarly to electric water heaters, natural gas water heaters have insulated tanks to reduce standby losses. However, due to the existence of the flue, additional losses are difficult to avoid.

For all storage tank water heaters, standby losses are an important efficiency consideration. For combustion based water heaters air flowing through the flue at standby condition, as well as the heat exchanger's (HX's) effectiveness during operation increases thermal energy loss [13]. However, according to NRCan [10], by addressing these issues, high efficiency models can commonly outperform standard models in terms of heat loss by 40%.

1.4 Solar Energy

1.4.1 Solar Energy Resources

Of the solar radiation that approaches Earth from outer space, 55% reaches the surface [14]. The global annual average radiation absorbed by land, oceans and the atmosphere is approximately $240\ W/m^2$ [15], leading to a figure of approximately $200\ W/m^2$ of annual average solar radiation striking the Earth's surface. Over the course of a year, approximately $3.2\ x\ 10^9\ PJ$ of solar energy strikes the surface of the Earth. Comparing this to the global total energy consumption of $3.5\ x\ 10^5\ PJ$ [1], it can be shown that the annual supply of solar energy dwarfs the global energy consumption by over 9000 times.

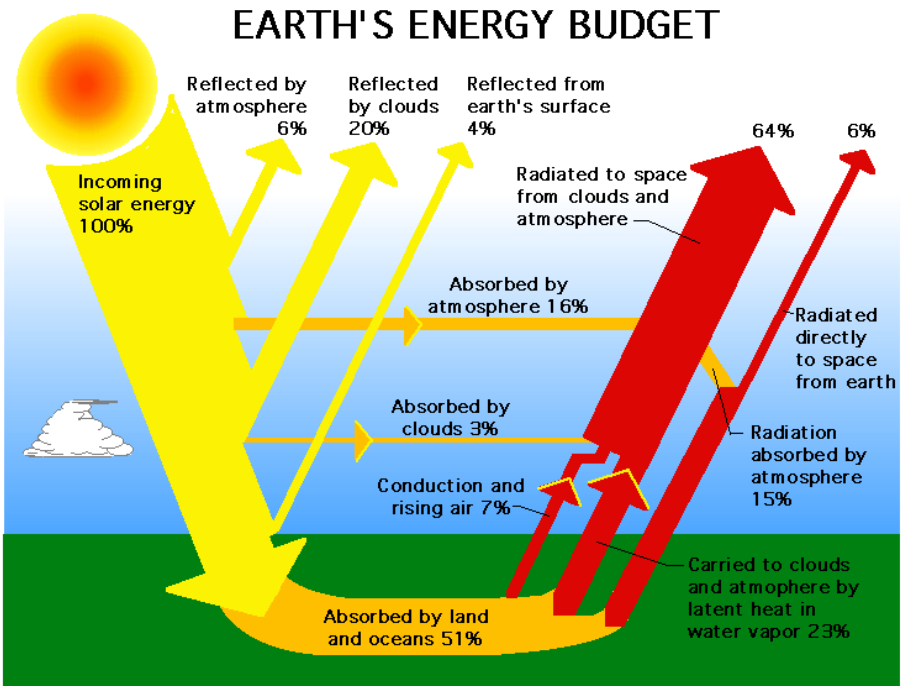

Figure 1.7 Breakdown of Earth's solar radiation [14]

Despite the vast supply of solar energy available on Earth, harvesting even a small portion in order to provide a sustainable energy supply has proven to be a challenge. As of 2008 solar energy provided only 0.04% of U.S. residential site energy and 0.3% of U.S. commercial site energy [9]. Though there may be a significant cost to harvesting solar energy, data from the U.S. DOE [9] can be interpreted to show that for 2005 the annual U.S. residential energy intensity was between 10 and 20 watts per square metre of heated space. Comparing this intensity to the global average solar intensity of $200\ W/m^2$, there is a significant potential to harvest solar energy when using appropriate technologies.

1.4.2 Solar Domestic Water Heating

Solar domestic water heaters are one of the most common ways in which solar energy is harvested. A schematic of a typical solar domestic water heating system is shown in Figure 1.8. A typical system consists of three main components, namely: the solar collector, hot water storage tank and pump. Active solar water heaters use a circulating fluid to absorb heat from a solar collector, and deposit the heat within a hot water storage tank. Other designs such as systems with vacuum tube collectors rely on a thermo-siphon effect to move heat to the water. For systems designed for cold climates, heat exchangers are common as the circulation loop often requires antifreeze to be used.

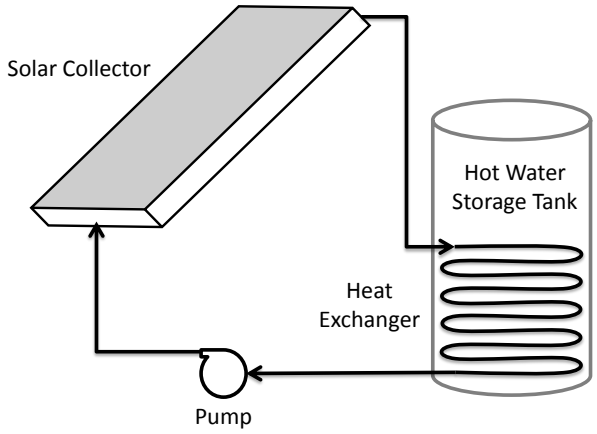

Figure 1.8 Typical solar domestic water heating system

1.4.3 Introduction to Solar Assisted Heat Pumps (SAHP)

In order to reduce energy consumption in building heating applications, solar thermal hot water collectors in combination with heat pump (HP) units have been investigated. For long it has been known that the combination of these technologies have the potential to reduce site energy consumption [16]. The concept takes inspiration from conventional solar domestic hot water (SDHW) systems, but has the potential to supply additional heat using a heat pump, thereby improving the performance of the solar collector [17]. Heat pumps consist of four major components; the compressor, condenser, expansion valve, and evaporator. In operation, a heat pump moves heat across the gradient from low to high temperatures with the assistance of work input to the compressor. The result is a low temperature refrigeration effect on the evaporator side of the heat pump, and a higher temperature heating effect on the condenser side of the heat pump. The performance improvement of the solar collector is accomplished by reducing the supply temperature to the solar collector, using the heat pump's refrigerating capacity, and thereby reducing thermal losses from the collector [17].

Though there appear to be two major categories of solar assisted heat pump (SAHP) systems, direct expansion (DX-SAHP) and indirect (I-SAHP), there are a vast number of possible configurations. In further chapters, the term heat pump assisted solar domestic hot water (HPASDHW) will be used to describe systems that incorporate a heat pump, but are also able to collect solar energy without the use of the heat pump. A DX-SAHP is a configuration that directly uses the solar collector as an evaporator in the heat pump cycle.

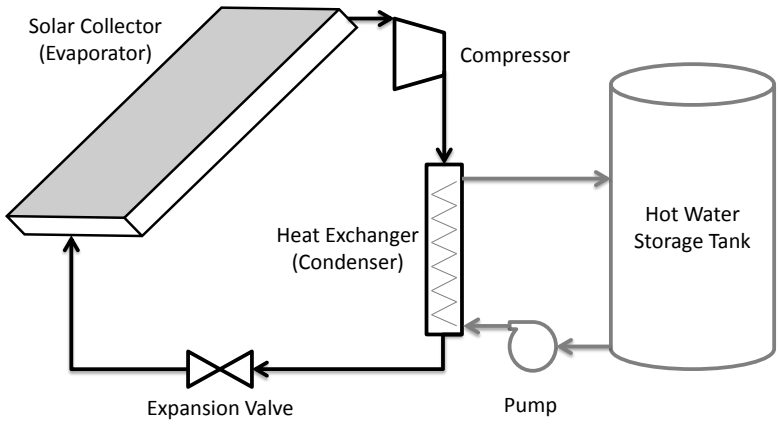

Figure 1.9 Direct expansion solar assisted heat pump (DX-SAHP) water heater

The I-SAHP is a configuration that includes a separate solar collection loop with the heat pump placed between the collection loop and the thermal storage loop. Heat exchangers allow for interaction between the solar collector, storage tank and heat pump.

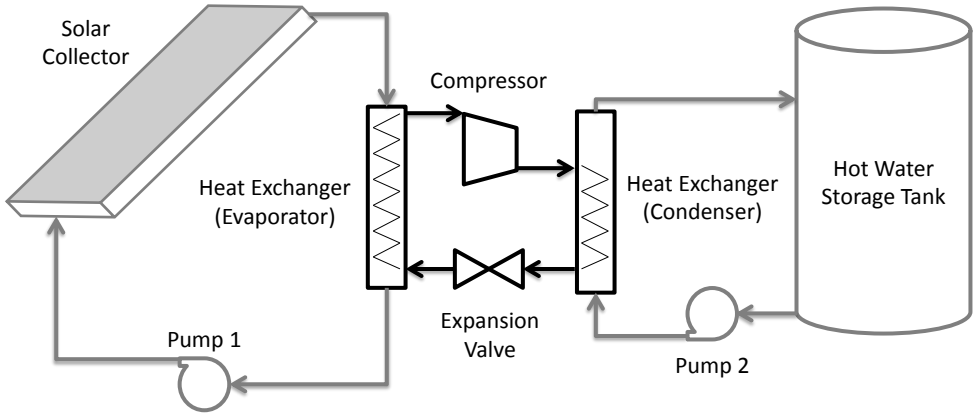

Figure 1.10 Indirect solar assisted heat pump (I-SAHP) water heater

Many systems in literature focus on providing residential hot water. These systems may also be scaled for use in large buildings. Some studies consider systems to provide space heat, or even cooling and heating simultaneously [18], which is particularly promising for use in large buildings that often require year-round cooling in core zones. Further, SAHP systems may be combined with ground source (GS) systems to form solar assisted ground source heat pump (SAGSHP) systems [19]. For all configurations it is important to consider whether or not these systems are cost effective, and if they actually reduce the source energy consumption of the building.

1.5 Outline of Thesis

This thesis covers the topic of heat pump assisted solar thermal systems for domestic water heating, including the modelling and experimental validation for one such system. In this chapter the motivation for research in the field of solar thermal and combined heat pump systems is presented. It also includes an investigation of how energy is used in buildings, common methods of water heating, an introduction to solar energy and the solar assisted heat pump as well as an outline of this thesis.

Chapter 2 provides a literature review describing research relevant to SAHP and HPASDHW systems. This chapter first briefly presents conventional solar domestic water heating systems. The major components that make up a heat pump assisted solar domestic water heating system are discussed with respect to relevant research in the field. The chapter concludes with a review of DX-SAHP, I-SAHP and HPASDHW systems, highlighted by studies of these water heating systems in the Canadian climate.

Chapter 3 provides a detailed description of the heat pump assisted water heating system of interest, called the Dual Side I-HPASDHW system. Potential performance advantages are stated that make the system an intriguing point of study. A detailed description is provided for the design and development of an Experimental Test Unit (ETU) capable of simulating both the Dual Side I-HPASDHW system, and a secondary system to be investigated by University of Waterloo PhD Candidate; Carsen Banister.

Chapter 4 presents the program TRNSYS and describes its use simulating the ETU. The basic way in which systems may be simulated is explained, and key simulation inputs such as the time-step are investigated. An explanation of the built-in models useful in simulating the ETU is provided and is largely based upon each model's mathematical description. Custom models are presented in a similar manner, providing information on each model's function. Where appropriate, the explanation of both built-in and custom models includes calibration data used to determine key model inputs to match ETU performance.

Chapter 5 presents the results of validation exercises, summarized in a series of plots. The chapter begins with an explanation of the simulation and several expectations. A sample of results from a 24 hour test of the ETU is presented to describe the quality of experimental simulation provided by the ETU. The mutual influence of hot water circulation and DHW electrical heating element usage is shown to provide context to further results. Lastly, four 24 hour tests are presented, directly comparing

the ETU performance with TRNSYS simulations, highlighting qualitative and quantitative matches and deficiencies.

Chapter 6 provides a summary of conclusions and recommendations based upon information obtained throughout the design, development and validation process. Conclusions are first drawn concerning the validation of the TRNSYS model used to match ETU performance. Further, conclusions regarding the design and control of the Dual Side I-HPASDHW are presented. Recommendations are then provided concerning the future use of the TRNSYS model and regarding the design and control of the Dual Side I-HPASDHW system. The chapter concludes by outlining an array of recommended future studies involving the Dual Side I-HPASDHW as well as other HPASDHW systems to be investigated.

The Appendix begins with the methods used to characterize components of the Experimental Test Unit equipment. Characterization is presented with data from preliminary experimental tests and, in some cases, simulations. Characterization for the heat exchanger and heat pump includes a description of how collected data is translated into custom TRNSYS components for the simulation. An uncertainty analysis is provided along with sample calculations to demonstrate how error in experimental measurements results in error in calculated values.

Chapter 2 Literature Review

2.1 Conventional Solar Domestic Water Heating Systems

Since solar assisted heat pump (SAHP) systems have evolved from solar domestic hot water (SDHW) systems, there are numerous similarities between the two. Therefore, it is important to provide a background in SDHW systems. Despite the diversity of possible configurations, in Figure 2.1 common SDHW systems are presented. System (a) shows a natural circulation system where flow is driven simply by natural circulation [20]. System (b) demonstrates a forced circulation system where pumping is required, and is usually controlled by a differential thermostat [20]. This means an adequate temperature difference must be achieved between the top of the collector and the bottom of the storage tank in order for the pump to be activated. Systems (c) and (d) show designs generated for collectors in colder climates where freezing is a concern, and therefore antifreeze is circulated through the collector. This necessitates the use of heat exchange devices, which may be external to, or contained within the storage tank [20]. In system (d) the second tank houses the auxiliary heater and provides additional storage capacity. It is important to note that all three methods of auxiliary heating presented in Figure 2.1 are interchangeable [20]. However, it is possible that external auxiliary heating will allow for extended solar collection periods since lower temperatures may be maintained in the storage tank. Lastly, whenever the temperature to the load exceeds the maximum hot water supply temperature, tempering valves are used to mix cold water into the supply [20].

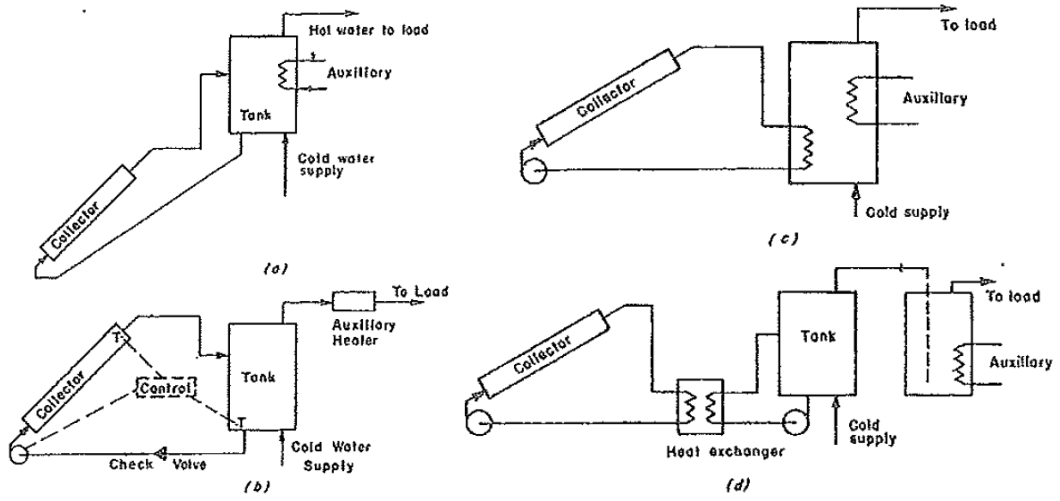

Figure 2.1 Schematic of common configurations of SDHW systems. (a) a natural circulation system (b) one-tank forced-circulation system (c) system with antifreeze loop and internal heat exchanger (d) system with antifreeze loop and external heat exchanger [20]

According to Natural Resources Canada (NRCan) [10], when using a conventional SDHW system, up to 50% of an average household's hot water demand can be supplied by solar energy. In order to increase this fraction of solar energy and improve the sustainability of auxiliary heating, heat pumps (HPs) may be introduced into SDHW systems [17].

2.2 Solar Assisted Heat Pump Major System Components

2.2.1 Solar Collectors

The solar collector is a primary component of solar assisted heat pump systems. This is the point at which the solar energy is collected, and for SAHP systems, is usually a flat plate collector which may be of the glazed or unglazed variety. The performance of solar collectors is often described with the "Hottel, Whillier, Bliss" (HWB) correlation as presented in Duffie and Beckman [20].

$$\dot{Q}_u = A_c F_R \left[S - U_L \left(T_{f,i} - T_a \right) \right]^+ \tag{2.1}$$

Where:

$\dot{Q}_u$ is the useful heat collected
A_c is the collector area
F_R is a heat removal factor describing the collector's heat transfer characteristics
S is the radiation reaching the absorber surface
U_L is the thermal loss coefficient
$T_{f,i}$ is the fluid inlet temperature
T_a is the ambient temperature

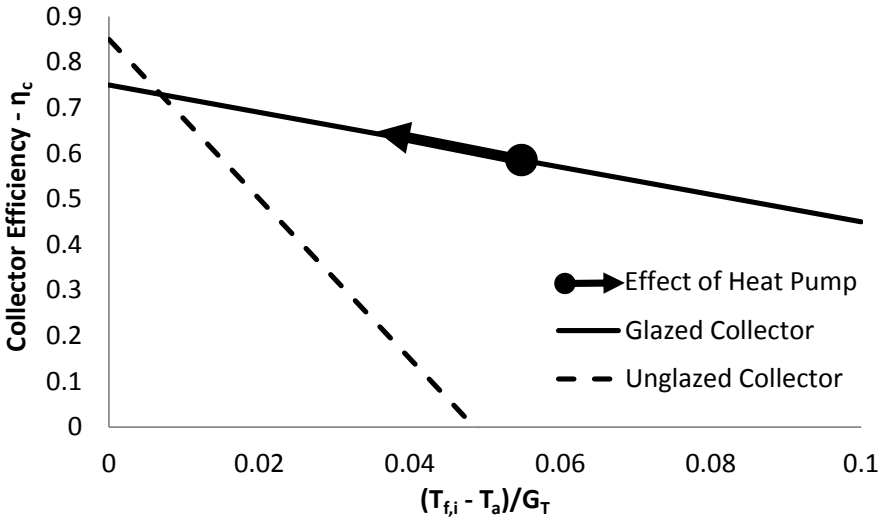

Figure 2.2 Characteristic solar collector efficiency curves (G_T = total incident radiation on a tilted surface)

The curves presented in Figure 2.2 are not taken from particular tests, but are typical representations of collector behaviour similar to those described in [20]. A glazed collector can accept

high temperature inlet fluid and maintain its efficiency much more effectively than an unglazed collector. This is due to the reduced loss coefficient, U_L. The y-intercept in Figure 2.2 represents the optical efficiency of the collector. It is possible that unglazed collectors may outperform their counterparts in this aspect; however, this is dependent on the coatings and glazings used for each collector.

The addition of a heat pump has the effect of lowering the inlet fluid temperature to the collector. With respect to Figure 2.2, the impact of the heat pump is to shift up the curve to the left, therefore increasing the collector efficiency and drawing more heat into the system. If the collector inlet temperature is reduced by the heat pump to a level sufficiently below the ambient temperature, it is possible to achieve collector efficiencies over 100% based upon the conventional definition. This is possible since, in addition to gaining heat from solar radiation, there may be a net transfer of heat from the ambient air to the collector. Since unglazed collectors cost less, and the addition of a heat pump lowers the fluid inlet temperature, unglazed collectors are common in SAHP systems. In cooler climates, the use of a glazed collector will allow for effective solar energy collection deeper into the heating season.

2.2.2 Hot Water Storage Tanks

Though other forms of thermal storage are possible, hot water storage tanks are extremely common in solar water heating systems. In a solar water heating system, appropriate thermal storage allows for solar collection throughout the day, and provides a supply of hot water during periods of little or no solar radiation.

There are many forms of hot water storage tanks. Booster tanks simply add storage mass and have direct connections to move fluid between tanks. Indirect water heaters provide thermal storage and include an internal heat exchanger in order to utilise an external heat source. In Figure 2.3, a typical SDHW tank is shown. This schematic includes a double wall heat exchanger, which is required by code in many jurisdictions in order to exchange heat with an antifreeze mixture. Within the middle portion of the tank, solar water heaters often include a high capacity backup electrical heating element and thermostat in order to provide heat when solar heating is inadequate. Though models with internal double wall heat exchangers are common, solar booster tanks are also available which utilise separate external heat exchangers.

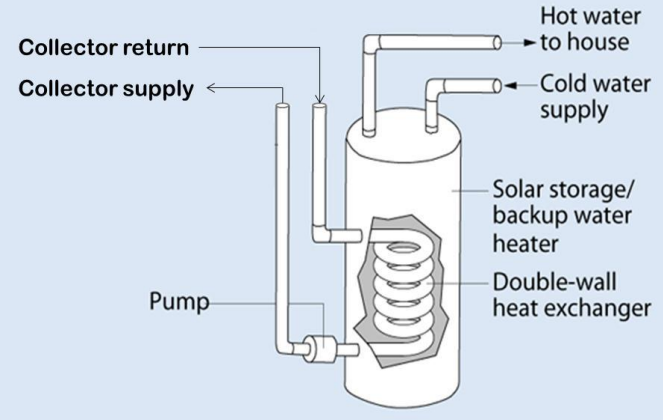

Figure 2.3 Solar domestic water heater tank: adapted from [21]

Like storage tank water heaters, solar water heaters include a cold water supply to the bottom of the tank with a hot water return at the top. As with high efficiency storage tank water heaters, standby losses are common concerns for solar hot water tanks. For this reason, solar water heater tanks are normally highly insulated, often more-so than ordinary storage tank water heaters. Heat exchanger effectiveness is also important to solar water heating systems since the collector inlet temperature should be kept as low as possible. If the effectiveness of the heat exchanger is low, the source side of the system will operate at a higher than necessary temperature. Other issues such as thermal stratification and sizing of hot water storage tanks can be very important when coupling the tank with a SAHP.

Thermal stratification is the variation of temperature with respect to the depth of the hot water tank. In a stratified water tank, hot water will move to the top of the tank due to a lower density, while cold water will tend to settle at the bottom of the tank due to a higher density. Thermal stratification has been shown to improve the performance of solar hot water systems [22]. Since cold water collects at the bottom of the tank, it can be supplied to the collector thereby improving the collector efficiency. This effect may also be exploited by SAHP systems and would allow for improved solar energy collection. One may note that the heat exchanger in Figure 2.3 is placed intelligently to take advantage of stratification. The heat exchanger is positioned such that the coldest temperature from the bottom of the tank can be returned to the collector to improve efficiency. Meanwhile the collector return is placed near the middle of the tank, meaning that a pocket of hot water can be maintained at the top of the tank even if the collector return is only a moderate temperature.

With the importance of thermal stratification being well understood, a significant amount of research has been focussed around the optimization of systems with respect to stratification. In one study by Hollands and Lightstone [23], the major causes of tank destratification are reviewed to outline the benefits of low flow solar systems. These methods included inlet jet mixing, plume entrainment, as well as heat conduction and side losses. It was shown that for inlet jet mixing, the effect can be mitigated by reducing inlet water velocity. Plume entrainment was the second mode of destratification and is caused by the introduction of either cold water in a warm part of the tank or warm water in a cold part of the tank. The study showed, using side-by-side tests, that the effect of plume entrainment can be curbed to a high degree by introducing water to the tank through a porous vertical manifold, see Figure 2.4, located within the tank. The device functions by allowing the density of incoming water to equalise to the density of water in various tank levels before exiting the manifold. Lastly, heat conduction in the tank wall, as well as standby losses may result in convection currents that contribute to tank destratification.

Figure 2.4 Porous manifold to reduce thermal plume – shown horizontally, installed vertically

In Fanney and Klein [24], a series of side-by-side experiments were conducted to investigate the impact of flow rates and return tube configurations using two otherwise identical systems with select modifications. A return tube investigation was conducted with single tank direct solar systems. The higher flow system ran a flow rate of $0.02\ kg/s$ per m^2 of absorber area. This system was equipped with a simple stratification enhancing return tube consisting of a $610\ mm$ tube with $9.5\ mm$ holes equally spaced at approximately $25\ mm$. In the other system, a lower flow rate of $0.0033\ kg/s \cdot m^2$ was used that, according to previous studies, was the optimal flow rate. This lower flow system was equipped with a standard return tube. Experiments showed that the system with a stratification enhancing device was quite successful in matching the performance of a low flow system. Other side-by-side tests were conducted with identical return tubes to investigate the effect of flow rates. Lower flow

systems demonstrated improved performance for direct systems. However, for indirect systems with an external heat exchanger, it was found that increasing the flow rate improved the performance of the heat exchanger and more than compensated for any subsequent destratification of the hot water tank.

In Huang and Lee [25], the importance of properly sizing the hot water tank to daily hot water draws was uncovered. If the system has a great excess of thermal storage, the initial daily water temperature in the tank will be too high and reduce the coefficient of performance (COP) of the heat pump. This problem may be mitigated through better tank stratification and improved flexibility in the system and controls. For a fixed system size with defined hot water draws, the tank size can be optimized in terms of cost. Increasing the amount of thermal storage increases initial cost, while decreasing the amount of thermal storage beyond a certain point will result in more auxiliary heating. In Nuntaphan, Chansena and Kiatsiriroat [26], an Indirect (I-SAHP) system was investigated mathematically with various hot water tank sizes. In this study, the principal investment required to install the system increased linearly with increased storage capacity. In reference to Nuntaphan, Chansena and Kiatsiriroat [26], it is important to note that the principle investment in a SAHP system may not be a strong function of storage capacity. A search of commercially available hot water storage tanks reveals that although the cost of storage increases with capacity, this increase is not necessarily linear.

2.2.3 Heat Pumps

Conventional vapour compression heat pumps are devices that are capable of moving heat from low temperature to high temperature with the assistance of energy input. The energy input is provided at the compressor and is almost exclusively in the form of electricity. The basic thermodynamic heat pump cycle includes the following processes:

- Evaporation
- Compression
- Condensation
- Expansion

A heat pump moves heat from a lower temperature reservoir to a higher temperature reservoir, and it is possible to move more energy against the temperature gradient than is consumed by the heat pump. As a result, heat pump performance is described by a COP rather than efficiency, which is defined as:

$$COP = \frac{Desired\ heat\ transfer\ rate}{Required\ energy\ input\ rate} \tag{2.2}$$

When the heat pump is used to refrigerate a given load, the desired heat transfer rate is the rate of heat removal at the evaporator. Conversely, in heating mode the COP improves as the desired heat transfer rate is defined as heat delivered at the condenser. More heat is delivered out of the condenser than is absorbed by the evaporator, and this is revealed through a simple energy balance. If unintended heat transfer to the surroundings is ignored, the heat transfer in the condenser becomes the sum of heat transfer in the evaporator plus the power used to drive the compressor.

Heat pump COP is highly dependent on the temperature difference maintained across the heat pump. Specifically, very high temperature differences are problematic. There are also limitations to how low or high the respective source and supply temperatures may be. These operating restrictions have been a major challenge for air source heat pumps and have limited their use for heating in very cold climates. This is one reason why ground source heat pumps have become common. For SAHP systems, the addition of solar energy may ease these temperature based limitations, although these conditions may still arise during periods of low solar radiation.

Just as there are vast configurations of SAHP's, there are many classifications of heat pumps. In Figure 2.5 typical heat pump configurations, air-to-air and water-to-water heat pumps, are shown. Combined source (air and water) and combinations of each may also act as the heat pump in SAHP systems depending on the design. As a condition of the heating load served by the system, the size of each heat pump can vary drastically. A heat pump responsible for space heating/cooling as well as hot water may be very large, while a heat pump integrated only with residential domestic hot water may be very small. In fact, many of the smaller systems considered for SDHW require custom or altered heat pumps. For example, in Nuntaphan, Chansena and Kiatsiriroat [26], an automotive air conditioning compressor was used to achieve a properly sized heat pump design for a hot water system.

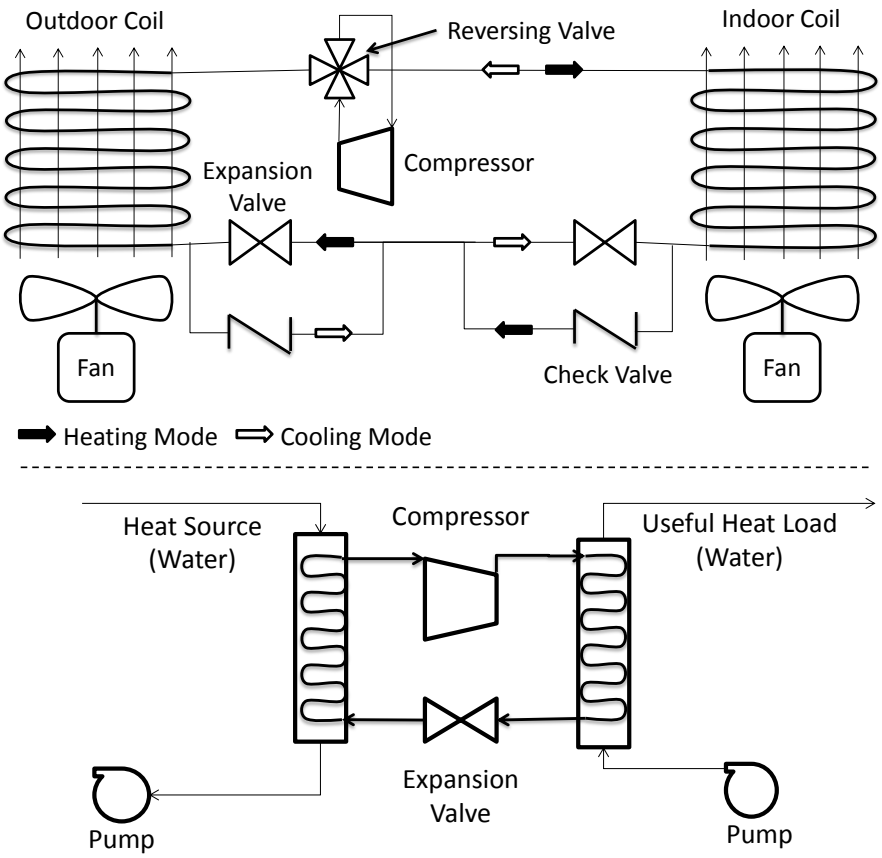

Figure 2.5 Air-to-air (top) and water-to-water (bottom) heat pumps: reproduced from [27]

Various working fluids have been investigated for use as both primary and secondary fluids for heat pump cycles in SAHP systems. In Jin and Spitler [28], the impact of running a water-glycol antifreeze mixture through the evaporator's heat exchanger was investigated. This analysis was important for ground source heat pumps, but is also useful for heat pumps using cold climate solar collection loops as a heat source. Other analyses consider alternate heat pump refrigerants such as non-azeotropic refrigerants. Non-azeotropic mixtures are combinations of refrigerants which tend to separate upon phase change due to a difference in saturation conditions. As a result, the phase change temperature does not remain constant, but is allowed to glide upwards or downwards as the mixture evaporates or condenses. As discussed in Nuntaphan, Chansena and Kiatsiriroat [26], non-azeotropic mixtures have the potential to significantly improve heat pump performance. Since the condenser and evaporator are allowed to vary in temperature, the temperature differences within the refrigeration cycle are reduced. Namely temperature differences between evaporator exit and condenser inlet, as well as between the condenser exit and evaporator inlet are reduced. These improvements may be realized by SAHP

systems, and were taken advantage of by the system described in Nuntaphan, Chansena and Kiatsiriroat [26]. In addition to potential performance benefits introduced by non-azeotropic refrigerants, a further benefit to SAHP systems may be expanding the envelope of acceptable operating temperatures.

The compressor is an extremely important component of the heat pump as it is responsible for driving the cycle. Many have studied the implications of compressor technology on heat pump COP for a variety of types and uses. In Kuang, Wang and Yu [18], compressor capacity modulation was studied. In this study, a variable speed compressor was used along with an electronic expansion valve in order to run a direct expansion (DX-SAHP) unit. The results presented improvements in heat pump COP from standard operation ($COP = 1.5 - 3.5$) to a modulated system COP ($COP = 2.5 - 5.0$). Scroll compressors have become popular in heat pump applications and are available from a number of large compressor manufacturers. In Kuang, Wang and Yu [18], correlations were presented to determine heat pump performance based upon data readily available in catalogues. These correlations are being updated in order to include the use of scroll compressors. Combining scroll compressor technology with capacity modulation results in the digital scroll compressor. This technology allows for improved seasonal average COP, while also being able to provide heat at times of low ambient temperatures [29]. However, the incremental cost of adding modulation to the compressor in a SAHP system may make this technology prohibitive for the time being.

Regardless of the measures taken to improve heat pump COP, it is still important to consider how the electricity used to power the heat pump is generated. For example, when comparing a heat pump heating system to a gas based furnace, the site energy consumption may go down considerably with the use of a heat pump while the source energy consumption may be equal. This is true if the COP is offset by the efficiency of electrical production in the region. In the consideration of greenhouse gas emissions and fossil fuel consumption, a heat pump operating in Ontario or Quebec makes much more sense than one operating in other provinces or many U.S. states which primarily use fossil fuels for power generation. The improvement in Ontario and Quebec is due to the high portion of nuclear and hydro contributions to the generated electricity. Any benefits of the heat pump are greatly diminished when a fossil fuel based grid is used to provide the electricity.

2.3 Solar Assisted Heat Pump Systems

Through a combination of components, SAHP systems may be created that commonly resemble SDHW systems. Controls for SAHP systems are also often similar to those of common SDHW systems

presented in Figure 2.1. However, more complexity may be added to the controller of a SAHP in determining when it is reasonable to run the heat pump. This complexity depends on the system configuration and the efforts made to improve system performance. When heat pumps are introduced to a hot water system, the inlet temperature of the solar collector may be lowered, and therefore the collection of solar energy may be extended into periods of lower radiation [17].

2.3.1 DX-SAHP and I-SAHP Characteristics

The DX-SAHP appears to be the most common SAHP system due to its advantages in moderate-to-warm climates. Since the DX-SAHP directly refrigerates the solar collector inlet, thermal collector losses are less of a concern. This allows for the use of a cheaper unglazed solar collector and in the process eliminates a heat exchanger, providing both economic and thermodynamic improvements [30]. One further advantage is the elimination of auxiliary heating, and comes from the system's ability to act as an air source heat pump when there is little-to-no incident radiation on the collector [31]. For two-tank systems, there is a potential to use the refrigerating and heating capacity of the heat pump simultaneously. This can be done both with DX-SAHP systems such as that presented in Kuang, Wang and Yu [18], as well as I-SAHP systems.

Though DX-SAHP systems are more popular, I-SAHP systems have a number of advantages. A very important advantage of the I-SAHP system is the fact that these systems do not necessarily require the heat pump to run in order to collect solar energy. When solar energy is in high supply, it may be collected in a more conventional SDHW style, thereby eliminating the electrical consumption of the heat pump. This prospect is realized in Sterling [17], where I-SAHP systems are referred to heat pump assisted solar domestic hot water (HPASDHW) systems since the heat pump is no longer the solitary energy mover. In this type of system, the use of a glazed collector allows for effective collection of solar energy well into the heating season. However, the glazed collector negates the option of using the solar collector as an effective air source heat exchanger. In Bridgeman and Harrison [32], the authors explained that a DX-SAHP system requires a significant length of refrigerant pipeline and therefore, a greater volume of expensive refrigerant may be necessary. Other refrigerant related costs were shown in Bridgeman and Harrison [32], namely, expensive refrigerant fittings would be necessary for the collector and on-site charging of the refrigerant may lead to additional installation costs.

2.3.2 Solar Assisted Heat Pump Operational Considerations

Since SAHP systems most commonly feed domestic hot water tanks, it is important to understand the impact of hot water draws on the system. In Anderson and Morrison [33], transient

behaviour was investigated and characterized for a DX-SAHP system with an in-tank condenser coil. In this investigation, various sized loads in the form of hot water draws were introduced to hot water storage tank, and the SAHP was used to recharge the tank. Heat pump (HP) operation was triggered by a thermostat located near the bottom of tank.

Table 2.1 Heat pump COP for various conditions when installed in a SAHP system - summary from [33]

Test Load	Level of Stratification	Daytime COP (Approx.)	Night time COP (Approx.)
Full Load	Low	2.5 - 7	2.5 - 5
Half Load	Moderate	2.75 - 4.75	2 – 3.5
Short Cycle	High	2.5 - 3	1.75 – 2.5

In all tests, the heat transfer rate of the heat pump HP increased when more source heat was available, implying higher levels of solar radiation and therefore a higher source temperature. However, compressor power appeared to be significantly influenced by the load only, where power consumption increased with increasing load temperature. Under full load and part load conditions, the COP was maximized at the beginning of each cycle, an effect which can be attributed to lower entering load temperature. It is clear from Table 2.1 that larger loads result in better system performance. Again, the COP was improved for larger loads where the mean water temperature in the tank, and therefore HP entering load temperature, was kept low. Since compressor power was only significantly influenced by load temperature, and heat transfer rates were influenced by the amount of heat available, night time COP values for the DX-SAHP system were consistently less than daytime COP values.

In the past, the reliability of heat pumps operating between highly variable temperature limits has been questioned, particularly for DX-SAHP systems [25]. Therefore, Huang and Lee [25] presents a long term performance study in which a prototype with a total running time of 20000 hours over the course of five years was investigated. The study also presented a 13000 hour period of continuous operation with no mechanical failures in this time. Though further testing will be continued, the authors have shown enough reliability to move forward with commercialization of their unit.

2.3.3 SAHP and HPASDHW in the Canadian Climate

In Freeman and Harrison [34], an I-SAHP system for domestic hot water was investigated using a computer simulation completed in the simulation program TRNSYS. TRNSYS is a transient simulation program that allows users to link a number of component models together through their inputs and outputs. The I-SAHP investigated was similar to that shown in Figure 1.10; however, the loop removing

heat from the condenser operated without a pump, instead relying on natural convection to circulate fluid. For the TRNSYS simulation, custom components were developed to model the heat pump, natural convection heat exchanger and the heat pump controller. The function of the heat pump module relied on a lookup table to provide performance data. This table was developed using first law heat pump analysis and EES (Engineering Equation Solver), a program that simplifies the use of thermodynamic property tables. The simulation was conducted for five major Canadian cities, namely: Halifax, Montreal, Toronto, Winnipeg, and Vancouver.

The study by Bridgeman and Harrison [32] was a continuation of the work by Freeman and Harrison [34]. In Bridgeman and Harrison [32], an experimental I-SAHP water heater unit was tested with the main objective of validating the heat pump model generated in the previous study. As shown in Figure 2.6, an electrical heater imitated a solar collector and was applied to the evaporator side loop of the heat pump in the experimental setup. The condenser in this unit was connected to the stratified hot water tank by a natural convection loop. In Bridgeman and Harrison [32], I-SAHP system simulations were compared with electric water heating, a SDHW system, and lastly an air source heat pump water heater. Simulations showed that more energy was collected by the SAHP unit than SDHW systems and air-to-water heat pumps in times of poor weather and in the winter season. This study predicted that the life-cycle cost of SAHP and SDHW systems are comparable for most locations. The SAHP showed improved life-cycle cost between 12% and 29% compared to SDHW systems for the cities of Halifax and Vancouver, cities in which relatively little solar radiation is available for collection.

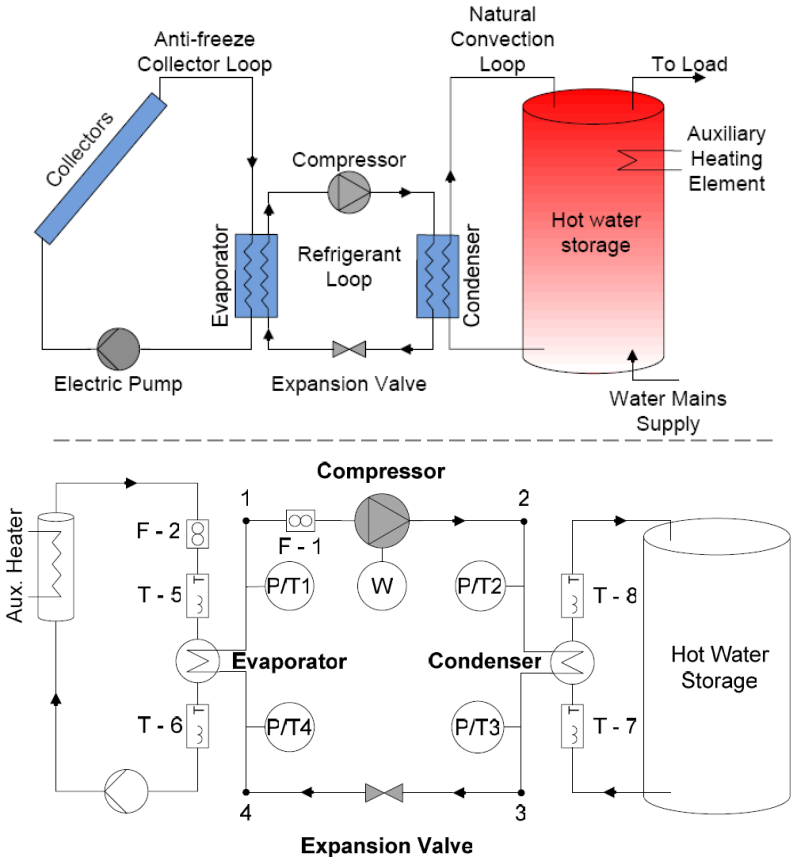

Figure 2.6 Schematic diagram of an I-SAHP System (Top) and an analogous experimental unit (bottom) [32]

After comparing the simulations from Freeman and Harrison [34], to experimental work done in Bridgeman and Harrison [32], significant variations were found, where the preliminary simulation over-predicted the heat pump COP [32]. Variations were attributed mainly to the assumed effectiveness of each heat exchanger. For the evaporator, simulations were conducted with a constant effectiveness of 93%; however, depending on conditions, a range between 68% and 90% was observed experimentally. For the condenser, the error was found to be even worse, and may be due to the complexity of modelling a natural convection loop. When simulations were repeated with corrections to the heat exchanger effectiveness, a much better match between theoretical and experimental results was found. However, the COP and power input of the heat pump still demonstrated up to 10% error between simulation and experimental results in certain cases. The experimental COP values were reported from 2.8 to 3.3 for source temperatures between $10℃$ and $30℃$ [32].

The thesis by Sterling [17] is a feasibility study focussing on two I-HPASDHW systems for solar domestic water heating. The study outlined a simulated analysis of system performance using the

TRNSYS software. The simulated performance of each system was compared, and further, compared with simulations of electric water heating and more traditional solar domestic hot water systems.

The first water heating system was named the Dual Tank indirect heat pump assisted solar domestic hot water system (Dual Tank I-HPASDHW) [17]. This system consisted of a solar hot water collection loop connected to a domestic water heating tank by two heat transfer systems, namely a heat pump and heat exchanger, Figure 2.7. The large tank was located in the solar energy collection loop and was allowed to float up and down in temperature. For the analysis, the source side of the system that includes the large tank used a water-glycol mixture as the heat transfer fluid. This allowed the collector to remain outside in the winter months without drain-back and expanded the source temperature range at which the heat pump may operate. When the large tank had sufficient temperature, the heat exchanger was used to heat domestic hot water. The heat pump was allowed to operate when the heat exchanger was not sufficient, and under most conditions provided $5 - 10\ kW$ of heat transfer. In this system, the cooling effect of the heat pump allowed for extended periods of solar collection compared to an ordinary SDHW system.

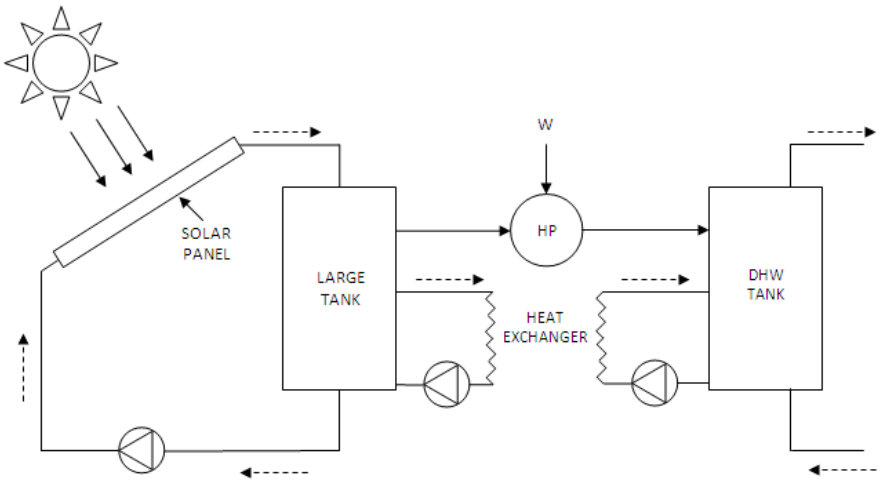

Figure 2.7 Dual Tank I-HPASDHW system for domestic water heating [17]

The second water heating system was named the Solar Side indirect heat pump assisted solar domestic hot water system (Solar Side I-HPASDHW) [17]. This system consisted of a solar hot water collection loop connected to a domestic water heating tank with a heat exchanger. In this system, a heat pump was connected in the solar loop, and was parallel to the solar collector, Figure 2.8. The heat pump in this system had a $1 - 2.5\ kW$ heat transfer capacity and directly cooled fluid being pumped to the solar collector inlet, thereby improving the collector performance.

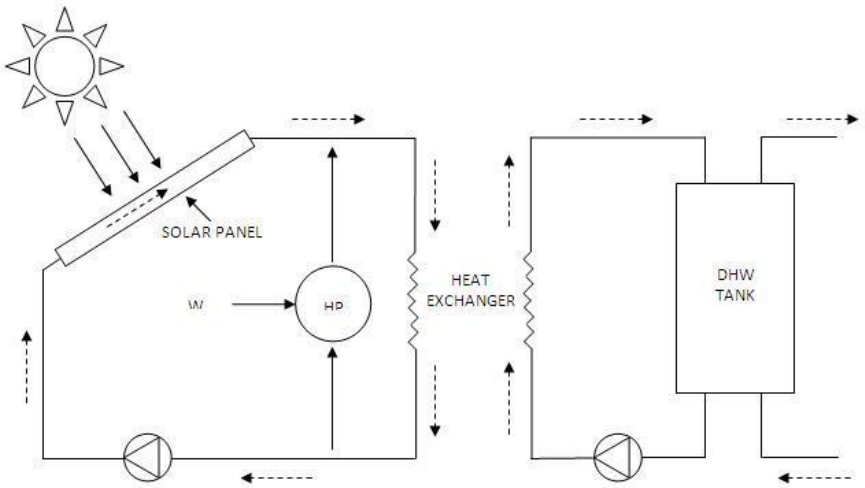

Figure 2.8 Solar Side I-HPASDHW for domestic water heating [17]

For both systems the heat pump operation was optional, providing the prospect of collecting energy in a more traditional SDHW style [17]. This option has the potential for a significant reduction in electrical consumption by avoiding unnecessary electrical consumption by the heat pump. Though the operational modes allowed by each system may provide energy savings, they introduce complexity into the control of each system, particularly for the Solar Side system. For the control of the Solar Side system a complex controller was programmed through a Microsoft Excel-linked component in TRNSYS. The complex control required a number of inputs including several temperatures, the heat transfer rate to the heat pump, and the solar radiation striking the surface of the collector. Based upon the answers to four questions, the complex controller decided whether the pumps should be on to allow for solar energy collection, and whether the heat pump should be on to assist in the collection of solar energy. The questions are as follows [17]:

- 1 - Is the domestic hot water top tank temperature too high to proceed?
- 2 - Can substantial energy be collected without the use of the heat pump?
- 3 - Can substantial energy be collected with the use of the heat pump?
- 4 - Is heat pump operation worthwhile?

Question 1 was used as a high limit cut-off where the entire system would be shut down when the tank temperature became too high [17]. Questions 2 and 3 were used to decide when the system should be operating to collect solar energy, where if at least one answer was 'yes', the operational mode of the pumps would be on. If Question 3 was answered 'yes' while Question 2 was answered 'no', the heat pump would be turned on. Note that if Question 3 was answered 'no', Question 2 would also be answered 'no'. Lastly, if both Question 2 and Question 3 resulted in a 'yes' answer, Question 4 would be

used to make the following decision; whether or not the heat pump should be operating. The decision of Question 4 was made using a decision matrix accounting for incident solar radiation on the collector, time of day, and tank temperature. This controller allowed the system to collect solar energy in a traditional SDHW style when appropriate, while using the heat pump to provide extended periods of collection in the cold season, poor weather conditions, earlier in the morning, and later into the afternoon.

In Sterling [17], year-long simulations were conducted for all systems analyzed. These simulations were limited to the geographical location of Ottawa, Ontario, Canada. Detailed analysis of the system and control operation was provided for days of typical performance in the months of February, July and December. It was found that the addition of the heat pump had the desired effect of increased solar collector efficiency and extended run time. The Solar Side system demonstrated a reduction in energy consumption with respect to the Dual Tank, electric, and the traditional solar domestic water heating systems. The Solar Side system was found to rely more heavily on electrical backup heaters, which was to be expected due to the lower volume of thermal storage in conjunction with a highly fluctuating heat source. The Solar Side system demonstrated a performance advantage in the summer, while the Dual Tank system's additional tank provided a performance advantage in the winter. With additional storage capacity, the Dual Tank system's superior performance in the winter months was expected. The Dual Tank's disadvantage in the summer requires more explanation and may relate to the thermal capacity of the float tank.

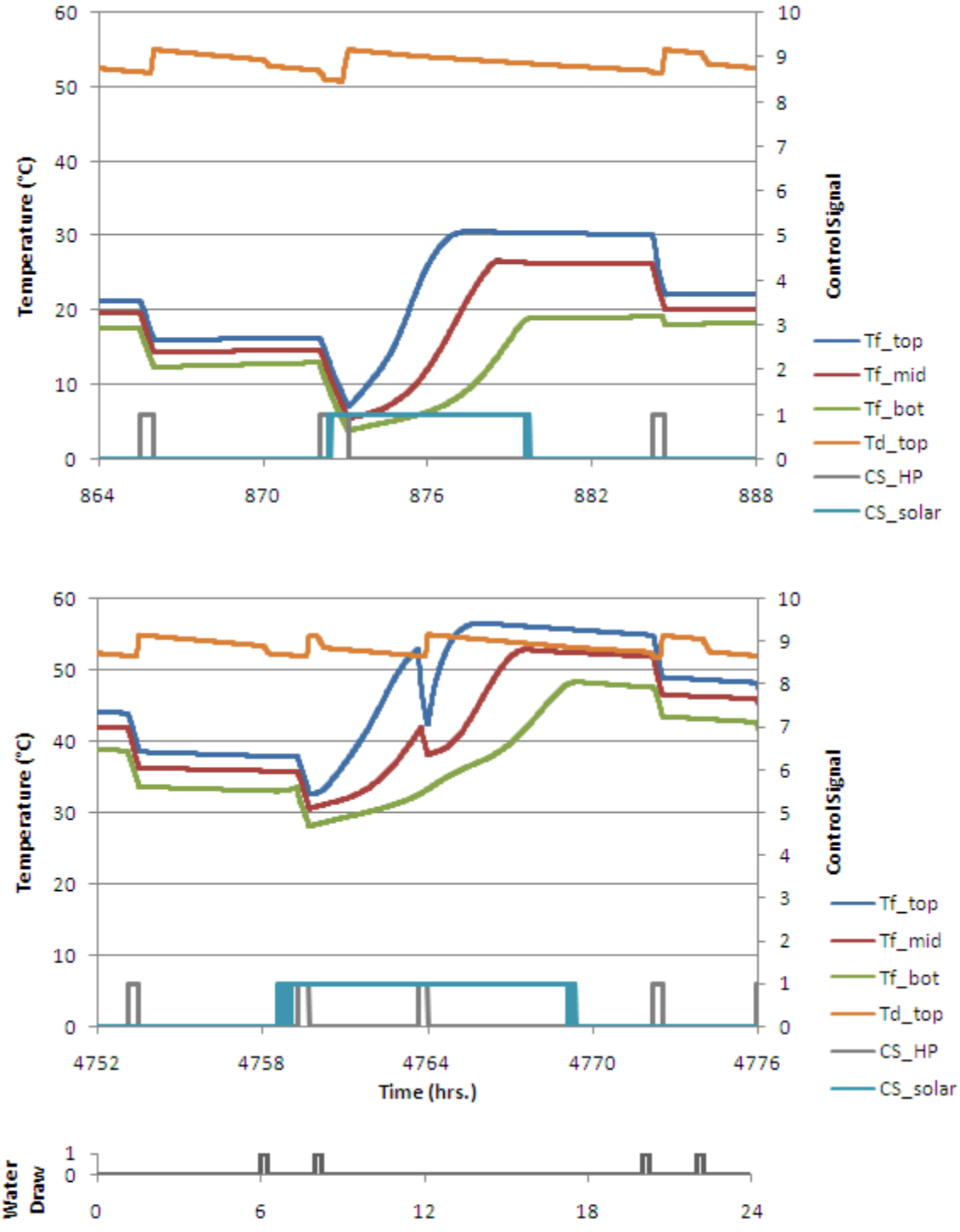

Figure 2.9 Dual Tank I-HPASDHW system operation on a typical February day (top) and a typical July day (bottom) reproduced from [17]

In order for the Dual Tank system to provide heat to the domestic hot water tank without requiring power input to the heat pump, the float tank must first be heated to a sufficiently high temperature. This introduces a capacitance effect to the system which may create an imbalance between energy supply and load demand, and possibly unnecessary use of the heat pump. This can be seen in Figure 2.9 where the heat pump runs in the middle of a summer day despite high levels of incident radiation. The heat pump is required since the float tank has insufficient temperature for the heat exchanger to be used. Although the time of operation on the typical July day for the heat pump in both the Solar Side and Dual Tank systems appears similar, one must remember that the heat pump for the Dual Tank system is substantially larger. Therefore, this system is consuming significantly more heat pump electricity than the Solar Side system. It is also worth noting that the temperature at the bottom of the float tank often exceeds the bottom temperature of the domestic tank, diminishing the potential collector efficiency. Further, the additional standby loss of the additional tank may contribute to the diminished summer performance in comparison on the single tank system.

Table 2.2 Summary of annual water heating system performance modified from [17]

System	Annual Electrical Consumption (MJ)	Solar Fraction
Electric DHW	20 070	0
Traditional SDHW	8 714	0.58
Dual Tank I-HPASDHW System	7 387	0.67
Solar Side I-HPASDHW System	6 524	0.66

The thesis concluded with several recommendations [17]. Each of the heat pump assisted solar domestic water heating systems should be investigated for a number of locations, possibly across the major cities of Canada. Due to the uncertainty in the simulations, prototype systems should be built and tested in order to verify the simulated performance. Lastly, since the systems are sensitive to the timing of load demand in the form of hot water draws, varying water draw profiles should also be investigated.

2.4 Summary of SAHP and HPASDHW Performance

The performance of SAHP systems is widely varying and is highly dependent on design and climatic conditions. In order for SAHP systems to obtain a significant share of the market, they must compete with combustible fuels, resistance heating, conventional SDHW, ground source heat pumps, air source heat pumps, and even gas engine driven heat pumps such as that presented in Lazzarin and Noro [35]. In Hepbasli and Kalinci [36], heat pump water heaters are reviewed, examining a wide variety of studies. For SAHP systems, Hepbasli and Kalinci [36] showed a range of collector efficiencies and heat

pump COP's found in literature. Collector efficiencies between 8% and 108% are presented, while the range of COP's is 1.7 to 6.

As is done in Hepbasli and Kalinci [36], it is common to reference a heating system's energy usage to electrical heating. It is clear that the efficiency of any heat pump system is tied to the COP. In Hepbasli and Kalinci [36], ground source heat pumps and air source heat pumps showed COP ranges of $1.656 - 3.307$ and $1.8 - 5.66$, respectively. These units can be compared to electric heating directly through their COP. However, direct comparisons are difficult with SAHP systems as they may contain a solar fraction. In Chandrashekar, Sullivan and Hollands [16], it was shown that solar assisted heat pumps result in lower energy consumption compared to heating by electricity and air source heat pumps. Solar fraction increased from 58% for conventional SDHW to approximately 67% for two I-HPASDHW systems based upon the simulations of Sterling [17]. In Huang and Lee [25], the SAHP system analyzed outperformed electrical resistance heating by three times, and conventional SDHW by two times in terms of energy consumption, however, these results are reported for a favourable climate.

Very few studies compare SAHP systems to fossil fuel heating. This is in part due to a difficulty competing with low gas prices and because it is generally accepted by renewable energy researchers that it is important to move away from fossil fuel heating in the future. However, if one imagines a 33% fuel-to-electrical efficiency in a highly fossil fuel based electrical grid like the United States, the SAHP in Huang and Lee [25] becomes comparable to gas heating in terms of fossil fuel consumption. This demonstrates the point made earlier, that the improvement in performance over electrical heating is mitigated by the inefficiency involved in electrical power generation. Though there must be a transition away from reliance on fossil fuels, it is important to remember the present link between electrical production and fossil fuels in many areas.

In terms of cost, with respect to resistance heating, the SAHP in Nuntaphan, Chansena and Kiatsiriroat [26] demonstrated a payback period of 2.3 years, where a DX-SAHP was analyzed in a favourable climate. Savings with respect to conventional SDHW are highly dependent on location. For example, in Freeman and Harrison [34], life-cycle costs of SAHP and SDHW units were found to be comparable for three Canadian cities, while showing moderate benefits for the SAHP for the remaining two cities. In Bridgeman and Harrison [32], it is suggested that the SAHP may be a good alternative to gas heating; however, no cost analyses have been provided to compare SAHP to gas heating. At this point in time, it appears that SAHP systems are not cost competitive with natural gas, a situation which may change significantly with time. It is important to note that using a HPASDHW system rather than a

SAHP system reduces the dependence on the heat pump, and is able to increase the solar fraction. The improvements of a HPASDHW system over a traditional SDHW system presented in Sterling [17] represent a promising opportunity as SDHW systems have already secured a portion of the water heating market.

In this thesis, the simulation of an I-HPASDHW system is investigated. The work by Sterling [17] focussed on comparative system simulations for competitive water heating systems, and this thesis is a continuation of that feasibility study. This thesis aims to establish the level of confidence with which such a water heating system may be simulated using the Transient System Simulation program TRNSYS. The most substantial factors affecting the accuracy of simulations are to be determined, highlighting the sensitivity of certain TRNSYS models. Finally, factors affecting the performance of I-HPASDHW systems are to be revealed including practical design concerns, component selection and control strategy.

Chapter 3 System Description and Experimental Test Unit

3.1 System Description and Design Intent

In this thesis, the system configuration presented in Figure 3.1 is of particular interest and is referred to as the Dual Side indirect heat pump assisted solar domestic hot water (I-HPASDHW) system. The system is comprised of the following major components:

- Solar collector
- Brazed plate heat exchanger
- Water-to-water heat pump
- Hot water buffering tank
- Hot water storage tank
- Two hot water circulation pumps
- Two diverter valves (zone valves)

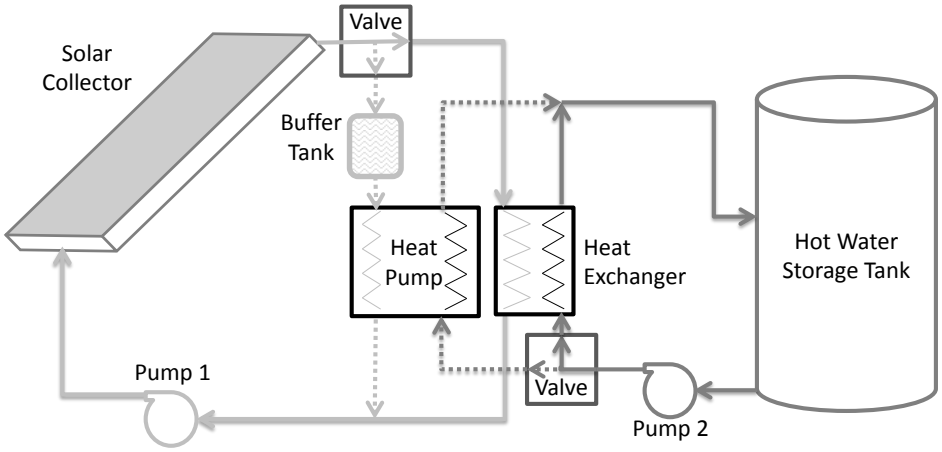

Figure 3.1 Heat pump assisted solar domestic water heating system (Dual Side I-HPASDHW)

The Dual Side I-HPASDHW system has evolved from the Solar Side I-HPASDHW investigated in Sterling [17]. Much like the Solar Side I-HPASDHW system, the Dual Side system has two primary running modes; namely, 1-Solar to heat exchanger (HX mode), and 2-Solar to heat pump (HP mode). In HX mode, the system operates in an identical manner to a traditional solar domestic hot water (SDHW) system. On the source side, solar energy is collected by circulating a heat transfer fluid through the loop. The diverter valve is in default position, sending fluid through the heat exchanger, see Figure 3.1. On the load side cold water is drawn from the bottom of the hot water storage tank, and again sent through the heat exchanger by the default valve position. Both mass flow rates are held constant and equal at $5\ kg/min$ in keeping recommendations for solar domestic hot water systems. In HP mode, the diverter valves switch position to direct flow through the heat pump. The hot water buffering tank ensures that

upon switching modes, the heat pump inlet temperature is held within its operating range. The hot water buffering tank also reduces heat pump cycling. The energized heat pump removes heat from the source side, and delivers heated water to the hot water storage tank. The flow rates in this mode are again held constant and equal; however, the flow rate in HP mode is $10.75\ kg/min$ and is governed by the required flow of the heat pump.

In order to improve the performance over the Solar Side system, the connections of the heat pump have been adjusted such that, in HP mode, heat transfer on the source side occurs through a singular heat exchanger. Eliminating a heat transfer path carries an inherent thermal benefit by achieving load temperatures closer to the heat pump's condensing temperature. An additional benefit of the Dual Side system comes from the fact that the heat pump provides net heat removal from the source loop. This is in contrast to the Solar Side system where the heat pump provides a net heat addition to the source loop. In operation, this means that the Dual Side I-HPASDHW system is able to draw the temperature of the source loop down thereby improving the efficiency of the solar collector. Despite the Dual Side system's performance advantage, the heat pump's net heat removal from a source loop with low thermal mass produces an inherent sensitivity to heat pump sizing, and complicates the control strategy.

3.2 Experimental Test Unit (ETU)

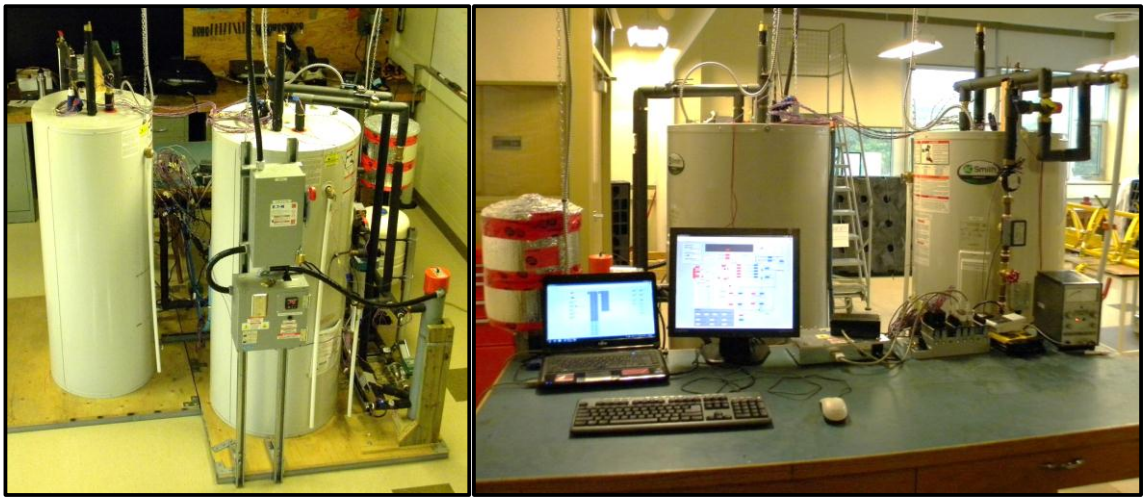

Figure 3.2 Experimental Test Unit for I-HPASDHW systems

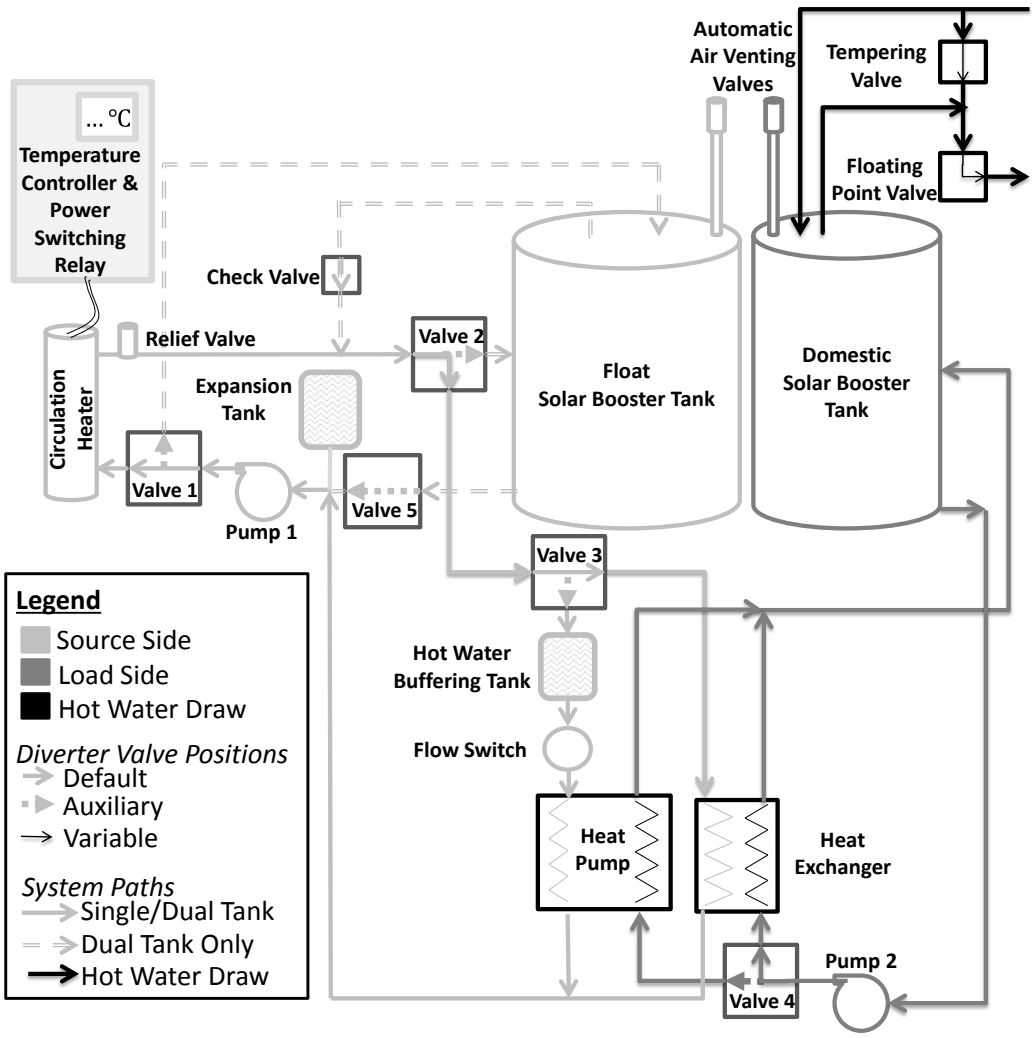

Figure 3.3 Experimental Test Unit schematic for I-HPASDHW systems

The Experimental Test Unit described herein, see Figure 3.2, has been designed to accommodate the experimental investigation of two I-HPASDHW systems. One such system is the single storage tank Dual Side I-HPASDHW shown in Figure 3.1, while the other system is equipped with an additional storage tank, and will be referred to as the Dual Tank I-HPASDHW system. The ETU was developed by William Wagar in conjunction with University of Waterloo PhD Candidate; Carsen Banister, where Mr. Banister is investigating the Dual Tank I-HPASDHW system. Construction of the ETU was led by William Wagar, and partners each contributed to the development of controls and automation of the test unit.

Table 3.1 ETU equipment specifications

Equipment	Make and Model	Size	Details
Circulation Heater	WATLOW CBEC27J10	6 [kW]	electric screw-plug heater
Temperature Controller	WATLOW EZ-ZONE PM6C1CJ-ARAAAAA	1/16 DIN	panel mount duty cycle heater control
Power Switching Relay – Solid State	ZPAC 600-40-DC-01	600 [VAC] 40 [A]	4-32 [V] DC switching (EZ-ZONE controller)
Domestic – Solar Booster Tank	AOSmith SUN 80 110	302.8 [L]	with 4.5 [kW] electric heater element
Float – Solar Booster Tank	AOSmith SUN 120 110	450.4 [L]	with 4.5 [kW] electric heater element
Hot Water Buffering Tank	Metlund Hot Shot 12-A502	4.5 [gal]	dual port buffering expansion tank
Heat Pump	Ecologix GX-W2W36	3.8 [kW]	water-to-water with R-134a refrigerant
Flow Switch	OMEGA FS303	3/4 [in]	Set-point range of 1.8-2.4 [GPM]
Heat Exchanger	Alfa-Biz SL15-25	44 [kW]	brazed plate (25 plate)
Circulation Pumps	TACO 008-VVSF6-IFC	1/25 [HP]	variable voltage variable speed control
3-way Electronic Valves	Dwyer Instruments 3ZV1032	3/4 [in]	14.5 [psi] close-off pressure
2-way Electronic Valve	Dwyer Instruments ZV1032	3/4 [in]	22 [psi] close-off pressure
2-way Floating Point Valve	Dwyer Instruments ZV20312	3/4 [in]	43 [psi] close-off pressure
Check Valve	WATTS 376372	3/4 [in]	brass body C_v = 11.5
Automatic Air Vent Valve	WATTS FV-4M1	3/4 [in]	acts as air purge and anti-vacuum device
Self-Closing T&P Safety Relief Valve	WATTS LL100XL	¾ [in]	pressure relief for circulation heater
Tempering Valve	WATTS LF1170MZ-US	3/4 [in]	accurate within ± [1.7°C]
Expansion Tank	WATTS PLT-20	8.5 [gal] tank volume	3.4 [gal] acceptance at 20 [psi] pre-charge

3.2.1 Hot Water Storage

The ETU is anchored by two residential electric solar booster water heaters. In this application each tank is placed in a closed loop. The hot water storage tank common to both systems is intended to double as the household's domestic hot water storage tank, and is therefore referred to as the domestic hot water (DHW) tank. The DHW tank is the smaller of the tanks at $302.8\ L$, where approximately $300\ L$

of capacity is a typical size for a SDHW storage tank. The larger $450.4\ L$ tank is used only by the two tank system, and is intended to float up and down in temperature. The Float tank acts as a heat source in poor solar conditions, and is charged with solar energy as a load when the demands of the DHW tank are satisfied. For a real world installed system, the entire source side of the system, including the Float tank, would be filled with a water-glycol mixture in order to handle sub-zero source temperatures. Due to limitations of the laboratory, the Experimental Test Unit uses only water as a heat transfer fluid.

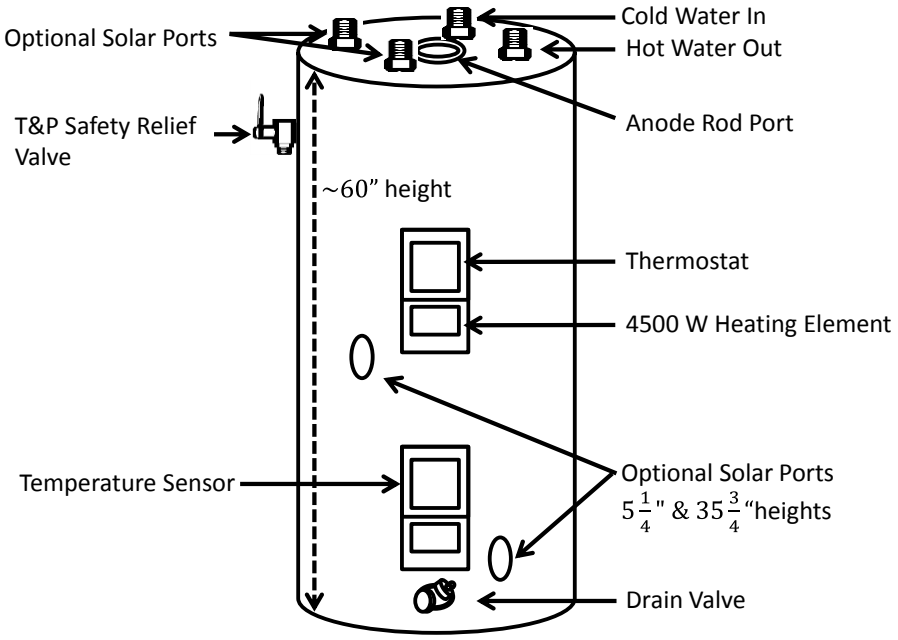

Figure 3.4 Residential electric solar booster water heater diagram: adapted from [37]

The particular tank models used were selected for the following features:

- 2" thick R16 foam insulation for low standby heat losses
- Additional connection ports for installation of temperature probes and air purge valves
- Single $4500\ W$ element capable of maintaining hot water recovery at 21 gallons per hour
- Selective electrical element placement in the upper half of the tank, maintaining cold water at the bottom of the tank

Figure 3.5 Flow diffuser for DHW tank solar return port

As discussed in Section 2.2.2, maintaining thermal stratification in solar hot water storage tanks is important for effective solar energy collection. Since the heat pump requires a flow rate that would be considered very high for a SDHW system, and high flow rates result in an inlet jet that is damaging to thermal stratification, a diffuser was installed in the DHW tank return port, Figure 3.5. The installed diffuser reduces exit velocity by 3.5 times, distributes the entrance flow, and attempts to force flow to exit with a horizontal velocity, all in an effort to prevent destratification. The diffuser alone may not successfully deal with the issue of thermal plume. However, installing the diffuser such that water enters horizontally and mid-way up the tank is in an effort to discourage mixing. The configuration is intended to allow the inlet water to find the matching density level within the tank.

3.2.2 Zone Valves

In order to alter flow paths of fluid in the Experimental Test Unit, both 2-way and 3-way diverter valves are used. By opening or closing the appropriate valves, the two operating modes of the Dual Side system are achieved, and additional modes may also be achieved to simulate the Dual Tank system. The available system modes are presented in Table 3.2, showing the valve conditions for each mode. Note that when a valve is switched on, it is actuated away from its default position. Valves $1-4$ are 3-way diverter valves, while valve 5 is a 2-way valve to simply open or close off a given flow path. Valve positions from Table 3.2 can be used along with Figure 3.3 in order to follow the flow path of each mode. For the simulation of the Dual Side I-HPASDHW system, only modes: $0, 1, 2$, and 6 are applicable. In these modes, the source loop is heated in order to simulate a solar input, and source heat is transferred to load heat through either a heat exchanger or heat pump. It may be noted that flow paths are also controlled by a check valve plumbed into one of the float tank branches.

Table 3.2 Operating modes for the I-HPASDHW ETU

Mode	Mode Name	Valve Positions	Powered Equipment
0	Everything OFF	Valves ON: None	None
1	Solar to HX	Valves ON: None	Circulation heater, circulation pumps
2	Solar to HP	Valves ON: 3, 4	Circulation heater, heat pump, circulation pumps
3*	Solar to Float	Valves ON: 2, 5	Circulation heater, circulation pump 1
4*	Float to HX	Valves ON: 1	Circulation pumps
5*	Float to HP	Valves ON: 1, 3, 4	Heat pump, circulation pumps
6	HP Warm-up	Valves ON: 3, 4	Circulation heater, circulation pump 1

For the specified three-way zone valves, fluid must be supplied from the bottom port. Each zone valve is actuated by an AC motor and maintains a default position using a return spring. The motor, or spring forces a rubber paddle to seat on the left or right port, providing flow to only one port at a time.

The particular model was selected for its quick acting characteristic with an opening and closing time of 11 and 5 seconds, respectively.

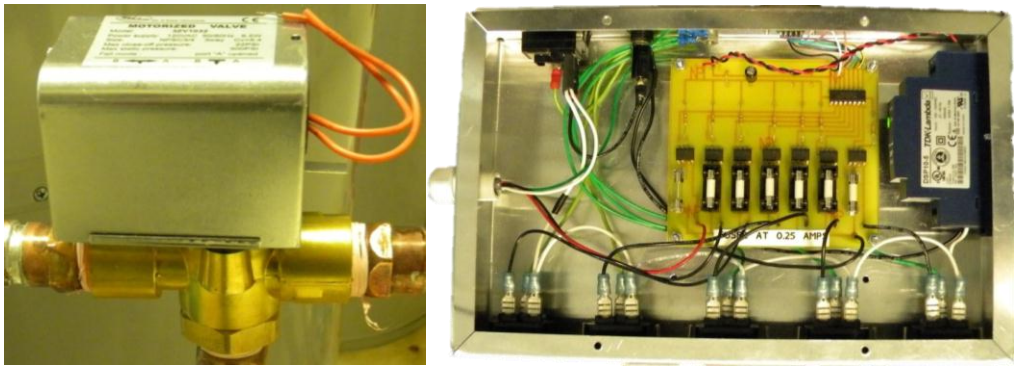

Figure 3.6 Three way zone valve (left) and electronic valve control box (right)

All controls for the ETU are programmed using LabVIEW virtual instruments (VIs) and with the exception of the Circulation heater signalling, control signals are actuated through a National Instruments data acquisition (DAQ) module. The control of each zone valve is facilitated by the electronic valve control box. This box receives a digital $5\ V$ transistor-transistor logic (TTL) standard signal from the DAQ, triggering the corresponding relay for $115\ V\ AC$ power switching.

3.2.3 Fluid Flow Systems

Source and load water circulation for the ETU is provided by two identical hot water cartridge circulator pumps. These pumps are variable voltage, variable speed pumps (VSPs) capable of handling temperatures up to 110 ℃. The TACO 00-VV hot water circulators were selected in order to supply both the high flow rate required by the heat pump and the lower flow rate desired for traditional solar collection. The pump speed is controlled by sending a $0 - 18\ mA$ current signal from the DAQ. Across the control terminals on each pump, a $560\ \Omega$ resistor is added to produce a voltage signal $\approx 0 - 10\ V$. Feedback for pump controls is provided by liquid flow meter readings acquired through the DAQ. Although the circulation pumps are capable of producing the low flow rate desired for traditional solar collection, it was not possible to maintain a stable flow rate with such low flow resistance in each loop. To overcome this problem, flow restricting gate valves were added to the heat exchanger's exit branch on both source and load side loops. Tuning the gate valves substantially improves the flow stability at low flow rates.

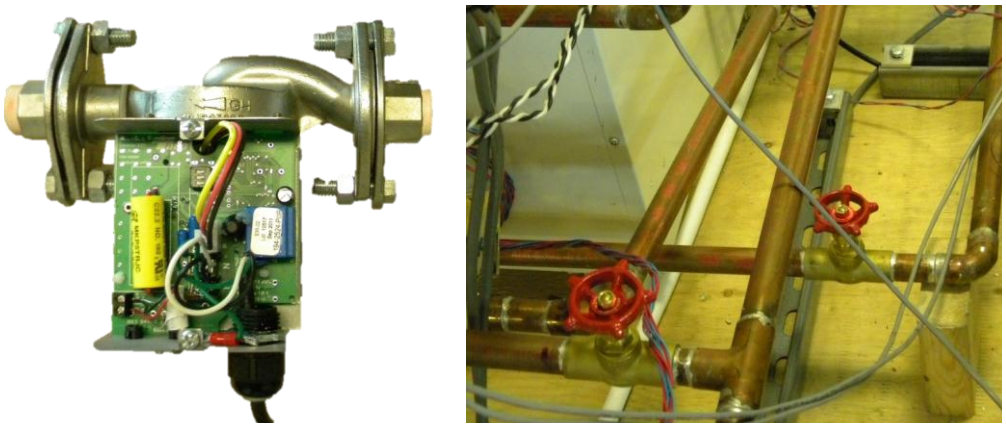

Figure 3.7 Hot water circulation pump (left) and heat exchanger flow tuning valves (right)

In order to simulate the consumption of hot water (hot water draw) as would be present in a household water heating system, an automated flow control system was devised. In an identical fashion to a residential hot water system, mains water is supplied to the bottom of the hot water tank, and the hot water line draws from the top of the tank. The cold mains inlet pressurizes the entire tank to a mains pressure, usually around $40\ psi$. The hot water exit of the tank in a household is held closed by valves at the taps. To simulate the taps for the consumption of hot water, the ETU is equipped with a 2-way floating point electronic valve. This valve is able to hold back mains pressure and close off the hot water line in stand-by condition. When the valve opens, mains water pushes hot water out of the system to simulate a hot water draw.

Figure 3.8 Floating point electronic valve with gate valve for simulated hot water draw

Unlike the zone valves previously described, the floating point valve has no spring return. Rather, it is opened by directing power in one direction to the AC motor, and closed by redirecting the supply power. When the valve is unpowered it remains in the last set position. The floating point action

of the valve allows for control of the hot water flow rate out of the domestic tank. As with the source and load circulation systems, the hot water draw system uses a gate valve in order to tune the flow rate and provide better control to a desired flow rate.

3.2.4 Circulation Heater

The circulation heater plays an important role in the ETU, namely, it is responsible for the simulation of a solar heat input. The electrical circulation heater mimics the heat input of a solar thermal panel, and can be controlled to heat water at variable power levels between 0 and the maximum capacity. The WATLOW CBEC27J10 has a rated capacity of $6\ kW$ at $240\ V$; however, due to a $208\ V$ supply voltage and potential thermal losses, the deliverable capacity is about $4.2\ kW$ of heat. The reduced heating capacity of the circulation heater means that the heater can simulate $4\ m^2$ of solar collector area for most days but may not have the capacity to simulate $4\ m^2$ of collector area when the solar irradiation significantly exceeds $1000\ W/m^2$.

Figure 3.9 Circulation heater and power switching electronics box

The power output of the heater is controlled through a duty cycle, where the circuit may be switched on and off several times per second. This power switching is accomplished by interrupting just one branch of the circuit using the ZPAC solid state power switching relay. The timing of the duty cycle is managed by the WATLOW EZ-ZONE digital temperature controller. The digital temperature controller receives a control signal from LabVIEW through USB-485 serial communications. Ideally the digital temperature controller would simply receive a set-point temperature, referred to as closed loop control. Unfortunately closed loop settings were not adequate to maintain reliable control as the heating loop experienced drastic overshoot and undershoot. Instead, the controller was configured using a piece of software called EZ-ZONE Configurator to implement open loop control. Open loop control requires a

power set-point $(0 - 100\%)$ supplied through LabVIEW. Feedback control of the temperature or thermal power output in open loop control is managed by a custom programmed LabVIEW virtual instrument. The heater control VI has two main settings, the first of which is an output temperature based control used to hold steady temperatures for equipment characterization. The second setting controls the power delivered to the water for the simulation of a solar hot water panel.

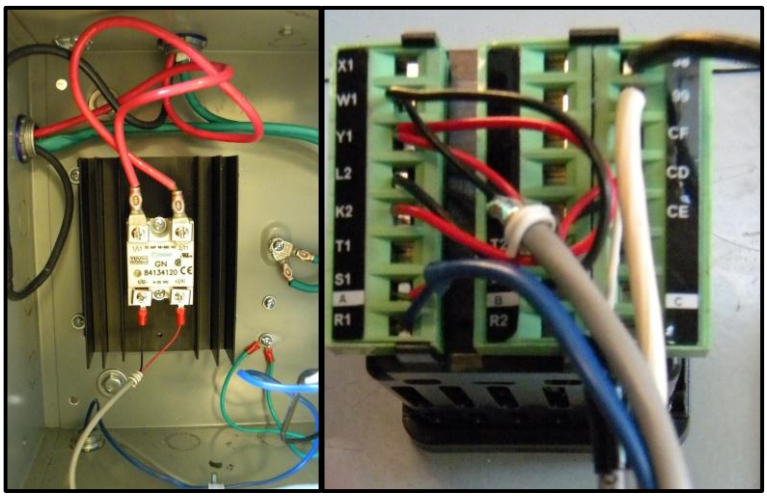

Figure 3.10 Power switching relay (left) and digital temperature controller (right)

With a powerful heater integrated into the ETU, over-temperature protection is a serious concern. In order to monitor the process temperature of the circulation heater, a dual measurement temperature probe is threaded into the top of the heater, see Figure 3.11. One of the process temperature readings is reported to LabVIEW controls, while the second reading is reported to the digital temperature controller. The first line of defence in terms of over-temperature protection is coded into the LabVIEW heater control VI. The VI monitors the process temperature, and automatically turns the heater off if the measurement lies outside the following range: $-5℃ < T_p < 90℃$. The upper limit keeps water from boiling, while the lower limit is in place to protect against thermocouple failure. When a type T thermocouple fails by a loss of electrical connection it reports a very large negative number. Since the control includes a lower temperature limit, the heater would be shut down in the event of a thermocouple failure. In addition to monitoring the process temperature, the heater control VI will also disable the heater if the measured flow rate of water is too low or if the valves are not in an appropriate position for the heater to run.

The next layer of over-temperature protection lies within the EZ-ZONE temperature controller. Since the controller is facilitating open loop control for the ETU, its automatic over-temperature

protection is not available. However, the controller is equipped with a mechanical relay output that is intended to operate an audible alarm. With this output available, the controller was configured to close the mechanical relay when the process temperature lies outside of the same temperature range used in LabVIEW: $-5℃ < T_p < 90℃$. The temperature controller's mechanical relay (terminals L2 and K2) was connected in parallel to the signalling wires (terminals W1 and Y1) that run from the digital temperature controller Figure 3.10 (right) to the power switching relay shown in Figure 3.10 (left). This means that in the event of equipment or software failure that negates the LabVIEW protection, the EZ-ZONE controller will disable the heater once the process temperature is outside of the desired range. When the digital temperature controller reads an out of range temperature, the mechanical alarm relay is closed, thereby short-circuiting the control signal sent to the solid state power switching relay. This action disables the solid state relay, leaving it in the closed position. Lastly, in the event of a complete control failure, for instance if the power switching relay were affixed in the ON position, a backup temperature and pressure (T&P) safety relief valve is in place to provide mechanical protection, see Figure 3.11.

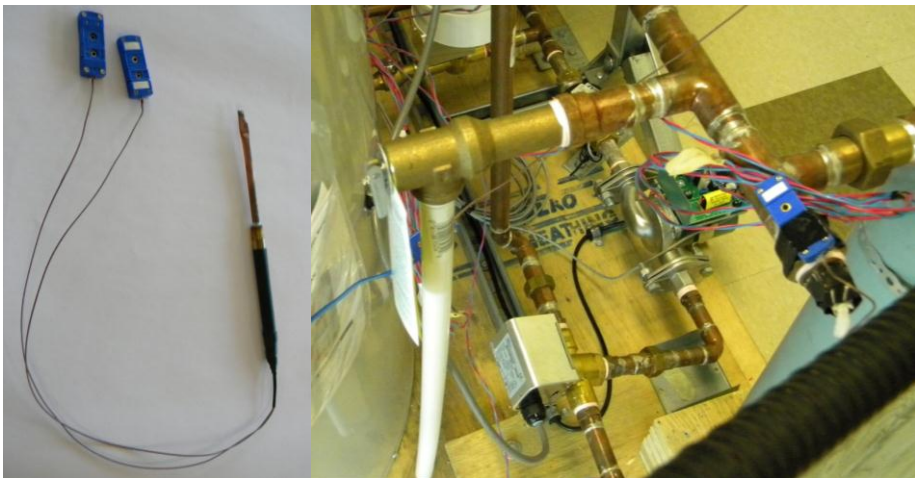

Figure 3.11 Circulation heater dual measurement temperature probe (left) and T&P safety relief valve

3.2.5 Heat Transfer Devices

The HPASDHW test unit comprises two devices used to transfer heat from the source to the load side of the system. A heat exchanger is used to move heat from source to load when there is sufficient solar irradiation. When it is necessary to enhance the heat transfer from source to load, a liquid to liquid, or more specifically in this case a water-to-water heat pump is used.

The selected heat exchanger is a brazed plate heat exchanger intended for use in solar thermal systems with as many as 8 solar collectors. The SL15-25 is made of stainless steel with copper brazing

and has a rated capacity of $44\ kW$ at $15\ USGPM$ with a 60℃ temperature difference. In an effort to eliminate the interaction between the heat exchanger and the environment, the heat exchanger was sealed in a box constructed from R5 rigid foam insulation.

Figure 3.12 Heat exchanger with insulation (left) and installation (right)

The GX-W2W36 is a water-to-water non-reversing HP built at Ecologix Heating Technologies Inc. This HP was custom built since no pre-packaged model was readily available in the desired capacity range. The heat pump was designed with a ZR16K4E-PFV scroll compressor, using a R134a refrigerant. The compressor gives the HP approximately $1\ ton$ of refrigeration capacity at rated conditions and suitable performance at expected system temperatures with a rated coefficient of performance (COP) between 3 and 5. The heat pump contains two coaxial refrigerant-to-water heat exchangers making up the evaporator and condenser. These heat exchangers are oversized (nominally $1.5\ ton$) to provide flexibility for source and load flow rates, as well as improve the temperature lift of the heat pump. The heat pump is also equipped with a desuperheater for future consideration which hasn't been plumbed into the ETU. Refrigerant flow is metered by a thermal expansion valve, which adjusts the refrigeration cycle based upon incoming temperatures.

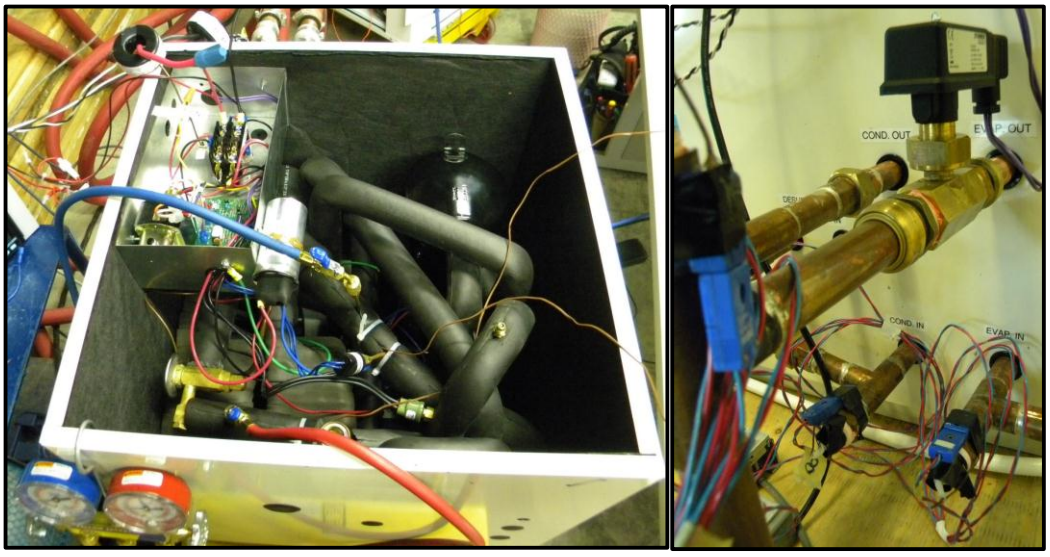

Figure 3.13 Heat pump charging and testing at Ecologix (left) installation and flow switch (right)

Switching the heat pump on and off is accomplished using a TTL based solid state relay, which can open or close the HP's $24\ V$ control circuit. This control circuit then operates a power switching mechanical relay. The unit is equipped with a short cycling delay which locks the compressor out for 5 minutes when the heat pump is switched off as well as upon initial power up. High and low pressure switches lock out the compressor when the inlet temperatures stray from the HP's operating range. The high pressure switch also acts as low flow protection for the load side of the heat pump, where heat will build up in the condenser and lock out the compressor if a loss of flow is experienced. On the source side of the heat pump, low flow and freezing protection is provided by a flow switch. Under low flow conditions (below $1.8 - 2.4\ GPM$), the flow switch breaks the HP's $24\ V$ control circuit, thereby shutting the HP down. This also protects against freezing in the evaporator since a buildup of ice will restrict flow through the evaporator.

3.2.6 Hydronic Accessories

Several hydronic accessories play an important role in the operation of the ETU. On the source side of the ETU, a closed system is formed. Therefore, an expansion tank is necessary to accommodate the thermal expansion of water in the system. The expansion tank was plumbed into the system before the pump such that it is not affected by changes in pump head. The closed system formed on the source side of the system also necessitates the use of an automatic air venting valve. Since the load side of the system may be closed off periodically by the hot water draw valve, an identical air vent valve was installed on the domestic tank. The air vent valves were placed at the highest point in each system atop

a stack plumbed into each tank. Air venting valves eliminate air from the system as it emerges over time from pockets trapped during the fill process, and simplifies filling and draining of the system. This allows for proper flow and pumping in the system.

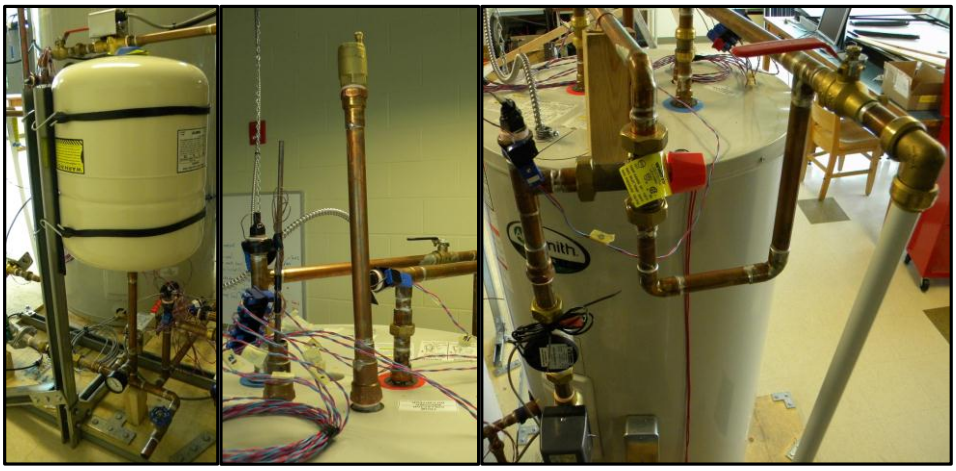

Figure 3.14 Expansion tank (left) air venting valve (middle) and tempering valve (right)

In order to provide a consistent and acceptable hot water delivery temperature to simulate a household's hot water consumption, a thermostatic mixing valve is used. This valve tempers the system's hot water output by mixing it with the appropriate amount of cold inlet water. The LF1170MZ-US hot water temperature control valve was selected for its $\pm$ 1.7℃ accuracy. The $\pm$ 1.7℃ accuracy is in accordance with section 8.7.6.2 of the Canadian Standards Association (CSA) standard for packaged solar domestic hot water systems [38]. The standard requires that tests on solar domestic hot water systems use a tempering valve capable of achieving an output temperature of $55℃ \pm 2℃$.

On the source side of the system, a hot water buffering tank is required in the heat pump branch. When the system runs in HX mode, the source side of the system operates at elevated temperatures. When switching to HP mode, water at elevated temperatures must be buffered to allow proper operation of the heat pump. To accomplish this, a dual port expansion tank, which is designed for cold water buffering in on-demand systems, is installed. In addition to the buffering effect provided, the tank dramatically increases the volume of water in the heat pump branch, and therefore extends heat pump run times and reduces equipment cycling.

Figure 3.15 Hot water buffering tank in heat pump inlet branch

3.2.7 Instrumentation

In order to monitor, control and evaluate the performance of ETU components as well as the system as a whole, the unit has been highly instrumented including 32 points of temperature measurement. Instrumentation for the ETU was selected using the requirements of the CSA standard for packaged solar domestic hot water systems as a guideline [38]. For uncertainty of calculations based upon the uncertainty introduced by instrumentation, see Appendix B.

Table 3.3 Instrument specifications

Instrument	Make and Model	Measured Parameter	Resolution	Accuracy	Range
Type T Thermocouples	Omega TG-T-30-SLE	temperature	----	Calibrated to ± 0.1°C	-200 to 350 [°C]
Liquid Flow Meters	Omega FTB4607	flow rate	75.7 pulses per gallon	± 1.5% of flow from 1.1-11.0 [GPM]	0.22 to 20.0 [GPM]
Current Transducer	Magnelab SCT-0750-010 and -025	current	----	± 1% at 10-130% of rated current	0 to 10 [A] 0 to 25 [A]
Potential Voltage Transformer	Magnelab SPT-0375-300	voltage	----	± 1% at 10-130% of rated voltage	23 to 300 [V]

Temperature measurements are extremely important to evaluating the performance of system components. With the accuracy of temperature measurements being of high importance, temperature probes rather than surface mounted sensors were installed. Custom temperature probes were constructed using higher accuracy special limits of error (SLE) grade Type T thermocouple wire. Completed probes were then plumbed into the inlets and outlets of major system components and other key locations. A majority of the probes were constructed using copper tube and brass plug fittings, where the end of the copper tube was flattened, soldered, and crimped around the thermocouple tip.

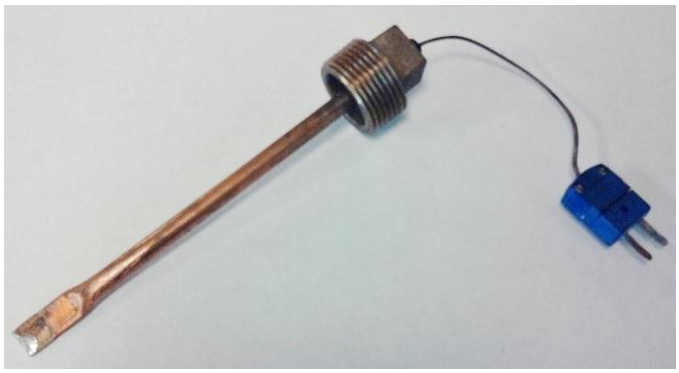

Figure 3.16 Custom temperature probe with type T thermocouple

In order to monitor tank temperatures, larger temperature probes constructed from $\frac{1}{2}in$ copper pipe were installed in each tank. These larger probes allow for 5 temperature measurements to be taken at locations evenly spaced vertically through the stagnation field of the storage tank. Thermocouples were mounted on the outside of insulating foam tape wrapped around a central steel rod, see Figure 3.17 (left). When the thermocouple lined rod is installed in the $\frac{1}{2}in$ copper pipe, the foam tape forces the sensor against the conductive wall of the temperature well.

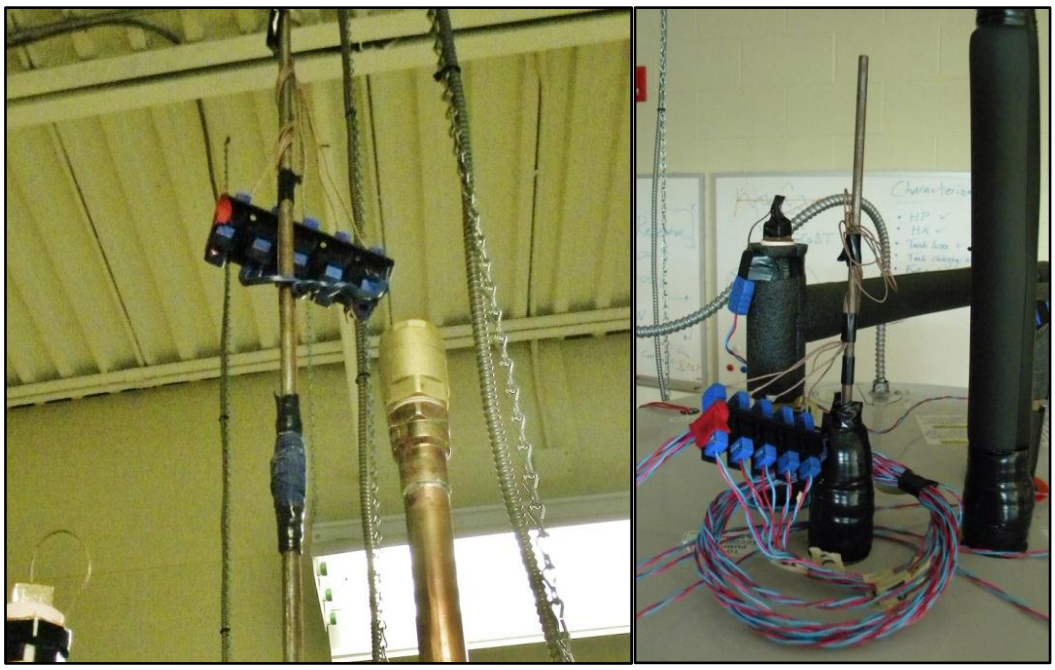

Figure 3.17 Thermocouple mounting (left) and installed temperature probe (right) for hot water storage tanks

For the purposes of control and calculation of heat transfer rates within the ETU, flow rate measurements are vital. Paddle-wheel style liquid flow meters recommended for both rate

measurements and flow totalization were selected. The paddle-wheel style flow meter produces an electrical switching action, and therefore a pulse output signal may be generated. In order to translate the flow meter's switching action to a TTL-standard pulse that can be read as a digital signal by the DAQ, additional circuitry was required. When the flow meter breaks the circuit, approximately $5\ V$ is sent to the DAQ. When the flow meter closes the circuit, the signal is shorted to ground and approximately $0\ V$ is sent to the DAQ. Each time the signal switches a pulse is counted. By tracking the frequency of pulses, and applying the $75.7\ \frac{pulse}{gallon}$ constant, a volume flow rate can be calculated. By considering a temperature-corrected density, volume flow rate can then be converted to a mass flow rate.

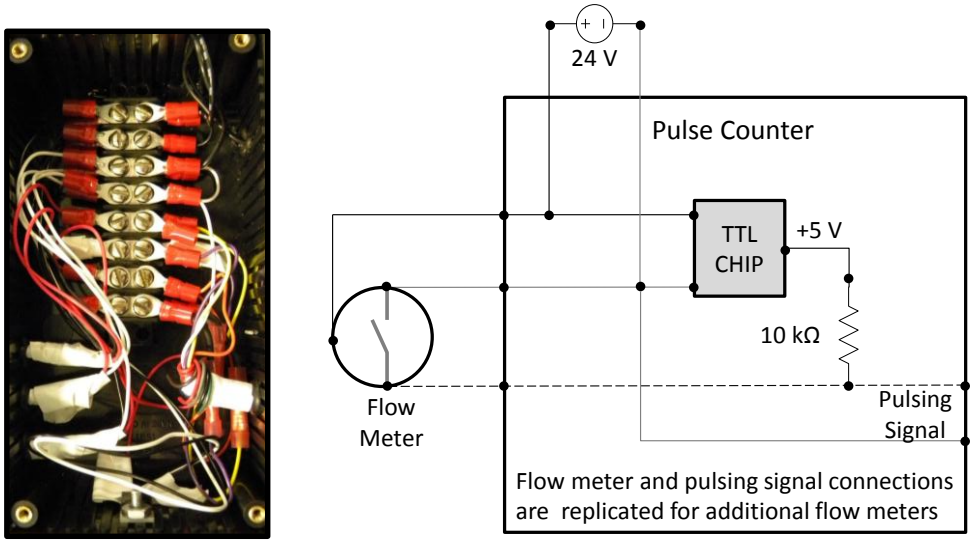

Figure 3.18 Circuitry (left) and wiring diagram (right) for metering flow

Since the total energy consumption of any HPASDHW system is a key to evaluating system performance, the ETU has been equipped with electrical power instrumentation. The most significant power consumptions may be measured in real time, namely the heat pump, and the domestic hot water tank's heating element. For each device a current and voltage measurement is taken in order to obtain a power value. In order to read the high currents and voltages of these devices through the DAQ, potential transformers and current sensors have been installed. Each of these electrical sensors provide a $\frac{1}{3}\ V$ signal to the DAQ at their rated inputs. Other power consumers such as valves and pumps can be considered separately. For example, the consumption of the diverting valves is known to be just $6.5\ W$ when energized. The pumping power may be measured and taken as a constant value for each flow condition.

Figure 3.19 Heat pump voltage transformer (left) and DHW tank current sensor (right)

3.2.8 Data Acquisition

For the control and characterization of the ETU, data is collected through wiring various components to a number of data acquisition modules. These modules are connected to a National Instruments Data Acquisition Chassis, see Table 3.4. Data is communicated through the chassis and transferred to a given virtual instrument through the DAQ Assistant in LabVIEW. To collect various data types, several custom virtual instruments have been built in LabVIEW for data collection.

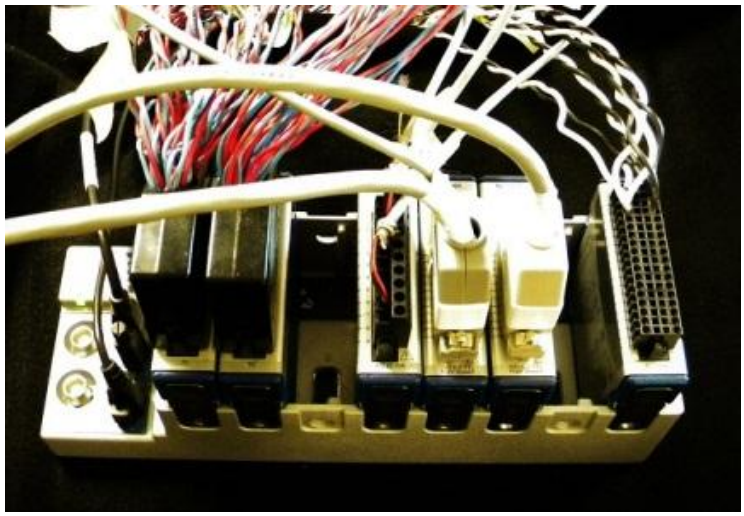

Figure 3.20 National Instrument modules (9213|9213|blank|9265|9401|9401|blank|9205) with chassis

Temperature readings are taken using two NI 9213 16-channel thermocouple specific modules with built-in cold-junction compensation. Digital communications are established through the NI 9401 module and are used to read flow meter pulses, signal zone valve actuation, and to signal heat pump operation. The digital module is capable of both sending and receiving digital signals, where the TTL

standard for digital communications is used. The NI 9205 analog input module was selected in order to read voltage and current sensors. The module is capable of reading $\pm 200\ mV, \pm 1\ V, \pm 5\ V$, and $\pm 10\ V$ signals with a $16\ bit$ resolution. Similarly, the NI 9265 analog output module was selected for variable speed pump controls. The analog output module produces $0 - 20\ mA$ signals and requires a $9 - 36\ V$ DC power supply.

Table 3.4 Data acquisition specifications

Device	Model	Quantity	Purpose
Chassis	NI cDAQ-9178	1	connect to multiple modules
Thermocouple Module	NI 9213	2	record temperatures
Digital IO Module	NI 9401	2	flow readings, valve and HP control
Analog Input Module	NI 9205	1	voltage and current readings
Analog Output Module	NI 9265	1	variable speed pump control

3.2.9 LabVIEW Controls

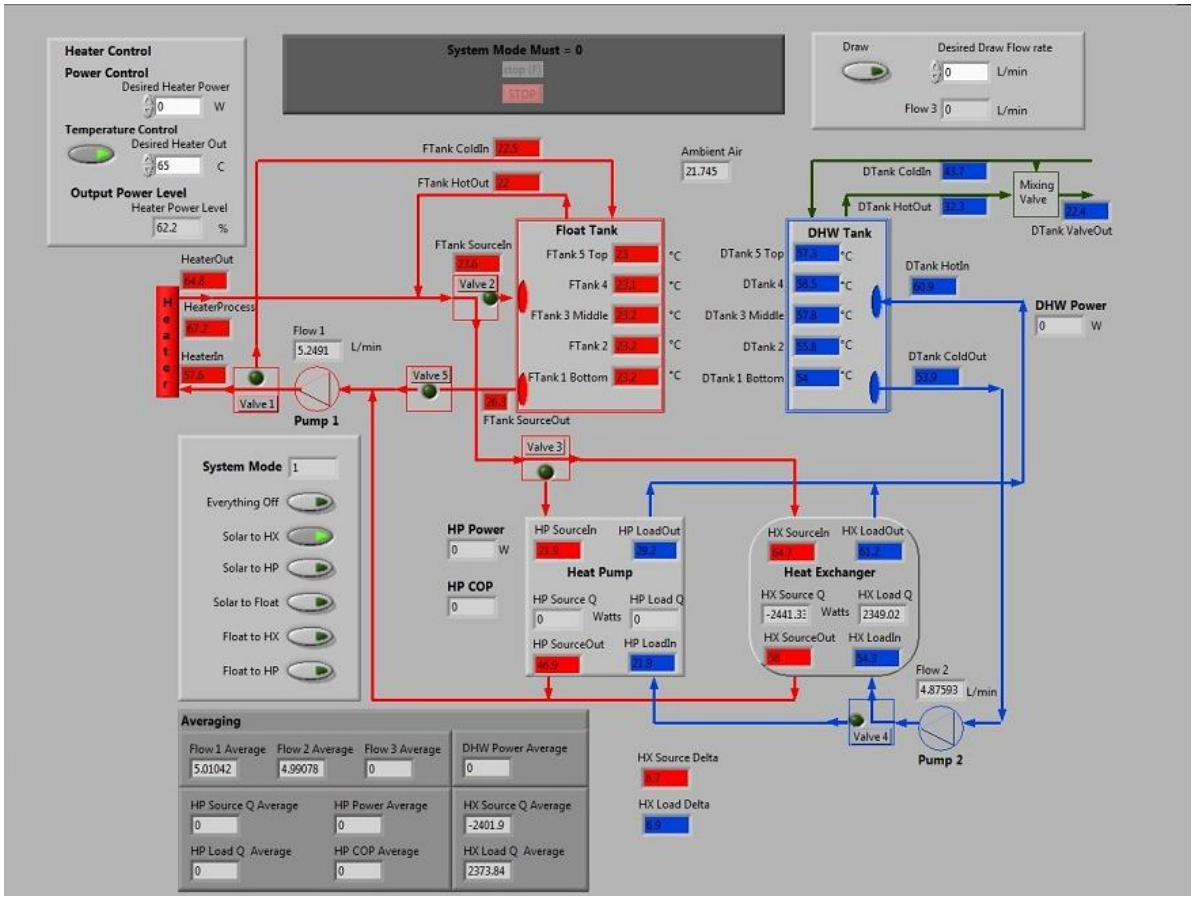

Figure 3.21 Experimental test unit schematic and LabVIEW Command Window

Control of the ETU is managed through a number of custom virtual instruments developed in LabVIEW. The controls are built in a hierarchy, where high level control, some averaging, and on-line display is executed through the Command Window. The Command Window is used to manually operate the ETU, and facilitates control through a number of lower level controls. Three of the panels on the Command Window allow for direct manual control of the system.

The system mode panel on the Command Window is used to accesses the Mode Control VI. This VI sets valve positions and desired pump flow rates based upon input from the Command Window. The draw panel in the top right corner also allows access to the Mode Control VI. Since the hot water draw is controlled using a floating point valve, the draw control is grouped together with the other valve controls.

The heater control panel allows access to the Heater Control VI. Two forms of control are available using the Heater Control VI. Control of the power delivered to the water is the default control mode, while a temperature set-point may also be specified. In all cases, the heater control ensures that proper valve positions, flow rates, and temperatures are present in order for the circulation heater to operate safely.

Global variables are used to communicate universally between virtual instruments running in parallel. Communications with the DAQ such as sending control signals and taking measurements are managed by a set of VIs that run in parallel with the Command Window. These control and measurement VIs are opened programmatically when the Command Window starts. The Command Window also exits or aborts lower level controls upon shut-down. However, with many important safety features being contained in lower level controls, aborting such programs must be done carefully. For example, when the Command Window is closed, it is vital that the heater power level first be set to 0. This is done by sequencing events in LabVIEW, including various time delays to allow actions to complete, and restricting commands under certain conditions.

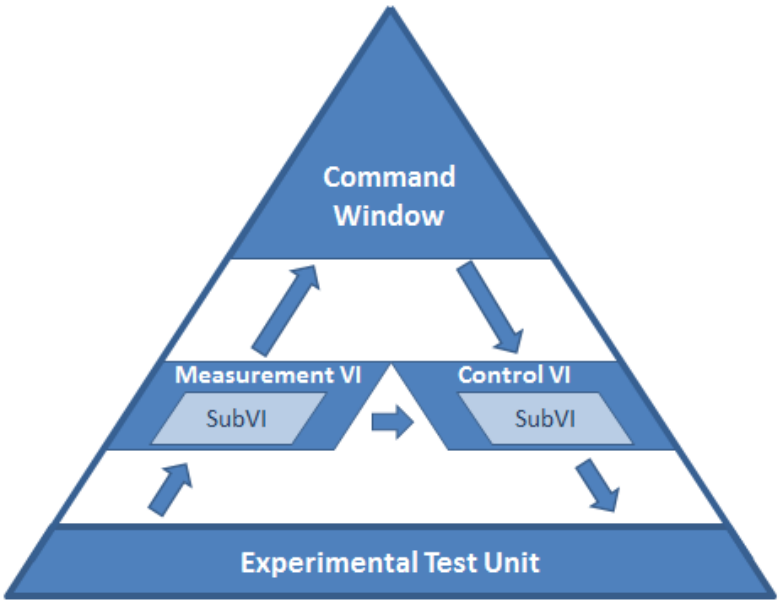

Figure 3.22 LabVIEW Virtual instrument hierarchy

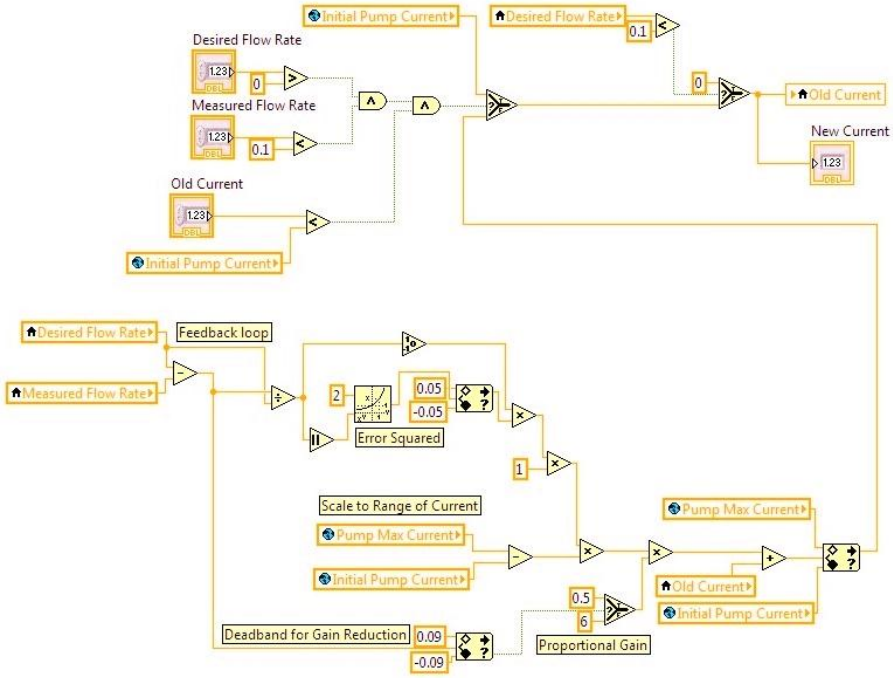

Figure 3.23 LabVIEW Pump controller SubVI

Repetitive calculations and control algorithms are managed through a set of lower level virtual instruments (SubVIs) which may be placed directly in the code of another virtual instrument. An example of a SubVI is shown in Figure 3.23. This virtual instrument generates a new pump control signal based upon the desired flow rate, the measured flow rate, and the previous control signal to the pump.

As a SubVI it is placed within the code of a larger virtual instrument, in this case, it is placed within the flow control VI that is responsible for signalling the circulation pumps. In Figure 3.23, the graphical nature of LabVIEW programming is shown.

In order to perform simulations, an additional high level control VI is necessary; namely the Simulator VI. This VI is used to feed inputs such as weather data and daily hot water draw profiles into LabVIEW from Microsoft Excel spreadsheets, control the system, and operate data recording VIs. Solar radiation inputs are used to provide delivered power set-points to the heater control. The Simulator VI includes a solar collector SubVI to account for collector efficiency. The solar collector model in LabVIEW was created to match the behaviour of the TRNSYS Quadratic Efficiency Collector with the exception of stagnation. The Simulator VI is then able to set system modes based upon a programmed control algorithm. The Simulator VI controls the ETU by programmatically operating the Command Window VI.

Chapter 4 I-HPASDHW Modelling in TRNSYS

4.1 TRNSYS Model Overview

TRNSYS is a transient system simulation program consisting of a simulation engine and an extensive library of mathematical models for various system components. Simulations are accomplished by iteratively solving sets of equations in discrete stages referred to as time steps. Each model reads updated input information for a given time step. The inputs are then used to determine outputs, and the process is repeated for the next time step. In TRNSYS, different types of variables are given different classifications. Parameters, for example, are variables that are supplied to each model, but are expected to remain constant throughout the entire simulation. Variables referred to as inputs are supplied to each model and are expected to change over time. Lastly, outputs are produced by each model and can be used as inputs to adjacent models. Some models, such as thermal storage components, require the simulation engine to solve differential equations, while others perform simpler manipulations [39].

Models are available for many applications ranging from renewable energy, buildings, heating, ventilation and air conditioning (HVAC), hydrogen, and other energy systems. TRNSYS also allows users to create their own custom models for new or novel components. In TRNSYS, models are distinguished with a Type, where a number is assigned to each Type and each model has a corresponding dynamic link library (DLL) file. Each model consists of a number of operations which are performed using inputs and parameters to produce outputs. TRNSYS simulations are performed in the user-friendly Simulation Studio, where a number of component Types may be connected to form desired systems. When model outputs are connected to corresponding inputs of other models, a complete set of equations and unknowns is formed. Inputs, outputs, and parameters for a given model are configured in the Simulation Studio through what is referred to as a performa, where each type of model placed in the simulation has its own performa. Global variables such as simulation start time, stop time, time-step, and tolerance are set through the Control Cards window [39].

In order to match simulations to the performance of the Experimental Test Unit, a variety of component models have been connected and configured in TRNSYS to form an equivalent system simulation. The system shown in Figure 4.1 represents the complete single tank system option provided by the Experimental Test Unit (ETU), and will be the focus of validation exercises. In order to simplify the validation of ETU performance, sub-systems of Figure 4.1 may be analyzed individually before the system is validated as a whole.

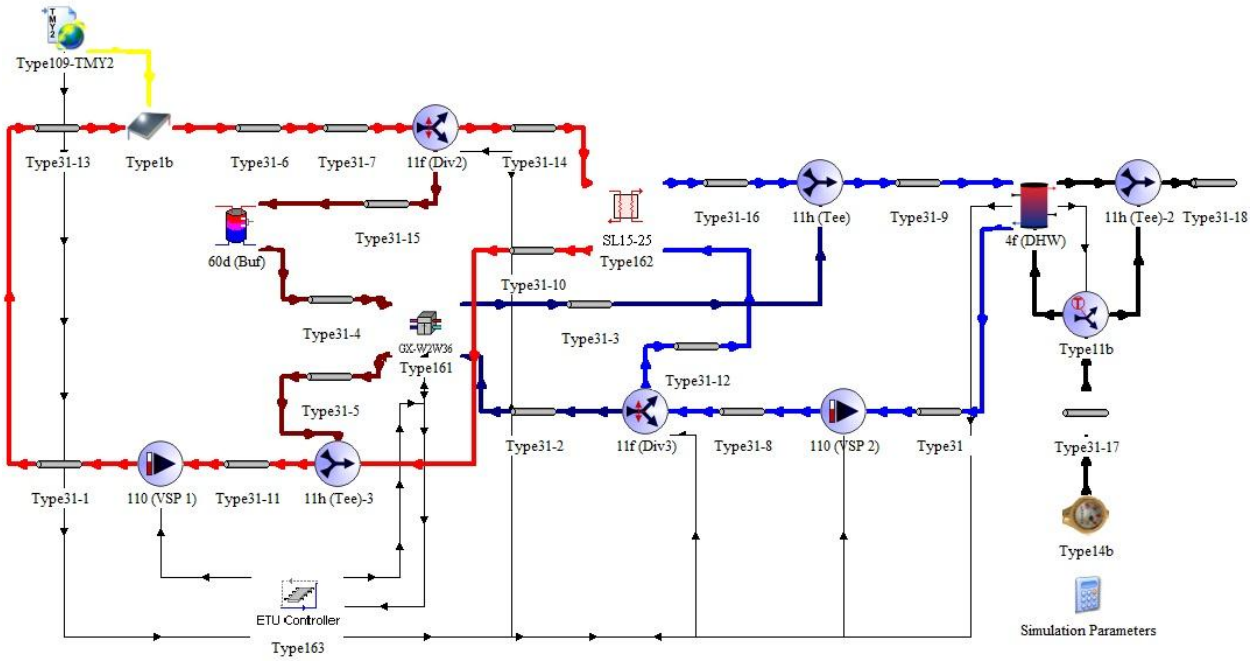

Figure 4.1 TRNSYS model for the Dual Side single tank I-HPASDHW system

The red loop to the left side of Figure 4.1 which encompasses the Type 1b solar collector component is the source side loop of the system. This loop is used to absorb solar energy and deliver it to one of two heat transfer devices, namely the heat exchanger or heat pump. Like the ETU, the heat exchanger is the default system path for the model. The source loop includes the solar collector, a variable speed pump, pipe components, as well as a flow diverter and mixer used to divert fluid for the operation of either the heat exchanger or the heat pump. The heat pump branch of the source loop also contains a buffer tank which is located prior to the heat pump source inlet.

The blue loop to the right side of Figure 4.1, which includes the second variable speed pump component (VSP 2), is responsible for delivering solar energy from the heat transfer devices to the stratified domestic hot water (DHW) tank. In addition to the tank and pump, this loop contains pipe models and flow diverters which are again used to divert the fluid path between heat exchanger and heat pump. Additional components connected to the DHW tank and positioned to the right of the system diagram are used to simulate hot water draws from the tank. Hot water draws are accomplished by using a forcing function, Type14b, to push cold water into the bottom of the tank and a mixing valve, Type11b, to temper the outlet fluid. This configuration simulates the opening and closing of taps for hot water draws in a household or on the Experimental Test Unit. In the TRNSYS model, cold water passes through the tempering valve prior to the domestic hot water tank. Although this does not match reality

and the ETU schematically, it is thermodynamically equivalent and is required by the Type11b routine. Note that output components used to gather, analyze, and export data are not shown in Figure 4.1.

Data from the ETU is collected at a time interval of 15 seconds. In order to read data from the experiment into the simulation, the simulation time step must be an integer division of 15 seconds. A variety of time steps have been investigated. The cumulative hot water draw was used to evaluate the effects introduced by the time step because it is not influenced by other factors in the system such as control decisions. After testing the cumulative draw at various time steps between the maximum of 15 seconds and a very small step of 1 second, a computational efficiency was found at a time step of 5 seconds. A 5 second time step is deemed acceptable since the resulting hot water draw deviates less than 1.5% of the desired hot water draw.

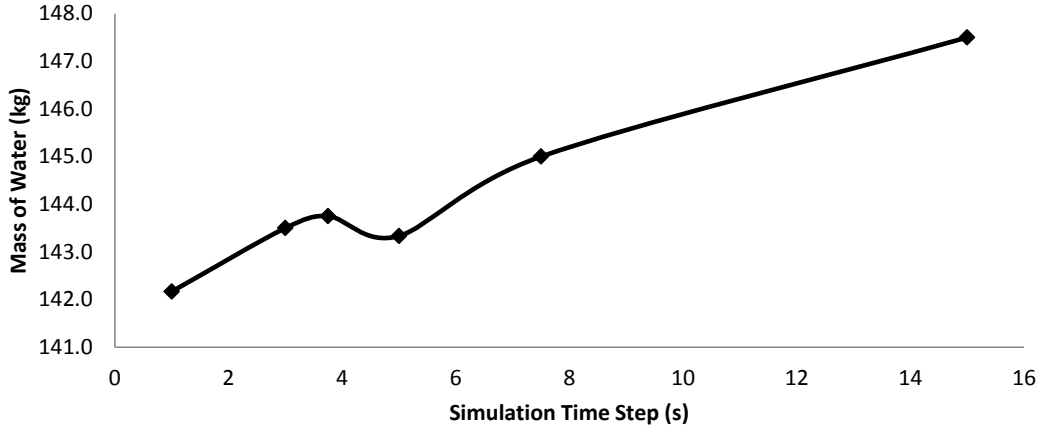

Figure 4.2 Cumulative hot water draw vs. simulation time step for TRNSYS simulation

4.2 TRNSYS Components and Calibration

Component models are described below along with important information used to match component performance to the Experimental Test Unit. Figure 4.1 shows the connection of TRNSYS components forming the system to be simulated. For the purposes of simulation, a number of built-in TRNSYS components were used. However, custom components were also created for improved accuracy and control flexibility. Characterization data used to create custom models or to tune built-in models can be found in Appendix A. For detailed information on built-in TRNSYS components, see University of Wisconsin - Solar Energy Laboratory [40]. For detailed information regarding custom TRNSYS components, full Fortran code may be found in Appendix C.

4.2.1 Type 1: Flat-Plate Collector (Quadratic Efficiency)

The Type 1 routine produces realistic solar thermal collector performance when subject to ambient conditions. In this simulation, optical mode 2 was used, which allowed the performance of the collector to be characterized by a quadratic efficiency curve. In optical mode 2, performance of the flat plate collector was modified with efficiency parameters and incident angle modifiers (IAMs). All of the necessary performance parameters were found in standardized solar collector tests such as those outlined by the Solar Rating & Certification Corporation (SRCC) OG-100 [41]. The Type 1 routine is capable of handling performance parameters specified based upon inlet, outlet or average collector temperature. For simulations featured in this thesis, efficiency parameters were based upon collector inlet temperature as is standard for North American solar collector testing. It is also important to note that efficiency parameters may also be based upon a number of differing area measurements for a given solar collector such as absorber area and gross collector area. The following equation was used to characterize solar collector efficiency [40]:

$$\eta = a_0 - a_1 \frac{(T - T_a)}{G_T} - a_2 \frac{(T - T_a)^2}{G_T} \tag{4.1}$$

Where:

η is the collector efficiency
G_T is the total incident radiation on a tilted surface
T_a is the ambient temperature
$T = T_{f,i}$ is the inlet fluid temperature supplied to the collector
a_0 is the efficiency intercept constant
a_1 is the efficiency slope constant
a_2 is the efficiency curvature constant

Incidence angle modification was used to account for off-normal performance with respect to the angle of incidence. Off-normal conditions strongly influence the optical efficiency of the collector ($\tau\alpha$), therefore, a modification ratio $\frac{(\tau\alpha)}{(\tau\alpha)_n}$ was required to account for the impact. An approximation is available for flat plate collectors relating the beam optical efficiency to the optical efficiency for normal incidence. Coefficients for the following equation are once again available from standard solar collector tests such as those produced by the SRCC [42]. The coefficients of the quadratic IAM Equation (4.2) are only valid within the range of $0 < \theta < 60$, where erratic results are produced by the model at greater incidence angles. Therefore, as suggested in University of Wisconsin – Solar Energy Laboratory [40], the linear approximation available in SRCC [42] was used and the second order constant b_1 was negated and set to a value of 0.

$$\frac{(\tau\alpha)_b}{(\tau\alpha)_n} = 1 - b_0\left(\frac{1}{cos\theta} - 1\right) - b_1\left(\frac{1}{cos\theta} - 1\right)^2 \quad (4.2)$$

Where:

$\tau\alpha$ is the optical efficiency of the collector
θ is the angle of incidence for beam radiation
b_0 is the first order IAM constant
b_1 is the second order IAM constant

Once IAM corrections are made, the Type 1 routine makes additional corrections for both off-rated collector flow rates and to account for multiple collectors placed in series. Both the flow rate and series corrections modify the overall collector heat removal efficiency factor. It may be noted that the flat plate collector model neglects the fluid capacitance of collector, and may therefore neglect transient collector behaviour in the transition from stagnation to steady flow conditions [40]. Although this does not match true solar collector performance, this influence should be short-lived in simulations and have a minimal energy impact. Collector stagnation effects also go unaccounted for in the operation of the circulation heater on the ETU since no heat can be supplied when the collector fluid is stagnant.

In the validation of the TRNSYS model, solar collector data for the Viessmann Vitosol 100-F flat plate collector was used. SRCC test data for the 100-F collector can be found from the SRCC [42]. Validation simulations were completed using a single 100-F collector with an area of $2.494\ m^2$.

Table 4.1 SRCC test results for Viessmann Vitosol 100-F Flat Plate Collector [42]

Parameter	Value	Unit	Notes
a_0	0.769	-	Test results are based upon: • Gross collector area: $2.494\ m^2$ • Inlet collector temperature • Working fluid: water • Flow rate: $3\ L/min$
a_1	3.614	$[W/m^2K]$	
a_2	0.01358	$[W/m^2K^2]$	
b_0	0.32	-	
b_1	0	-	

4.2.2 Type 4: Stratified Fluid Storage Tank

The Type 4 routine provides a model for stratified liquid storage tanks for sensible energy storage only. Storage tanks are modelled in discrete volume segments, with up to $N = 15$ elements of fully mixed uniform temperature, see Figure 4.3. Within this model, a number of user-selectable options are available. Inlet and outlet ports may be specified in default positions, fixed custom positions, and may even be modelled with the inclusion of a variable inlet valve to deliver fluid to the most appropriate tank element. The height of each volume element may be entered individually, allowing variable volume elements within the simulation.

The tank size was supplied to the model by entering a total volume, fluid properties, and the tank height which was found through the summation of element heights. Thermal loss properties were specified through heat loss coefficients, where an average tank loss coefficient was first specified and an incremental loss coefficient factor was available for each volume element. The model also included provisions for simulating two auxiliary heating elements, each with dead band temperature controls to mimic a standard hot water tank thermostat.

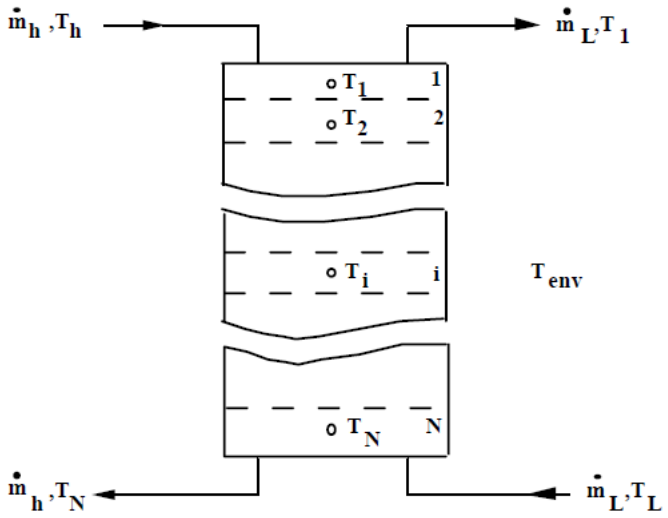

Figure 4.3 Type 4 stratified fluid storage tank [40]

Since solar collector performance is dependent on inlet temperature, system performance is sensitive to the level of stratification in the hot water storage tank, particularly the bottom tank temperature. Finding a reasonable match in stratification between the simulation and the ETU was therefore very important to matching the TRNSYS simulation to the ETU. Altering the stratification characteristics in the Type 4 model was accomplished by varying number and size of volume elements [40].

In a real stratified storage tank, thermal losses are not necessarily uniform. This is due to a number of thermal bridging components; inlet ports, outlet ports, drains, and relief valves. Incremental heat loss coefficients were therefore specified for each volume element to define element losses relative to the average tank loss coefficient. The loss coefficient for a given segment was calculated by the following equation. Note that all loss coefficients are negative values [40].

$$u_i = |u_m| + \Delta u_i \tag{4.3}$$

Where:

u_i is the loss coefficient calculated for the i^{th} volume element
u_m is the mean loss coefficient for the tank
Δu_i is the incremental loss coefficient for the i^{th} volume element to be specified by the user

The two electrical auxiliary heaters are available for use as the upper and lower element for an electric hot water storage tank, and may be controlled externally if desired. The thermostat controls function in one of two modes; independent or master-slave control. Independent control allows each thermostat to act without influence from the other. Master-slave operation enforces a condition that the lower element can only be active when the upper element is inactive [40].

Flow streams between volume levels in the hot water storage tank are the result of inlet and outlet flows to the tank. The impact of mass transfer on element temperature is characterized in the tank model by writing an energy balanced equation for each element in terms of temperature. This equation balances the change in element energy over time as a function of the incoming and outgoing flow streams. It is assumed that the positive flow direction is from low to high within the tank, an assumption which has been shown to be in accordance with experimental results [40].

Energy balance for the tank as a whole is characterized by a similar but more comprehensive differential energy balanced equation. This equation is solved by integration with respect to time. On the left side, the energy balanced equation is written in terms of temperature $M_i C_p \frac{dT_i}{dt}$. The right hand side of the equation includes terms for:

- Direct heat removal and addition by the load and source flows, respectively
- Heat loss to the environment
- Flow streams from adjacent nodes
- Heat addition from auxiliary heaters [40]

For the simulation of the ETU, the Type 4f model was most appropriate and was used to specify a tank with electrical backup heating and fixed user-specified inlet and outlet port positions. A ten-node tank model was found to provide an adequate match to the DHW tank installed on the ETU. The thermostat in the DHW tank of the ETU was found to respond to water entering the solar return inlet port. To account for this impact, the solar return port, DHW thermostat, and DHW element were all placed within node 5 of the DHW tank model.

Table 4.2 Overall and node-specific data for DHW tank model

Tank Parameter	Value	Unit	Notes
Number of nodes	10	-	Nodes in the lower half of the tank are larger in order to provide appropriate mixing levels in the model.
Volume	302.80	$[L]$	
Height	60.00	$[in]$	
Loss coefficient	-1.18	$[W/m^2K]$	
Element heating rate	3.1	$[kW]$	
Thermostat set-point	62.40	[°C]	
Thermostat dead band	5.90	[°C]	
Node #	**Height** $[in]$	**Incremental loss coefficient** $[W/m^2K]$	**Node contents**
1 (Top)	5.0	0.00	• Outlet port: to hot water load • T5 temperature sensor
2	5.0	0.00	
3	5.0	0.00	
4	5.0	0.00	• T4 temperature sensor
5	5.0	0.00	• DHW thermostat & element • Inlet port: solar return
6	7.0	0.00	• T3 temperature sensor
7	7.0	-0.48	
8	7.0	-0.755	• T2 temperature sensor
9	7.0	-0.755	• Inlet port: mains supply
10 (Bottom)	7.0	-1.03	• Outlet port: to solar • T1 temperature sensor

4.2.3 Type 11: Tee Piece, Flow Diverter, Flow Mixer, Tempering Valve

Type 11 is a flexible routine capable of modelling a number of common hydronic components including the following components used in the simulation of the ETU:

- 11h Tee Piece
- 11f Controlled Flow Diverter
- 11b Tempering valve

All of these modes of the Type 11 routine are intended for liquids such as water, where other modes are available for more complex fluids such as moist air [40]. The Type 11h Tee Piece completely mixes two inlet streams. It may be noted that one of the inlet conditions will often be a zero-flow condition. When this is true, Type 11h may be used in conjunction with a controlled flow diverting valve to switch between distinct fluid loops rather than operating in an analog fashion.

The Type 11f Controlled Flow Diverter receives one inlet stream, and diverts it between two possible outlets. The amount of fluid sent to each outlet is controlled by a user-specified proportional

signal between 0 and 1. In the TRNSYS simulation of the ETU, controlled flow diverters were used to completely switch flow streams from one exit to another. A control signal of 0 sent the entire stream of fluid to outlet 1, while a signal of 1 sent the entire stream to outlet 2 [40].

The Type 11b Tempering Valve model is similar to Type 11f, but differs from 11f in that the user must set a desired outlet control temperature. The proportion of flow to be sent to each outlet is then calculated by the model. As mentioned in Section 4.1, the simulated position of the tempering valve, B, is not schematically identical to a real tempering valve position A, see Figure 4.4. Although this model reliably simulates an ordinary tempering valve, for convenience of simulation the model requires it to be placed in position B [40].

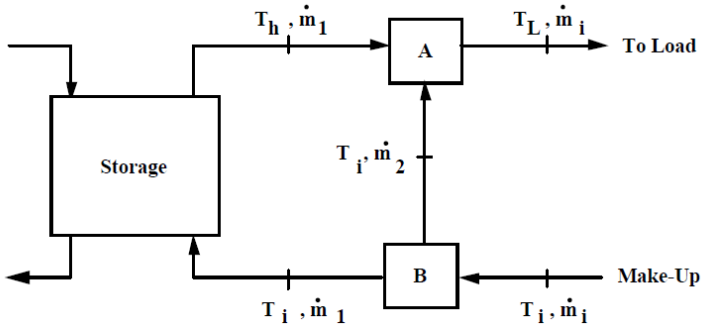

Figure 4.4 Schematic depicting TRNSYS tempering valve use [40]

4.2.4 Type 31: Pipe or Duct

This model allows for lengths of pipe to be added between components in the simulation and treats mass transfer as plug flow. Fluid within the pipe is modelled with uniform temperature segments with a maximum number of 25 segments per model. Outgoing segments of flow are forced out of the pipe by incoming segments. Along the axial direction of the pipe, heat transfer is neglected. Heat losses in the pipe model are accounted for similarly to those of the stratified hot water storage tank component. The energy change in each plug segment is accounted for by solving a differential energy balance equation. The energy balance is written in terms of temperature where the energy change of the fluid is expressed as $M_j C_p \frac{dT_j}{dt}$. The right hand side of the equation contains the convective heat transfer terms from the pipe [40].

In order to approximate the behaviour of the pipes used on the ETU, overall heat transfer coefficients for pipe components were determined by matching measured and simulated results. For ordinary pipe segments connecting ETU components, three different points on the ETU were brought to

a high temperature, then left to cool to room temperature. With the exception of pipe models used to add storage volume to the solar collector, and those used for the hot water draw, all other pipe models used in the simulation were given an overall loss coefficient to match the median result from the three-point experimental test. The pipe models used to add storage volume to the solar collector were meant to approximate the circulation heater on the ETU. Each pipe segment was placed in-line to the solar collector model, one on the inlet and one on the outlet, where each model represents half of the circulation heater's volume. The singular loss coefficient used in pipe models representing the circulation heater was determined with a further experimental test, allowing the circulation heater to cool over time. The comparison demonstrated in Figure 4.5 was the result of the cooling circulation heater being matched by a $5.5\ W/m^2K$ loss coefficient applied to the pipe model.

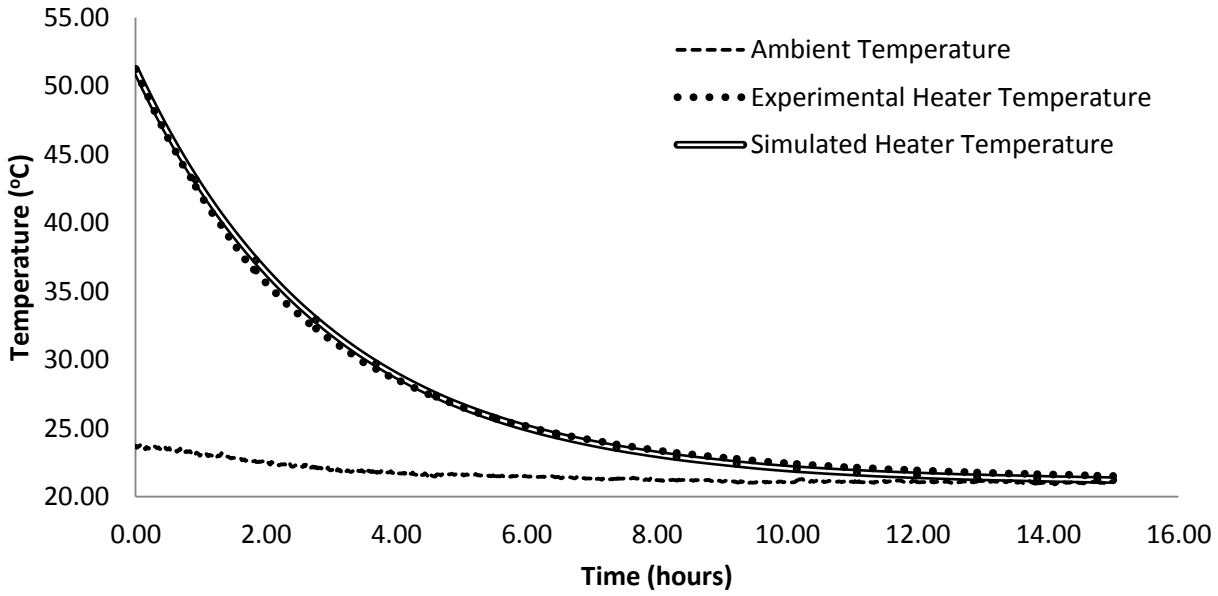

Figure 4.5 Calibrating circulation heater thermal loss coefficient

Table 4.3 Data for pipe models

Pipe Purpose	Loss Coefficient $[W/m^2K]$
Solar collector storage volume	5.5
Hot water draw connections	5.0
Equipment connections	0.075

4.2.5 Type 60: Stratified Fluid Storage Tank with Internal Heat Exchangers (Detailed)

The Type 60 routine is a more detailed version of the Type 4 stratified fluid storage routine. The Type 60 routine is intended to model sensible energy storage using water and provides a number of features for detailed simulations:

- Up to 100 fully mixed volume segments
- Equal or variable volume segments
- Incremental heat loss coefficients
- Fixed or variable inlet positions
- Internal submersed heat exchangers
- Non-circular cross-section
- Horizontal orientation
- Electric or gas auxiliary heating
- Temperature dead bands on thermostats [40]

The Type 60 routine differs from other TRNSYS component models with respect to its time step. Since the TRNSYS time step can influence tank models, the detailed fluid storage model includes an internal time step. The model calculates the critical Euler time step, and allows the user to select the fraction of this time step used in simulation. A fraction of $1/6$ is recommended for a balance between computational efficiency and accuracy [40].

In the simulation of the ETU, the Type 60d, vertical cylinder with one inlet and one outlet, was used to model the hot water buffering tank. The buffering tank was expected to act as a fully mixed tank as it had a relatively small volume, under $17\ L$, and processed a flow rate of approximately $10.75\ L/min$. For this reason, the detailed tank model was required in order to generate a single-node model to simulate a fully mixed tank.

Table 4.4 Data for detailed stratified storage tank model

Tank Parameter [Unit]	Value
Number of nodes	1
Volume $[gal]$	4.05
Height $[in]$	15
Inlet port height $[in]$	4
Outlet port height $[in]$	0
Loss coefficient $[W/m^2K]$	5.0

4.2.6 Type 110: Variable Speed Pump

The Type 110 routine provides the capacity to simulate a variable speed pump. The model generates a mass flow rate of fluid based upon a fixed maximum flow capacity and a specified linear control function between 0 and 1. The pump model does not include any transient behaviour upon start-up and shut-down. The default method of characterizing power consumption is through a direct linear proportion of the flow rate, where an option for defining a more complex correlation is provided. More complex flow-to-power correlations are defined using the following equation:

$$\dot{W}_p = \dot{W}_{p,max}[a_0 + a_1\gamma + \ldots + a_N\gamma^N] \quad (4.4)$$

Where:

$\dot{W}_p$ is the power consumption of the pump at a given condition
$\dot{W}_{p,max}$ is the maximum pump power
a is a set of coefficients used to relate flow rate to power consumption
γ is the pump control signal and the proportion of maximum flow rate for which the pump is operating
N is the number of coefficients required to explain pump behavior

It may be noted that at a 0 flow condition the power correlation may provide a non-zero pump power, however, the model enforces a pump power of 0 under this condition. Motor efficiency (wire-to-shaft), overall pumping efficiency (wire-to-water), and a motor heat loss factor are used to determine the quantity of pumping energy added to the fluid as heat [40].

In order to match pump performance in the model to results measured from the ETU, a custom linear power correlation was generated. This correlation was intended to match power consumption at the two fixed flow rates at which each pump on the ETU was set to operate. The motor heat loss fraction was taken as 1, which assumed that all pump energy losses are dissipated into the fluid as heat. This is a common assumption for pumps with liquid cooled motors. The overall pumping efficiency (wire-to-water), was found to be approximately 7% based upon measured consumption and theoretical fluid power calculations. The motor efficiency itself was assumed to be 25%, a value typical of motors in the $\frac{1}{25}\,hp$ range.

Table 4.5 Data for variable speed pump models

Parameter	Pump 1 $[W]$	Pump 2 $[W]$	Notes
$\dot{W}_{p,r}$	76.13	51.47	$\dot{W}_{p,r}$ and linear power coefficients are calibrated to match ETU performance at 300 kg/hr and 645 kg/hr
Parameter	**Pump 1**	**Pump 2**	
a_0	0.2322	0.7288	
a_1	0.7678	0.2712	

4.2.7 Simulation Tools

4.2.7.1 Type 9: Data Reader (Generic Data Files)

The Type 9 routine reads data into the simulation at consistent specified time-steps from a given data file, performs unit conversions and common calculations, and provides the model with a forcing function [40]. In the TRNSYS validation simulations, the generic data reader was used to read room

temperature data from Microsoft Excel worksheets recorded during ETU experiments. This data was then supplied to models which simulation heat loss to the environment; namely, pipe and tank models.

4.2.7.2 Type 14: Time Dependent Forcing Function

The Type 14 routine produces a repeating pattern of pre-defined behaviour with a dependence on time which can be used for a variety of tasks. In this simulation, the forcing function was used to generate a hot water draw profile by sending its output signal to other simulation components. Data points were entered individually for different times of day to form the pattern of hot water draws. Since the model uses linear interpolation between data points, creating step functions required multiple data points for each time specified time of interest [40].

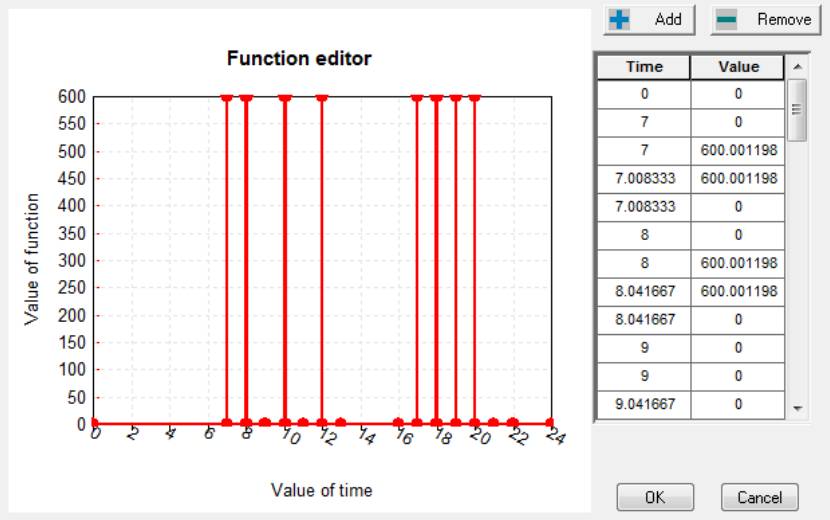

Figure 4.6 Sample CSA Size A (150 L) hot water draw profile from [38] replicated in the Type 14b TRNSYS component

For the experimental tests conducted on the ETU, the Canadian Standards Association (CSA) Size A $(150\ L)$ draw profile found in Table 3 of CSA [38] was used. Due to the operating properties of the hot water draw valve on the ETU, the actual hot water draw demonstrated a reduction in mass transfer of approximately 7% compared to the desired draw in terms of total cumulative flow. As a result, for simulations of the ETU in TRNSYS, a modified CSA Size A hot water draw profile was used, and totals approximately $140\ kg$ of hot water per day.

4.2.7.3 Type 24: Quantity Integrator

The quantity integrator collects a cumulative running total of selected parameters over a specified period of time. This tool makes totalizing data a simple task, and by default it is set to totalize values over the full simulation time period [40].

4.2.7.4 Type 25: Printer

The printer component is used to send simulation data to an output data file such as a Microsoft Excel spreadsheet. This component may be set to append or overwrite an existing data file, and will create a data file if one has not yet been created. The printer is capable of printing at time intervals independent of simulation time steps as well as starting and stopping within the simulation time. This tool can also manage timing in both absolute simulation time, or in time relative to the simulation start time [40].

4.2.7.5 Type 65: Online Plotter

The online plotter is used to produce a graphical representation of selected variables as they vary with time. This component provides the ability to quickly review simulation results or check for appropriate system behaviour for a simulation in progress. The model contains an option for storing simulation results to an output data file [40].

4.2.7.6 Type 109: Combined Data Reader and Solar Radiation Processor

The Type 109 routine reads data into the simulation at consistent specified time-steps from a given data file, performs unit conversions and common solar thermal calculations, and provides the simulation with a forcing function. The solar radiation processor is able to produce calculated values of direct and diffuse radiation for tilted surfaces [40]. For simulation purposes in this thesis, the processor was used to read standard TMY2 weather files, providing realistic weather conditions to the model.

4.2.7.7 Equation Tool

In TRNSYS, an equation tool is provided for performing simple calculations [40]. This tool may also be used to define and use parameters within the simulation by referencing the parameter name. This functionality may unify the repetitive entry of parameters that are common to multiple models. A parameter may be named and set using the equation tool. The named parameter may then be applied to a component model by entering the parameter name as a string input for a given model.

4.2.8 Custom Components

4.2.8.1 Type 161: GX-W2W36 Heat Pump

The Type 161 routine is a custom TRNSYS component created to simulate the performance of the GX-W2W36 heat pump installed on the ETU. The Type 161 routine is a zero-capacitance steady state model. The Type 668 heat pump component is a built-in TRNSYS component located in the TESS HVAC library. The Type 668 routine allows the user to enter discrete data points from an external file, where

performance data is interpolated from the provided lookup table. In this routine, the inlet source and load fluid temperatures are used as independent variables and the model uses this information to interpolate heat transfer and work rates.

Unlike the Type 668 routine, the Type 161 custom heat pump model uses three dimensional curve fit functions determined from experimental data. Relying on these functions eliminates the need for interpolation. Similarly to the Type 668 routine, source and load inlet temperatures are used as independent variables. Each energy transfer rate in the Type 161 model, $\dot{Q}_{source}, \dot{Q}_{load}, \dot{W}_c$, is a dependant variable and is described by a three dimensional function. Outputs such as coefficient of performance (COP) and outlet temperatures are then calculated by energy balance considering the fluid and the corresponding heat transfer rate. Note that the calculated COP does not include pump energy. An energy balance error is calculated to show the imbalance in experimentally generated data compared to the following equation:

$$\dot{Q}_{load} = \dot{Q}_{source} + \dot{W}_c \tag{4.5}$$

Where:

$\dot{Q}_{source}$ is the source heat transfer rate for the GX-W2W36 evaporator
$\dot{Q}_{load}$ is the load heat transfer rate for the GX-W2W36 condenser
$\dot{W}_c$ is the electrical energy consumption for the GX-W2W36 compressor

The Type 161 model provides accurate results limited to the temperature range of supplied data. Within the model, if one of the independent inlet temperature variables is out of range of the known operation limits, it is coerced to the nearest known data point. If the inlet source temperature is greater than the inlet load temperature, the source temperature is coerced to equality with the load temperature. For all situations, coerced temperatures are applied only to the curve fitting functions and are not applied directly to the calculation of outlet temperatures in the heat pump model. The approximate extent of known performance ranges from $10 \leq T_{source}$ [℃] ≤ 30 and $15 \leq T_{load}$ [℃] ≤ 50, where $T_{load} \leq T_{source}$ based upon inlet temperatures. In the measurement of actual heat pump performance, the lower end of the temperature limits were enforced by the use of mains water in the ETU, where source temperatures significantly below 10℃ would have resulted in freezing conditions. The upper temperature limits were enforced by the heat pump's operating range, which involves pressure limits within the heat pump's thermodynamic cycle. For the condition of no flow through the heat pump model, all outputs are set to 0 with the exception of outlet temperatures, where they are

simply set to the corresponding inlet temperature value. For detailed characterization information, see Appendix Section A.4.

In the Type 161 routine, a number of heat pump faults are enforced to match the operation of the real heat pump, and are able to effectively shut the heat pump down in the model. A control signal fault ensures that the heat pump model is receiving a valid control signal, and will shut the heat pump off if a signal is lost. An anti-short cycle timer has been added to the model which restricts heat pump operation for 5 minutes. The timer becomes activated upon initial power-up, as well as each time the heat pump operation changes from a running condition to a fault or off condition. High temperature faults are activated when the supplied source temperature exceeds 30℃ or when the load temperature exceeds 50℃. Low temperature faults are activated when either the source outlet temperature drops below 5℃, or the load outlet temperature drops below 0℃.

In order to allow for the future simulation of the Dual Side I-HPASDHW system with various heat pump sizes, additional parameters were entered into the Type 161 routine. The model includes a $ScaleHP$ input, which directly multiplies through with each energy transfer rate correlation. To scale down the size of the heat pump, $0 < ScaleHP < 1$. Any value over 1 will increase the size of the GX-W2W36. Since the COP of heat pumps typically decreases as a heat pump decreases in size, a COP_d input has also been incorporated. The derating value directly scales the compressor power through division. A $COP_d < 1$ will increase the required work input while a $COP_d > 1$ will produce a more efficient device. All scaling and derating operations make use of the performance map containing the characteristics of the actual GX-W2W36.

$$\begin{aligned} \dot{Q}_{source} &= ScaleHP \cdot f_{source}\{T_{source}, T_{load}\} \\ \dot{Q}_{load} &= ScaleHP \cdot f_{load}\{T_{source}, T_{load}\} \\ \dot{W}_c &= \frac{ScaleHP}{COP_d} \cdot f_c\{T_{source}, T_{load}\} \end{aligned} \tag{4.6}$$

Where:

$f_{source}\{T_{source}, T_{load}\}$ is a three-dimensional source heat transfer curve fit for the GX-W2W36
$f_{load}\{T_{source}, T_{load}\}$ is a three-dimensional load heat transfer curve fit for the GX-W2W36
$f_c\{T_{source}, T_{load}\}$ is a three-dimensional compressor power curve fit for the GX-W2W36

4.2.8.2 Type 162: SL15-25 Heat Exchanger

The Type 162 routine is a custom TRNSYS component created to simulate the performance of the SL15-25 heat exchanger installed on the ETU. The Type 162 routine is a zero-capacitance model that assumes steady state conditions and neglects heat loss to the surroundings. Although a built-in counter flow heat exchanger model with constant overall heat transfer coefficient is available, this model is not capable of considering the effects of fluid density.

The results of testing the SL15-25 heat exchanger on the ETU revealed that the effectiveness of the SL15-25 depends on operating source and load inlet temperatures. The most likely explanation for these unexpected results is a density related effect. The ETU corrects for water density when reading volume flow rates, allowing for mass flow rates to be calculated and held constant. With a constant mass flow rate, an increase in circulating water temperature has the effect of increasing volume flow rate, and therefore fluid velocity. This increase in fluid velocity is likely responsible for the increase in overall heat transfer coefficient in the heat exchanger, and therefore, the effectiveness increases with temperature. The overall trend of increasing effectiveness with increasing average inlet temperature was found to be linear and is described by the following equation.

$$\varepsilon = 1.01x10^{-3}(T_{avg}) + 0.579 \tag{4.7}$$

Where T_{avg} [℃] is the average of inlet source and inlet load temperatures.

Equation (4.7) is the basis of the Type 162 routine. Once the heat exchanger effectiveness is calculated, the heat transfer rate may be calculated. This heat transfer rate is applied to both the source and load sides of the heat exchanger, enforcing an assumption of no heat loss to the environment. Equations for calculating heat transfer rates from effectiveness are fundamental to any heat transfer text book covering heat exchanger analysis such as Çengel [43], and may be found in Appendix Section A.3.

Much like the heat pump model, the heat exchanger has a scaling feature to allow for future modelling of the system with varying sizes of heat exchanger. The $ScaleHX$ input directly multiplies through the effectiveness correlation. To scale down the size of the heat exchanger, $0 < ScaleHX < 1$. Any value over 1 will increase the size of the SL15-25. After calculation of the effectiveness, the effectiveness is coerced between a value of 0 and 1. Output temperatures are calculated by considering the heat transfer rate, mass flow, and specific heat of water flowing through the model. In a zero-flow

condition, the heat exchanger model produces a heat transfer rate of 0, and the outlet temperatures are set to match the inlet temperatures.

4.2.8.3 Type 163: ETU Controller

In order to make comparisons between the ETU and TRNSYS simulations under a realistic operating scenario, a simple but effective control strategy was necessary. The ETU Controller was originally developed in LabVIEW and contains hard-coded settings and procedures to generate control decisions. The control decisions are used to set system modes as the primary output of the controller. The ETU Controller was designed with the purpose of model validation in mind. The simple control strategy avoids excessive equipment cycling and allows for stability and predictability in control decisions, streamlining the validation process. Controls for the ETU and HPASDHW systems have not been optimized. The ETU Controller contains features that avoid the possibility of operating the ETU near restricted conditions, for example, reaching a $100℃$ temperature at any point in the system. Also, factors such as time of day energy billing, as well as weather and load prediction were not included. However, the design of the ETU Controller displays influence from the analyses found in Sterling [17]. Namely, the encouragement of heat pump operation at times of lower solar heat input has been programmed into the decision structure of the ETU Controller.

In order to effectively control a system like the Dual Side I-HPASDHW system, more advanced controls are required with respect to traditional SDHW systems. Instead of relying on a differential temperature controller, monitoring the available solar energy collection rate was important. By estimating the quantity of solar energy available for collection, steady control operations were made possible and excessive equipment cycling was avoided. In an installed system, the theoretical energy collection rate could be supplied by first obtaining the total radiation on a tilted surface using a photovoltaic sensor. The total radiation on a tilted surface would then be converted to a theoretical useful heat collection rate by using measured temperatures and collector efficiency correlations.

The ETU Controller was designed to operate the Experimental Test Unit with the theoretical solar input of a single Vitosol 100-F solar thermal panel and CSA Size A ($150\ L$) draw profile found in Table 3 of CSA [38]. The controller model used the intercept efficiency, efficiency slope, and efficiency curvature parameters of the Vitosol 100-F solar collector to approximate useful heat input. With solar radiation, ambient temperature, and bottom DHW tank temperature inputs, Equation (4.1) is applied for both heat pump and heat exchanger operating conditions in order to determine theoretical collector efficiency values. Collector efficiency values are then used to calculate theoretical collector heat inputs:

$$\dot{Q}'_u HX = \eta' HX(A_c)(G_T)$$
$$\dot{Q}'_u HP = \eta' HP(A_c)(G_T) \quad (4.8)$$

Where:

$\eta' HP$ is a theoretical collector efficiency based upon an inlet collector temperature of $25℃$
$\eta' HX$ is a theoretical collector efficiency based upon an inlet collector temperature of $TBot + 10℃$
$\dot{Q}_u' HP$ is a theoretical heat collection rate based upon the collector efficiency $\eta' HP$
$\dot{Q}_u' HX$ is a theoretical heat collection rate based upon the collector efficiency $\eta' HX$

At the beginning of the ETU Controller code, limiting conditions are checked, and may be used to abort large sections of code. If any of the limit conditions are true, the controller keeps the system in an off condition. For upper limit conditions, the reading must be maintained below the setting for the system to turn on. The opposite is true for lower limit conditions. When the system is off, the setting is used for control decisions and the dead band is inactive. When the system is on, the dead band becomes active. For example, from an off condition, $250\ W$ of input heat must be expected before the system may run. However, if the system has been previously running, a heat input below $200\ W$ must be expected before the system will shut down.

Table 4.6 Summary of ETU Controller cut-out limit conditions

Limit [$Units$]	**Limit Type**	**Setting**	**Dead Band**
Attainable Radiation [W]	Lower	250	50
DHW Top Temperature [℃]	Upper	80	10
DHW Bottom Temperature [℃]	Upper	65 (HX) 45 (HP)	5 5
Heat Pump Timer [min]	Lower	5	-

Theoretical collector heat inputs form a basis upon which control decisions can be made. Using theoretical heat inputs to control the system rather than measured heat inputs or differential temperatures provides control stability. To avoid equipment cycling, a set of thresholds have been set for theoretical heat inputs. Thresholds have been chosen to encourage the desired behaviours, such as heat exchanger operation in times of high solar radiation, and in addition provide dead bands to the control scheme.

Table 4.7 Summary of ETU Controller mode switching heat input thresholds

Operation	$Q_u'HP\ [W]$	$Q_u'HX\ [W]$	Notes
HP mode on	250	-	If adequate heat is available to run the heat exchanger, HX mode will take precedent over HP operation
HP mode off	200	-	
HX mode on	-	1000	
HX mode off	-	500	

The output of the ETU Controller model includes both the desired output mode and corresponding control signals for the heat pump, circulation pumps, and diverter valves. There are four modes used to operate the Dual Side HPASDHW system:

- Mode 0 – "Everything Off"
- Mode 1 – "Solar-to-HX"
- Mode 2 – "Solar-to-HP"
- Mode 6 – "HP Warm-up"

When operating Mode 2, the temperature of the source side fluid drops significantly since the heat transfer rate of the heat pump does not balance with the collected heat input from the solar panel. As a result, the heat pump must be cycled on and off. Once the source loop reaches a temperature of 5°C or below, the controller will switch the system to Mode 6, shutting the heat pump down. The objective of Mode 6 is to warm up the source side loop from approximately 5°C to 25°C. If the source loop temperature reaches 25°C and the heat pump anti-short cycle delay has expired, the controller switches back to Mode 2, re-energizing the heat pump.

Chapter 5 Experimental and Simulation Results

This chapter presents the results of a validation exercise intended to match Experimental Test Unit (ETU) performance with TRNSYS simulations. The results herein were intended for validation only, where the design and controls of the ETU were not optimized. Chapter 5 results should not be used to make conclusions regarding the performance of an optimized system. It may be noted that a number of achievable design and control changes are likely to substantially improve the energy performance of the system. Commentary and recommendations regarding the design and control of the Dual Side indirect heat pump assisted solar domestic hot water (I-HPASDHW) system may be found in Section 6.1.2.

The objective of matching the ETU performance with a TRNSYS simulation was to obtain a validated TRNSYS model of the Dual Side I-HPASDHW system. A validated TRNSYS model allows future investigations to be substantiated, where performance evaluation and improvement studies could be conducted for optimization of the Dual Side I-HPASDHW system. With appropriate measures and care, aspects of the validated Dual Side I-HPASDHW model could be used in future evaluations of other systems.

In order to conclude that the TRNSYS model has been validated, a strong correlation between experimental results and simulation is required. Ideally, the simulation would match experimental results within the experimental uncertainty of the experiment. For substantial deviations between simulated and experimental results, the limitations of the TRNSYS model must be understood along with the source of deviation and approximate level of simulation accuracy. Further, it is important in the evaluation of the system to understand the operation of the ETU Controller, and how its control decisions may have impacted simulation results.

To investigate the correlation between the ETU and the TRNSYS model, four full-day tests were conducted. One full-day test for each of the following seasons was simulated with the domestic hot water (DHW) electrical heating element energized; summer (August 13th), fall (October 28th), and winter (January 12th). Further, the August 13th test was also simulated using the ETU and TRNSYS without an energized heating element. All simulations were conducted for the geographic location of Ottawa, Ontario, Canada. Sections 5.1-5.3 present the results of TRNSYS simulations against the backdrop of ETU experimental results. In Section 5.1.1, the experimental results from the August 13th ETU test are presented with detailed analysis. Within this section, the effects of circulating water through the DHW tank are explored in order to shed light on the results of presented full day comparative tests.

In Section 4.1, the impact of the TRNSYS time step was investigated. In addition to deviation of the simulation based upon time step, there are a number of areas in which TRNSYS simulations are expected to deviate from experimental results. Some of these factors are expected to produce only minimal error:

- Collector stagnation is not considered in the ETU test
- Fluid capacity of the Solar Collector, HP, HX, valves, and pumps are ignored in TRNSYS
- Circulation heater fluid capacity is approximated with two pipe components in TRNSYS
- Thermal mass of piping and other plumbing components is ignored in TRNSYS
- Custom HP and HX models have been developed using quasi-steady state testing, therefore, much like built-in TRNSYS models, transient effects are not captured

The majority of error expected between TRNSYS simulations and ETU experiments is associated with the DHW tank model. Although the Type 4 Stratified Fluid Storage Tank model is well developed and has been experimentally validated, it is a simplified approximation of the real DHW tank and does not behave identically. Temperature gradients in the Type 4 Stratified Fluid Storage model are approximated using a number of uniform temperature nodes, where the number and size of nodes may be used to alter the stratification and fluid mixing characteristics. An example of how the Type 4 Stratified Fluid Storage model is an approximation of reality is evident when examining the effect of the entrance plume. It is well known that a strong entrance plume has the potential to destroy tank stratification in SDHW systems. This entrance plume effect, despite its substantial impact, cannot be taken into consideration by the model, which does not contain detailed fluid dynamics. With fluid mixing not considered in full detail, generating a tank configuration capable of accurately simulating high-flow HP operation and moderate-flow HX operation was not possible.

The behaviour of the DHW electrical heating element is also an approximation in the TRNSYS tank model since tank temperature gradients are approximated with uniform temperature nodes. When an electrical heating element is used, the temperature around the element becomes elevated. In the TRNSYS tank model, the heating element adds heat uniformly to a node occupying an entire horizontal cross-section of the tank with a given depth. In a real tank, heat builds up near the element, signalling the thermostat to stop sending electrical power. As a result of their respective behaviours, the actual DHW element will tend to cycle on and off over relatively short periods, while the model tends to leave the DHW element on for longer periods of time before turning off.

The positioning of the DHW thermostat and heating element in the Type 4 Stratified Fluid Storage model is also extremely important to matching the electrical energy consumption of the DHW

tank. In order to achieve a reasonable match between experiments and TRNSYS models, the thermostat and heating element must be placed in the same node in which solar return fluid enters. This placement of components causes the element's operation in the TRNSYS model to be triggered by hot water circulation, an occurrence which is observed in experimental tests.

When comparing temperature readings from experimental results to the output of corresponding uniform temperature nodes in the TRNSYS model; substantial temperature deviations may be observed. This is particularly true when large differences in temperature are found between a given node and an adjacent node in the TRNSYS model. Temperature deviations, in the realm of $\pm$ 5°C for a given node, have relatively far reaching impacts. The bottom tank temperature influences the collector efficiency when the system is collecting solar energy with the heat exchanger (HX). Further, and more detrimental to matching simulations, the bottom tank temperature influences cut-out conditions which are used to shut the system down when the bottom tank temperature limits are met.

5.1 ETU - TRNSYS Results and Comparison - August 13th - Ottawa

The experimental tests based upon the August 13th weather profile represent the most challenging cases to simulate. As a result, the August 13th tests are a logical starting point to investigate the performance of the ETU, and begin validation of TRNSYS simulations. Much of the discussion provided in Section 5.1 also applies to Sections 5.2 and 5.3, as some sources of error are present in multiple tests.

5.1.1 Sample of ETU Full-Day Test Results with Enabled DHW Heating Element

Many characteristic behaviours of the ETU may be easily observed by viewing various system parameters as a function of time. In this section, all curves were derived from data readings taken at 15 second intervals over the course of each 24 hour test. Several curves in Section 5.1.1 are presented as set-point data overlapped by experimental readings with corresponding uncertainty curves. The match between set-point curves and experimental readings indicates the performance of the ETU's controls. These controls must have operated the ETU sufficiently close to set-point values in order to attempt validation exercises.

It may be of note that for all full-day ETU tests, the DHW tank was prepared several hours in advance. Pre-stratifying the DHW tank provided a realistic starting point for full-day testing, adding credibility to the validation exercises. It may be noted that if substantial water draws were applied to prepare the tank without allowing sufficient settling time, more mixing effects would have occurred

which cannot be matched by the Type 4 Stratified Fluid Storage Tank model. Such mixing effects are evident in Figure 5.2, where the middle tank temperature (DTank3 Mid) rose between simulation hours 5400 and 5406 despite an absence of solar heat input.

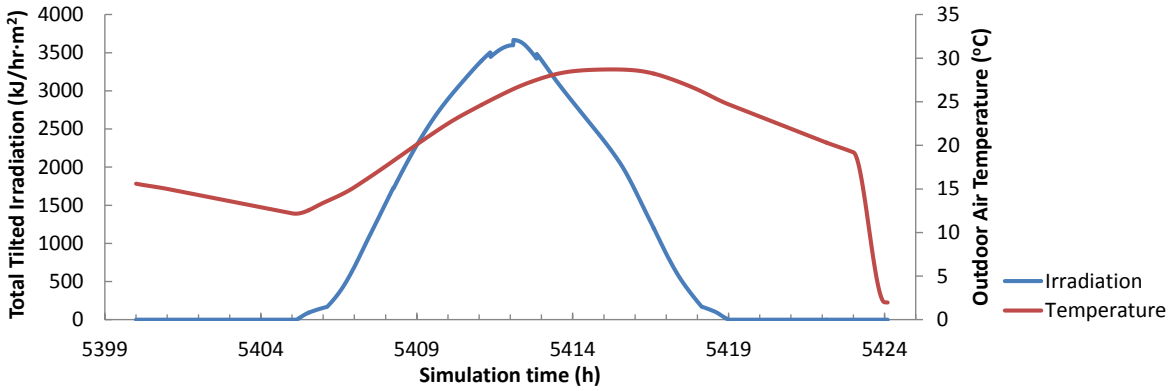

Figure 5.1 Sample solar irradiation and outdoor air temperature profiles used for ETU and TRNSYS simulations - Aug. 13th

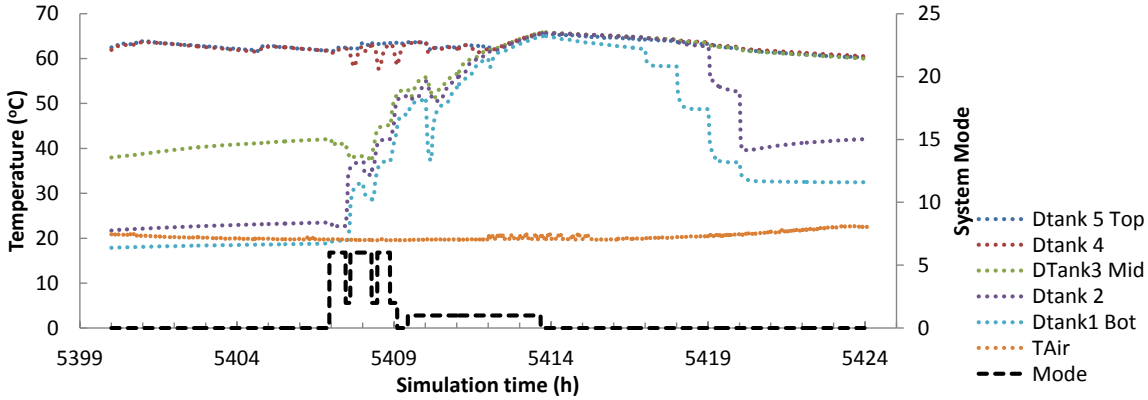

Figure 5.2 ETU system mode, DHW and air temperatures - Aug. 13th

The ETU Controller makes important decisions largely based upon measured temperatures. In particular, the bottom temperature of the DHW tank is responsible for a number of control decisions. In Figure 5.2, the temperature profile of the DHW tank is shown through the five temperature readings measured at increments of tank depth. Also shown in Figure 5.2 is the system's operation profile described by the system mode enforced by the ETU Controller.

Between the approximate simulation hours of 5407 and 5409, the ETU Controller cycled the system between modes 6 and 2 in order to maintain the source side temperature between 5°C and 25°C. In general, HP cycling begins in the HP warm-up mode (Mode 6), where the ETU Controller has determined that sufficient solar radiation is available to begin collecting heat, therefore signalling the

source side pump to circulate fluid. When the source side loop reaches a temperature of $25℃$, the heat pump (HP) and load side pump are energized (Mode 2), rapidly transferring heat from the source loop to the DHW tank until the source temperature reaches $5℃$. This rapid transfer of heat was reflected in experimental temperature readings, see Figure 5.2, where large increases in temperature were observed to coincide with a system mode of 2.

The ETU Controller continues the process of cycling between modes 2 and 6 until one of two triggering conditions becomes true. Once the DHW tank bottom temperature reaches $45℃$, the heat pump can no longer operate and the system is shut down. The alternate trigger is a sufficient level of solar radiation to switch to HX operation. In the August 13th test, the bottom of the DHW tank reached $45℃$ before enough solar radiation was present to switch to HX mode. Therefore, the system shut down for approximately 30 minutes, see Figure 5.2.

For HX mode to become active, a theoretical heat input of $\dot{Q}'_u HX = 1000\ W$ is required. Once the system runs in HX mode, no cycling is necessary. In this mode, the ETU is allowed to run with a higher DHW bottom temperature. To prevent certain temperatures in the ETU system from nearing the boiling point of water, the bottom tank temperature is limited to $65℃$ while the system is running. The bottom temperature limit becomes $60℃$ once the system stops running, forming a dead band. In Figure 5.2, the system mode can be seen switching from 1 to 0 as the bottom tank temperature arrived at the maximum of $65℃$.

In the August 13th test, as with other tests that were executed, once the system switched off in the afternoon, it never returned to an active heat collecting system mode. The reason for the termination of solar collection lies within the control strategy. In order for the HX to continue collecting solar radiation, $\dot{Q}'_u HX = 1000\ W$ of heat must be available and the bottom tank temperature must be below $60℃$. By the time the temperature limit became satisfied, see Figure 5.2, the available solar radiation had diminished below sufficient levels, see Figure 5.3. The use of HP mode was also restricted since the DHW bottom temperature exceeded $40℃$. By the time this temperature condition was satisfied, the available solar radiation had all but disappeared.

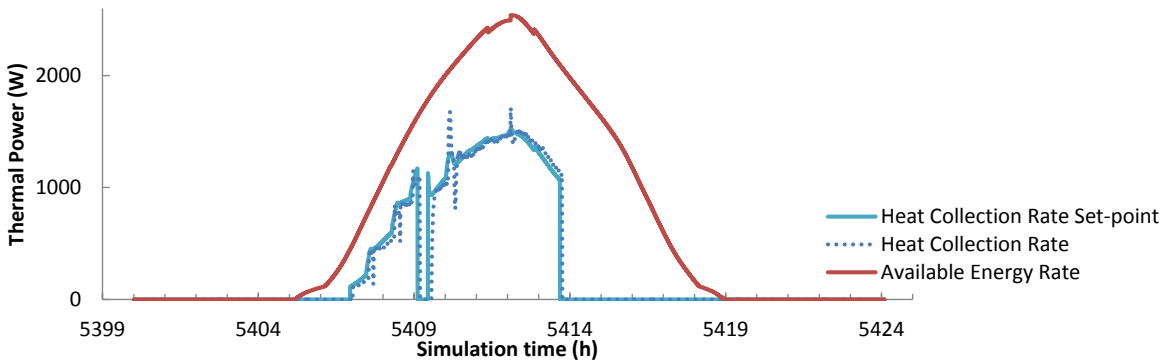

Figure 5.3 ETU available energy rate and simulated solar heat input with set-point - Aug. 13th

Figure 5.3 presents a number of curves portraying the rate at which solar heat was available and was collected throughout the full day test. The fraction of heat collection rate set-point to the available energy rate is equal to the efficiency of the solar collector at any given time. Figure 5.3 also demonstrates the behaviour of the ETU's heater controls by tracking the measured heat collection rate along with the heat collection rate set-point. Large short-lived deviations between the heat collection rate and its corresponding set-point were caused by transient system effects. These transient effects were triggered either by control mode changes of the system, or changes in DHW bottom temperature as a consequence of hot water draws. When either of these events occurred, there was a rapid shift in system conditions, requiring a period of time for adjustment. In general, the heater control tended to lag behind the set-point and its reaction time was intentionally limited in order to manage heater behaviour during transient conditions. Although the control had a lagging effect, Figure 5.4 demonstrates the effectiveness of the ETU's heater controls.

At this point, it is worth considering the purpose of the heat pump in the Dual Side I-HPASDHW system. By operating the HP, the source side temperature is lowered, and the solar collector efficiency increases. This allows for improved solar collection in times of cold outdoor air temperatures and lower solar radiation. Figure 5.3 clearly demonstrates this effect. Shortly after hour 5409, the system shut off after cycling the heat pump throughout the morning. Once the system returned to operation in HX mode, the rate of heat collection had dropped. While more solar radiation became available, a high bottom tank temperature meant that the solar collector inlet temperature had increased, and therefore the collector efficiency was reduced.

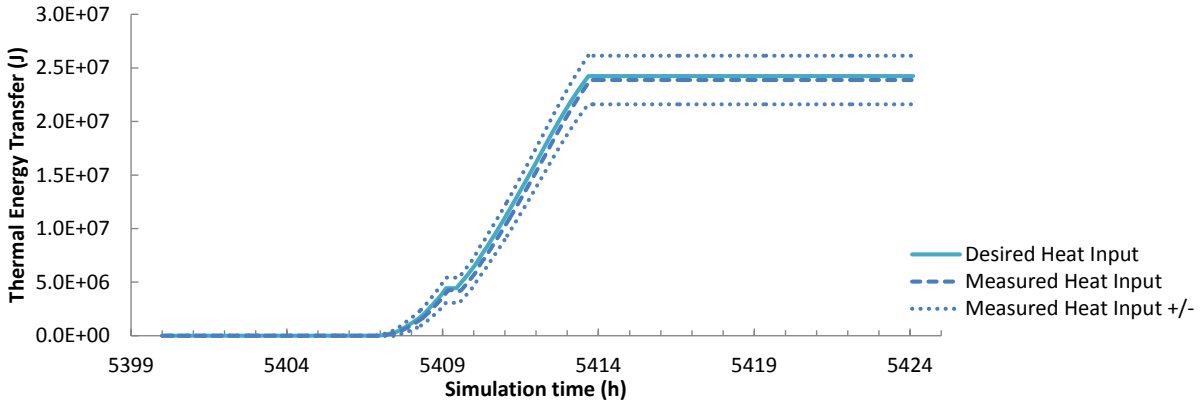

Figure 5.4 ETU cumulative simulated solar heat input - Aug. 13th

In Figure 5.4, the total amount of solar energy that was introduced into the system through the solar collector, or in the case of the ETU, the circulation heater, is presented as a function of time. The cumulative curve was achieved through the integration of heat collection rates throughout the test. The desired heat input curve represents the integration of the heat collection rate set-point depicted in Figure 5.3. The measured heat input was tracked, where the measured heat input +/- curves display the experimental uncertainty associated with the calculation of the corresponding quantity. The match between the desired heat input and measured heat input demonstrated the effectiveness of the ETU's heater controls. Though there was some visible deviation, at all times there was a successful match between the desired and measured heat inputs well within experimental uncertainty.

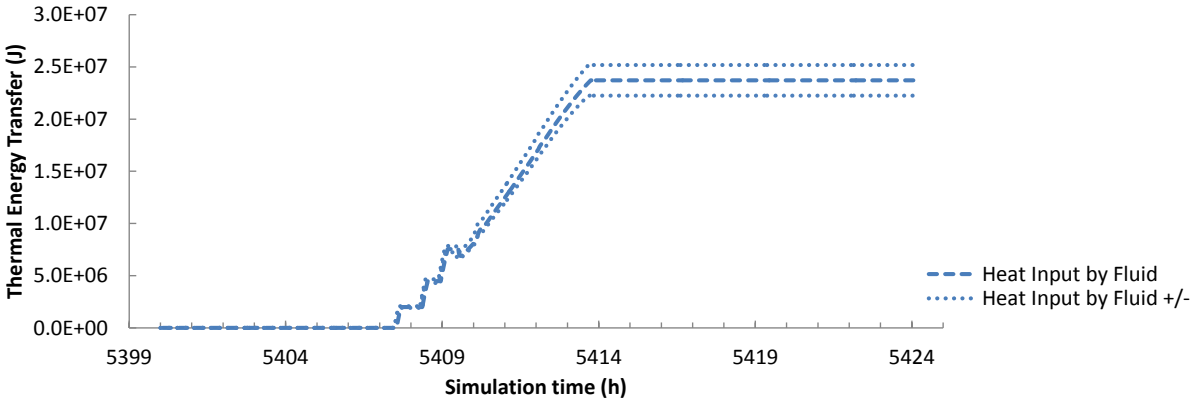

Figure 5.5 ETU cumulative DHW heat addition by fluid - Aug. 13th

Figure 5.5 presents the cumulative transfer of energy to the DHW tank from the rest of the ETU. The heat input by fluid measurement includes only heat delivered by the movement of fluid, and therefore, does not consider DHW heat addition by the electrical heating element. This cumulative heat

addition curve was formed by the integration of the heat transfer rate observed across the entering and exiting solar ports of the DHW tank. From hours $5407 - 5409$, the impact of heat pump cycling is clearly shown. The slope of the three short energy increases, observed between hours 5407 and 5409, indicated that very high heat transfer rates were achieved by the heat pump. Two corresponding flat sections appeared on the curve during this same time period. These sections indicated that no heat was delivered to the DHW tank when the HP warm-up mode (Mode 6) was active.

Between hours 5409 and 5410, there was a short period of time in which the curve decreased in value, which represented a loss of heat from the tank. This phenomenon can be explained by considering that the source loop fluid temperature was $25℃$ or lower as the heat pump cycling procedure had finished. After a period of time, heat exchanger mode became active near hour 5409, see Figure 5.2. At this point, some heat was lost from the DHW tank as heat was transferred in reverse from the DHW tank to warm up the chilled fluid in the source loop. After another short period of time, the source loop reached a sufficient temperature and began adding heat to the DHW tank through the heat exchanger.

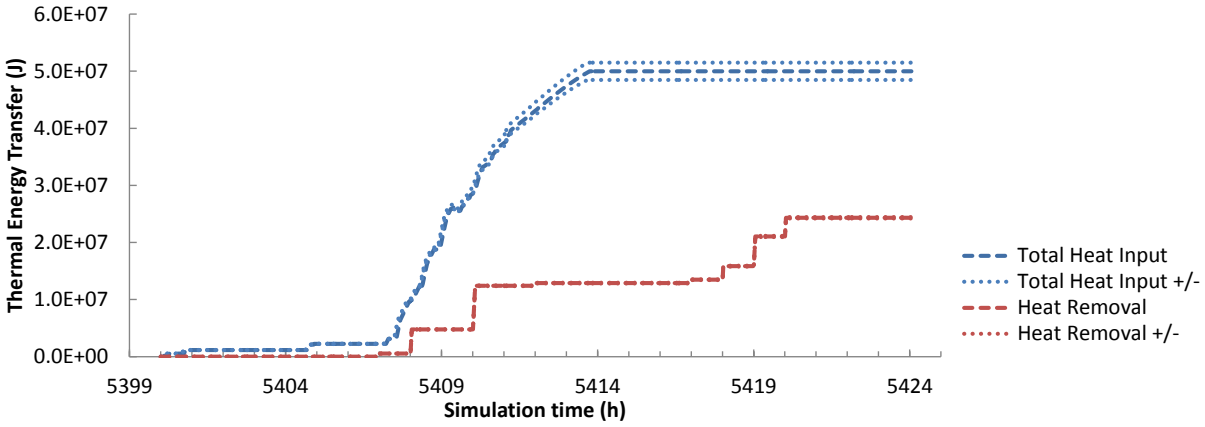

Figure 5.6 ETU cumulative DHW total heat addition and removal - Aug. 13th

Upon initial inspection of Figure 5.6, one may notice the uncertainty curves for heat removal demonstrate very little spread compared to the total heat input. The experimental uncertainty for heat transfer calculation is attributed largely to the uncertainty in temperature and flow rate measurements. When heat was added to the DHW tank by fluid, the heat transfer rate was relatively low and occurred for an extended period of time. As a fraction of the total heat input, the associated uncertainty became significant and the uncertainty curves became visible. When a hot water draw occurred, heat transfer rates were very high due to the high flow rates and temperature differences involved. The

corresponding uncertainty as a fraction of the heat removal in this case was very small. The relatively low level of uncertainty associated with high heat transfer rates means that uncertainty curves for heat removal are not easily visible.

Observing the DHW tank temperature profiles presented in Figure 5.2 indicates that overall, a significant quantity of heat had been added to the tank. Figure 5.6 shows that substantially more heat had been added to the DHW tank from solar and electrical energy than had been removed by hot water draws. One might also note that when heat addition by fluid presented in Figure 5.5, is compared with the total DHW heat addition presented in Figure 5.6, approximately half of the heat supplied to the DHW tank was by the electrical element. This was largely due to a mutual influence between fluid circulation and the action of the DHW heating element.

The backup electrical heating element installed on the ETU is controlled with a standard tank-mounted thermostat that is independent of the remainder of the ETU controls. The DHW thermostat, electrical heating element, and solar return port are all in close proximity, within 6" of each other with respect to the vertical dimension of the DHW tank. The result of this close proximity is a mutual influence between solar collection and DHW electrical consumption that is triggered by mixing effects in the DHW tank.

The first influence occurs when fluid from the bottom of the DHW tank is circulated and heated in either the heat exchanger or the heat pump. When this fluid is returned to the DHW tank through the solar return port, there is no guarantee that it will reach a temperature greater than or equal to the DHW thermostat set-point. If this solar return water is substantially cooler than the DHW thermostat set-point, the thermostat would be triggered and electrical energy, wanted or unwanted, would be added to the water in the tank.

The second influence introduced by the proximity of components in the DHW tank is a heating effect that moves downward through the tank over time. As water is circulated over long periods of time, a fraction of the solar return fluid becomes mixed with the warmer fluid above that has been heated electrically. This fraction of mixed fluid is carried downward through the DHW tank as the bottom half of the tank is continually processed by the load side pump. Eventually, as heated fluid circulates downward, fluid at the bottom of the DHW tank demonstrates a heating influence from the DHW element.

The mutual influences described above are clearly demonstrated in Figure 5.7. The phenomena were separated from other effects by disabling various ETU components. Figure 5.7 shows a full day test during which, the heat pump's compressor power was disabled, and no solar heating was simulated. As a result of the conditions, the system first operated the HP warm-up cycle, followed by an extended period of circulation from the DHW tank, through the disabled heat pump, and back to the DHW tank. Remembering that the heat pump was turned off for the entire test and no heat was added to the circulating fluid, the electrical element's impact on tank temperatures is clear. After just 2 hours of hot water circulation, temperatures in the lower half of the tank reached $45°C$, a temperature rise for which heat addition by the DHW element was entirely responsible. Modelling this behaviour is a significant challenge, particularly because the fraction of heat which travels downward is dependent on tank stratification and circulating flow rate. This behaviour was difficult to characterize and implement in a tank model, and cannot be fully accounted for in the available built-in TRNSYS tank models.

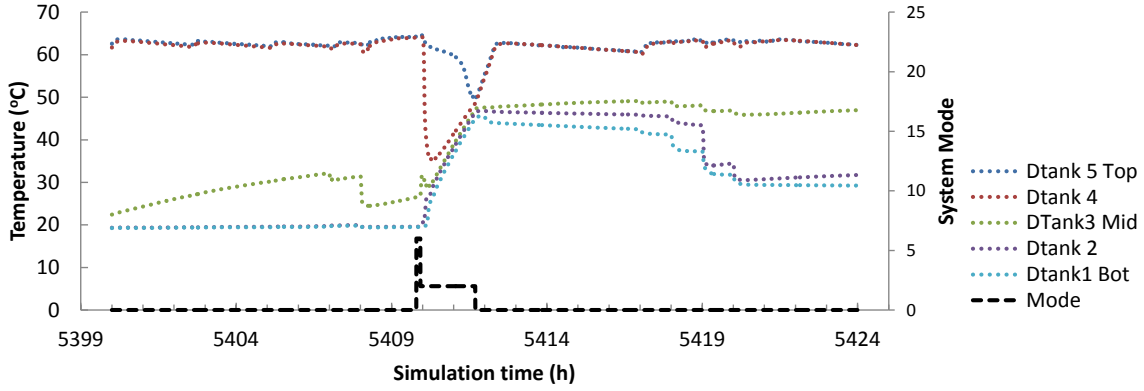

Figure 5.7 ETU DHW circulation and electrical element mutual influence test - heat pump disabled - no solar heat input

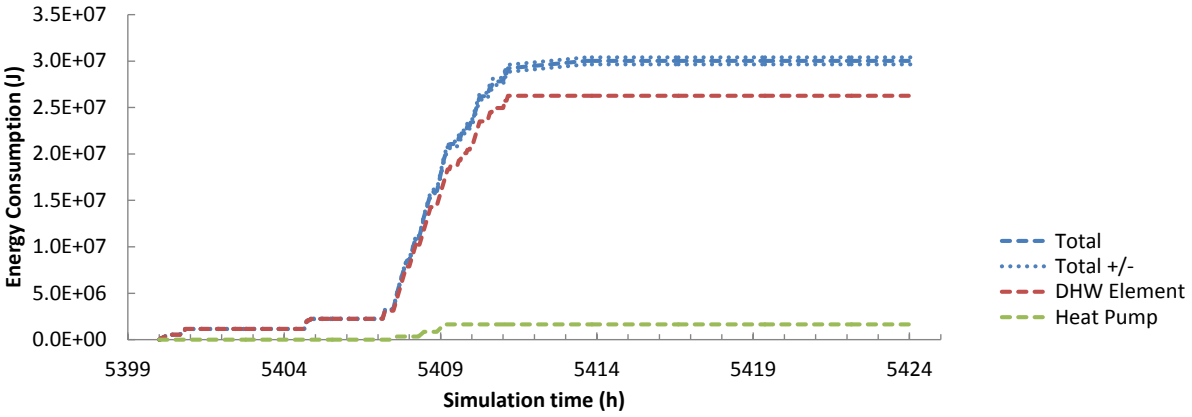

Figure 5.8 ETU cumulative electrical energy consumption - Aug. 13th

Figure 5.8 presents energy consumption over the course of 24 hours. In this figure, uncertainty curves are only presented for total energy consumption since they are not sufficiently visible on the other curves. The uncertainty involved with electrical power measurements is much less significant than the temperature measurements used in heat transfer calculations. It may be seen in Figure 5.8 that the electrical consumption of the heat pump, despite significant running time, was a very small portion of the total electrical power consumption. However, it is important not to confuse electrical consumption with heat delivered to the DHW tank since the heat pump had a coefficient of performance. Still, the DHW element consumption represented the overwhelming majority of electrical energy use. In addition to what is explicitly shown in Figure 5.8, pump and valve energy also accounted for a small portion of the total energy consumption curve.

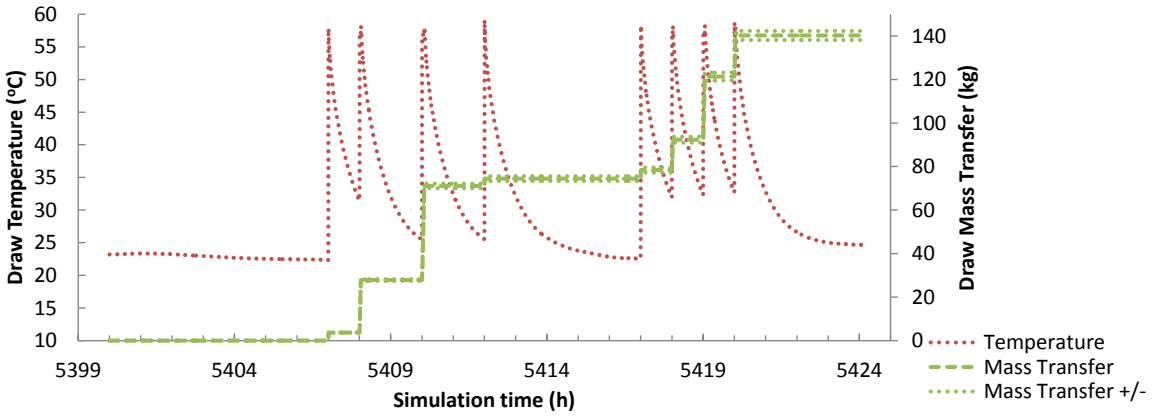

Figure 5.9 ETU hot water draw characteristics - Aug. 13th

In Figure 5.9, hot water draw temperatures and mass flow rates are depicted. The mass transfer curve shows the mass of water processed by the DHW tank throughout the day. The mass transfer occurred in 8 distinct steps. The draw controls on the ETU were set to provide $150\ kg$ of hot water per day. Due to the characteristics of the ETU's floating point valve, namely a quicker closing action than opening action, approximately $140\ kg$ of hot water were drawn from the DHW tank. During the step increments of hot water draws, the draw temperature exhibited a peaking behaviour. Between distinct hot water draws, the draw temperature sensor lost heat to the surroundings. However, each peak reached the approximate tempering valve set-point temperature of $57℃$. Although the draw valve did not provide the $150\ kg$of hot water desired, it is simple to match this hot water draw profile in the TRNSYS model.

5.1.2 ETU - TRNSYS Comparison with Enabled DHW Heating Element

Of all experimental tests carried out, the August 13th test with an energized DHW heating element demonstrated the largest deviation compared with the TRNSYS model. As previously discussed, the deviation between simulation and experimental results can be largely attributed to stratification in the TRNSYS tank model. The August 13th test with an energized DHW heating element was used to determine which TRNSYS tank configuration provided the best match to the experimental results. The selection of an appropriate tank configuration allowed for further simulations to be conducted. Within Section 5.1.2, tank models with increased and decreased levels of stratification are analyzed.

In order to determine the quality of match between simulation and experimental results, the cumulative heat delivered to the DHW tank by fluid was useful metric. Matching the cumulative energy added to the DHW tank required a reasonable match between the experimental and simulated system operation since it depended on a number of system behaviours. Other metrics like total energy addition to the hot water tank and total energy consumption appeared less sensitive to the quality of simulation. In later sections, it may be necessary to observe multiple figures simultaneously before system behaviours can be understood.

5.1.2.1 High Stratification TRNSYS Tank Model

In order to find the ideal tank model that provides the best possible match between simulation and experiment, tank models with varying levels of stratification have been investigated. The high stratification tank model used 15 nodes, the maximum number of tank nodes available in the Type 4 tank model. The total DHW heat addition by fluid for the highly stratified DHW tank is shown in Figure 5.10, where a substantial deviation in thermal energy transfer was observed towards the end of the day. This deviation was attributed to a high temperature cut-out condition that shut the system down in the simulation, where the experimental unit was allowed to run further into the afternoon. This high temperature cut-out condition occurred when the bottom DHW tank temperature reached 65°C.

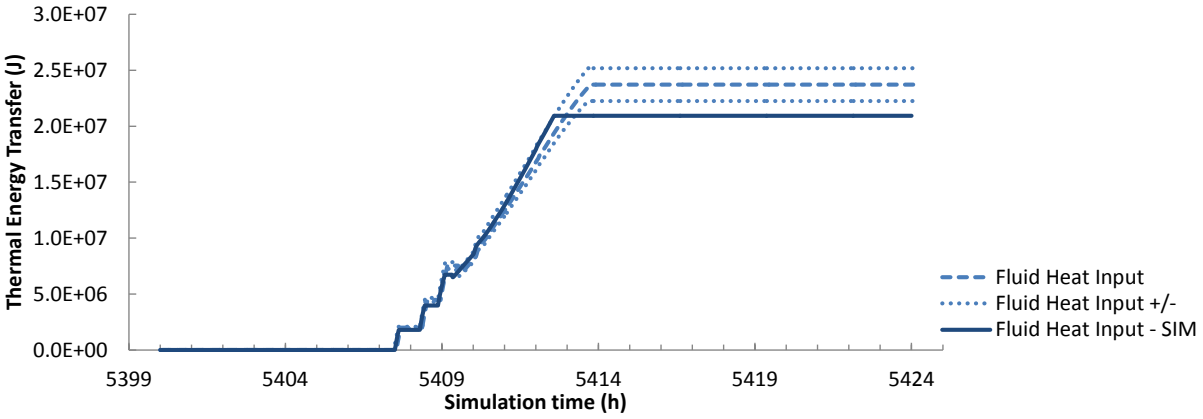

Figure 5.10 Comparison of ETU and TRNSYS model: cumulative DHW heat addition by fluid - high stratification - Aug. 13th

5.1.2.2 Low Stratification TRNSYS Tank Model

The low stratification tank model used 5 nodes, each corresponding to the placement of the temperature sensors installed in the DHW tank of the ETU. This number of nodes was used as the low-limit of tank stratification. The total DHW heat addition by fluid for the least stratified DHW tank is shown in Figure 5.11, where even more deviation in thermal energy transfer was observed towards the end of the day. This deviation was also attributed to the high temperature cut-out condition where the bottom DHW tank temperature in the simulation reached $65℃$.

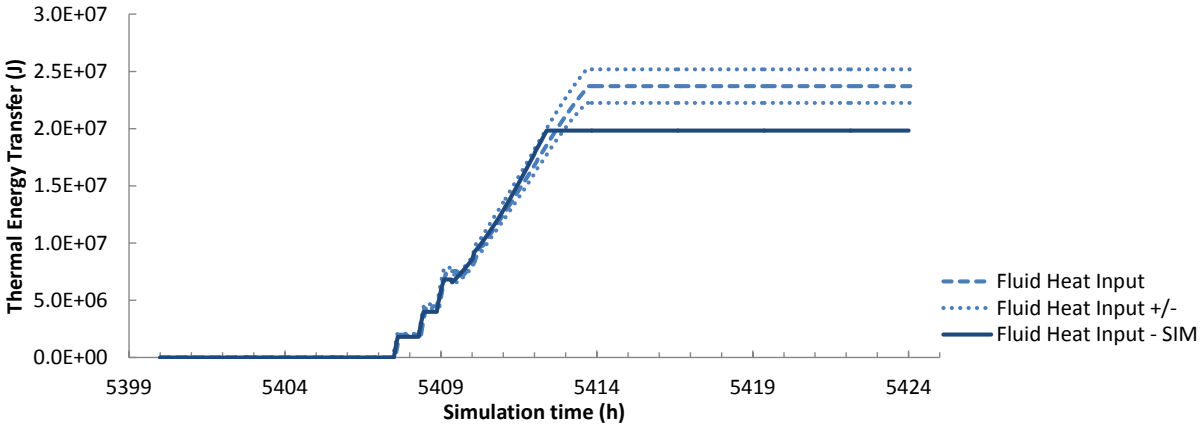

Figure 5.11 Comparison of ETU and TRNSYS model: cumulative DHW heat addition by fluid - low stratification - Aug. 13th

5.1.2.3 Moderate Stratification TRNSYS Tank Model

After iteratively attempting to match simulations to experiments with various Type 4 Stratified Fluid Storage tank model configurations, the best available configuration was found. The configuration providing the most accurate match between TRNSYS models and ETU tests was a 10 node tank model with increased stratification in the upper half of the tank. Figure 5.12 overlays experimental

temperature readings with corresponding simulated DHW tank temperature profiles from TRNSYS. From preliminary observations of Figure 5.12, a clear correlation between the experimental and simulated temperatures was observed; however, significant fluctuation did occur and was a clear demonstration that the TRNSYS simulations were an approximation of actual performance.

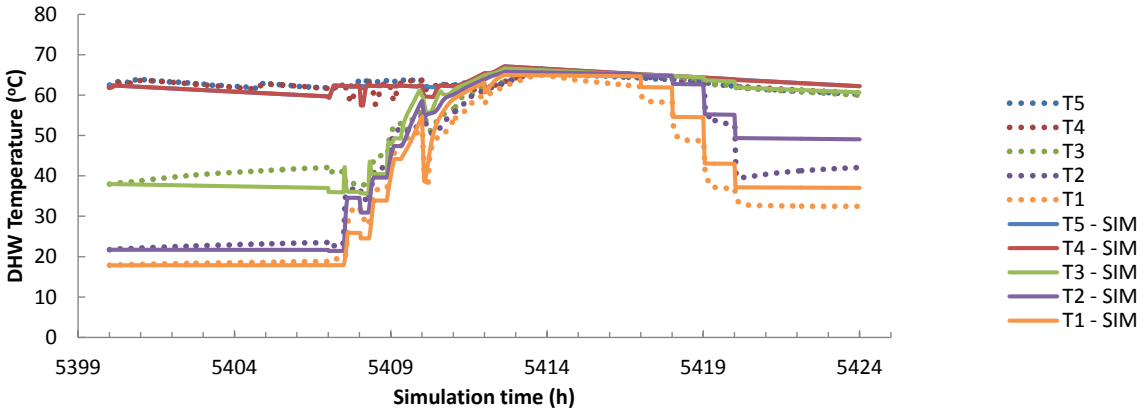

Figure 5.12 Comparison of ETU and TRNSYS model: DHW tank temperatures - Aug. 13th

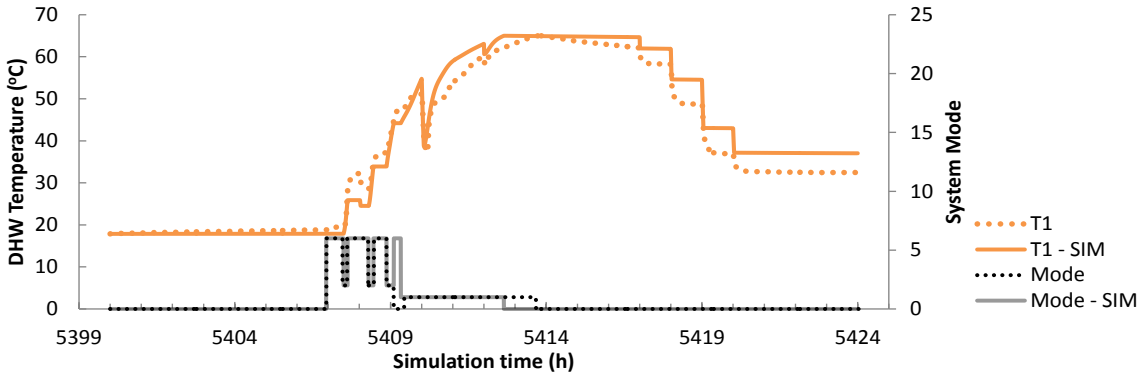

Figure 5.13 Comparison of ETU and TRNSYS model: DHW tank bottom temperature detail and system mode - Aug. 13th

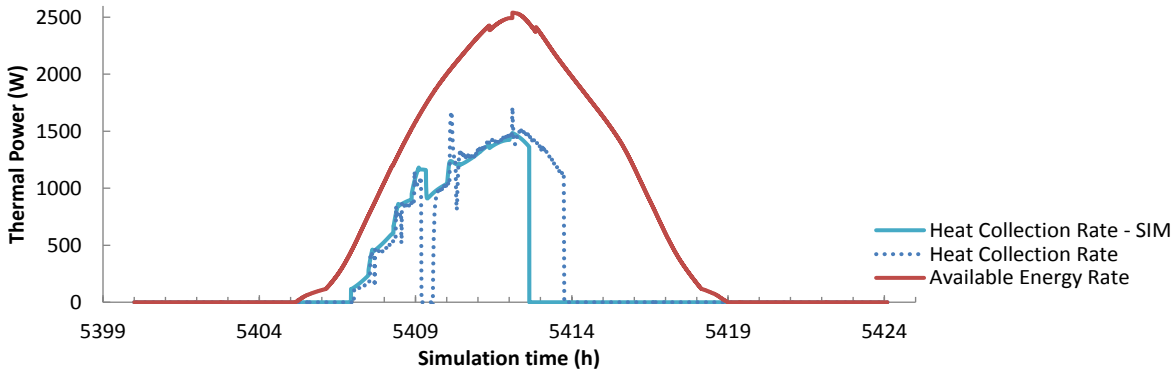

Figure 5.14 Comparison of ETU and TRNSYS model: available energy rate and simulated solar heat input - Aug. 13th

In Figure 5.14, it is clear that the solar heat collection period for the TRNSYS simulation was substantially different than that of the ETU experiment. The reason for solar collection being cut short by the simulation is demonstrated in Figure 5.13, where significant deviation in the bottom tank temperature was shown. Shortly after simulation hour 5409, the bottom tank temperature in the experiment reached $45°C$, causing the system to shut down. In the simulation, the bottom tank temperature remained below $45°C$ long enough to allow the system to switch to heat exchanger mode, and continue collecting energy without interruption. At approximately 5412.5 hours of the TRNSYS simulation, the system shut down and heat collection was ceased. In experimental results, heat collection extended much longer into the day, nearing hour 5414. The difference between simulated and experimental heat collection was caused once again by deviation in the DHW bottom tank temperature. In the simulation, the bottom tank temperature reached $65°C$ much quicker than in the experimental results.

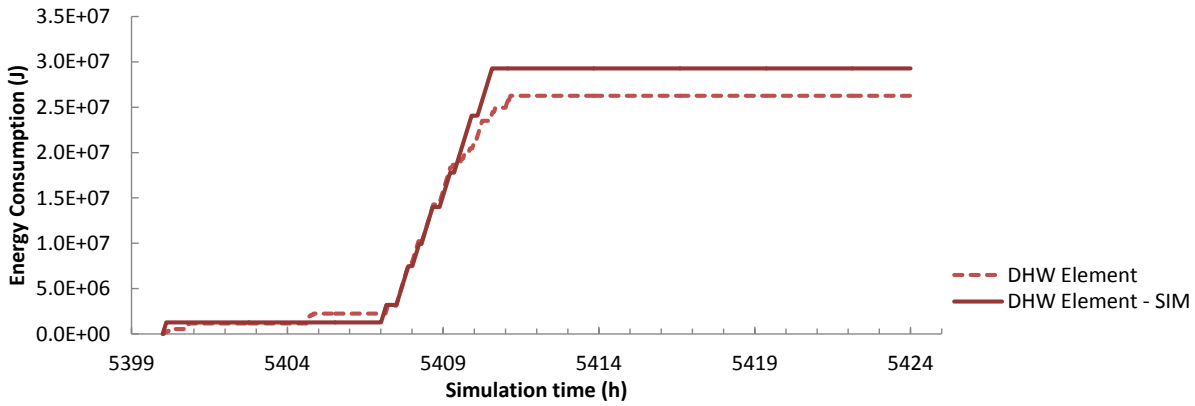

Figure 5.15 Comparison of ETU and TRNSYS model: DHW heating element energy consumption - Aug. 13th

Some deviation in bottom tank temperature was attributed to the approximation of stratification; however, in the case of this simulation, deviation was also attributed to excess heat addition by the DHW heating element while the system ran in HX mode. At this point it is important to remember the mutual influence of water circulation and DHW electrical heating element operation. Heat added to the DHW tank by the heating element while water is circulating through the system ends up being added to the bottom of the DHW tank after a sufficient period of time. Excess heat addition was observed starting shortly after simulation hour 5409, see Figure 5.15, while the corresponding deviation in DHW bottom temperature is visible in Figure 5.13.

The pattern of DHW element energy consumption highlighted the challenge faced in matching a TRNSYS model to the DHW tank installed on the ETU. When the heat pump was running, flow rates were

high and the model provided a reasonable match to the experimental results. Once the system began to run the heat exchanger, flow rates were reduced, and the model began to over-predict DHW heating element usage. In the experimental test, less mixing near the solar return port took place when fluid was circulating through the heat exchanger, compared to more mixing when fluid was circulated to the heat pump. In the TRNSYS simulation, a similar level of mixing near the solar return port was modelled for both heat pump and heat exchanger operation. Mixing and destratification phenomenon experienced at the solar return port had a significant impact on thermostat operation.

In Figure 5.16, DHW heat addition is shown for the moderately stratified tank. By the end of the simulation, the simulated heat addition by fluid deviated 10.3% from the experimental value. However, the simulated value only deviated 4.4% from the lower uncertainty bound of the experimental heat addition by fluid, where experimental uncertainty was considered. Regardless, it was still clear from Figure 5.13 and Figure 5.14 that the simulation had qualitative differences resulting in lost accuracy.

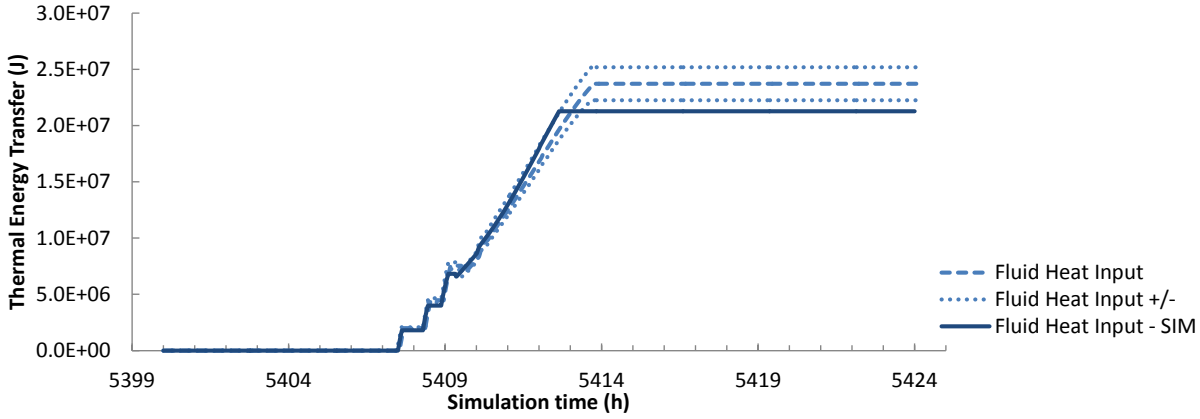

Figure 5.16 Comparison of ETU and TRNSYS model: cumulative DHW heat addition by fluid - Aug. 13th

When observing Figure 5.17; the choice to use heat addition by fluid, as opposed to total heat addition, as a metric to evaluate the accuracy of the simulation was validated. Despite the limited accuracy of the August 13th simulation, the total heat input to the DHW tank matched well within experimental uncertainty. The excess energy consumption by the DHW heating element demonstrated in Figure 5.15 is also visible between hours 5419 and 5413 in Figure 5.17.

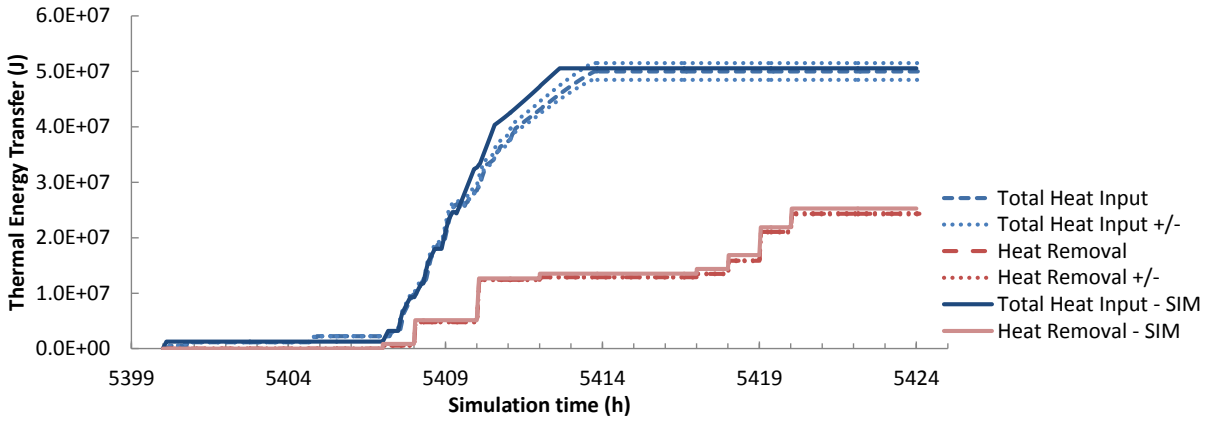

Figure 5.17 Comparison of ETU and TRNSYS model: cumulative DHW total heat addition and removal - Aug. 13th

The August 13th TRNSYS simulation cut short the collection of solar energy since excess heat was provided by the DHW heating element while the system operated in HX mode. As a consequence of this offsetting of solar energy collection, total electrical energy consumption increased in the simulated results with respect to experimental data. In Figure 5.18, the deviation in total energy consumption was explained almost in its entirety by the excess electrical heating element's energy consumption.

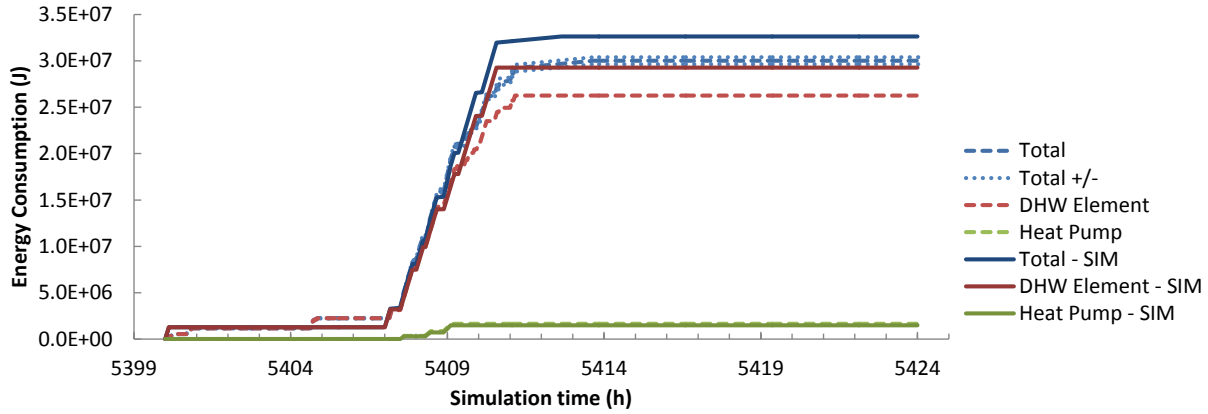

Figure 5.18 Comparison of ETU and TRNSYS model: cumulative electrical energy consumption - Aug. 13th

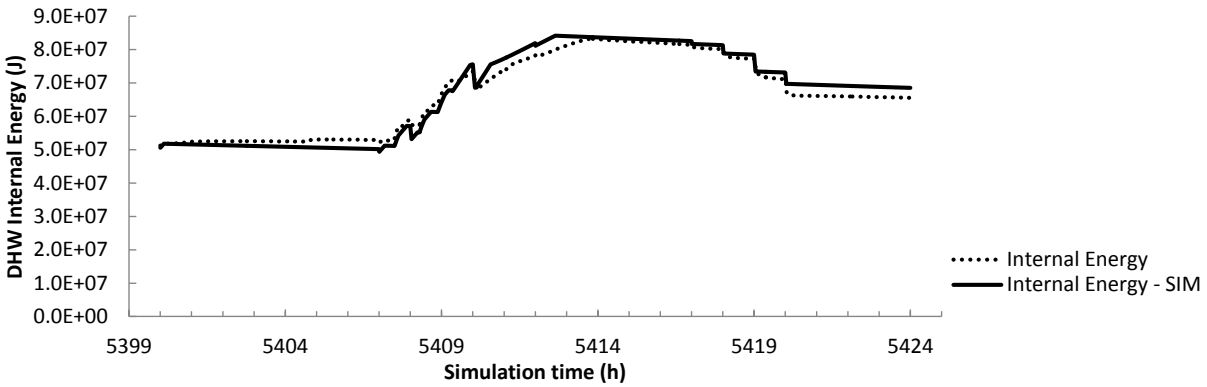

Figure 5.19 Comparison of ETU and TRNSYS model: DHW tank internal energy - Aug. 13th

In Figure 5.19, the internal energy of the experimental and simulated DHW tank is depicted. It is important to note that this metric was very much an approximation. Since internal energy of the DHW tank on the ETU was determined by just 5 temperature measurements, the curves presented in Figure 5.19 are only useful for portraying trends. Further, in calculating internal energy, a constant specific heat of water was assumed. Like with other metrics, the internal energy demonstrated a reasonable match between simulations and experiments while the heat pump was operating, followed by a deviation during HX operation.

5.1.2.4 Enforced DHW Heating Element Power with Moderate Stratification Tank Model

While investigating the August 13th test with an energized DHW heating element, much of the deviation between experiment and simulation was attributed to excess use of the heating element in the simulation. By enforcing the TRNSYS simulation's DHW element power using experimental results, the impact of the element was demonstrated. Note that a successful simulation must achieve a sufficient match to experiments without enforcing inputs using experimental data. The purpose of enforcing DHW element power is to clearly demonstrate that the DHW element was major source of simulation error. It is important to remember at this point that the DHW element was controlled by an independent thermostat. In the experiment, the element operation was sensitive to the temperature immediately adjacent to the thermostat. In the TRNSYS simulation, element operation was triggered by the temperature of the DHW tank node that contained the thermostat, element, and solar return port.

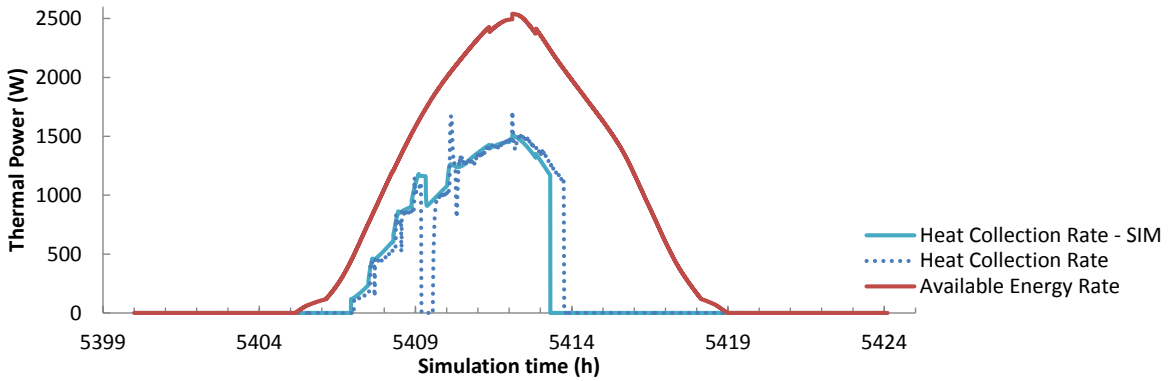

Figure 5.20 Comparison of ETU and TRNSYS model: available energy rate and simulated solar heat input - enforced element - Aug. 13th

Figure 5.20 shows that with an enforced DHW element power, a much closer match to the solar heat input was achieved. A substantial difference in behaviour was still visible; however, when integrated over the course of the simulation, the total amount of heat collected by the solar collector was nearly a perfect match between simulation and experiment. Note that, heat obtained through the solar collector and heat added to the DHW tank, are two separate metrics. Again, the stratification characteristics of the TRNSYS tank model allowed solar energy to be collected without interruption in the simulation. The difference in solar energy collected between hour 5409 and 5410 was corrected towards the end of the solar collection period. The bottom tank temperature in the simulation reached the maximum, 65℃, before the experimental temperature reached this limit. This was due to the excess heat added to the DHW tank between hour 5409 and 5410.

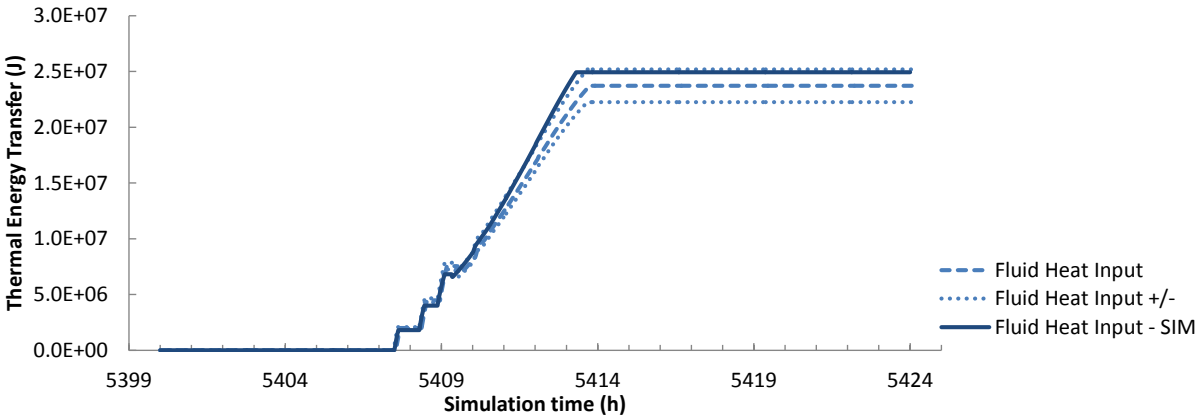

Figure 5.21 Comparison of ETU and TRNSYS model: cumulative DHW heat addition by fluid - enforced element - Aug. 13th

At times throughout the simulation, the cumulative heat addition by fluid strayed outside the bounds of the experimental uncertainty. Despite temporary deviations, the final fluid heat input was

found to be within experimental uncertainty, see Figure 5.21, indicating an improved match between simulation and experiment. The total addition and removal of heat to and from the DHW tank, not shown, still demonstrated a sufficient match between experiment and simulation. The heat addition and removal curves with an enforced element were very similar to those found in Figure 5.17. By enforcing the DHW element power, a clear improvement in matching energy consumption was found with respect to Figure 5.18. Enforcing the DHW element power provided a sufficient match between experimental results and the TRNSYS simulation. This proved that the deviation introduced by the DHW element was responsible for a significant portion of error between TRNSYS simulations and the experimental results.

5.1.3 ETU - TRNSYS Comparison with Disabled DHW Heating Element

Moving forward with the 10-node tank model, the best configuration found, the August 13th comparison between the ETU and TRNSYS simulation was repeated with a disabled electrical heating element. Evidenced by the DHW top temperature dipping below the $55 - 57$°C hot water delivery set-point, Figure 5.22 demonstrates that insufficient heat was available early in the day to avoid the use of the DHW heating element. Note that the tank's preparation temperature profile was largely responsible for this, and a real summer day is likely to begin with higher bottom tank temperatures.

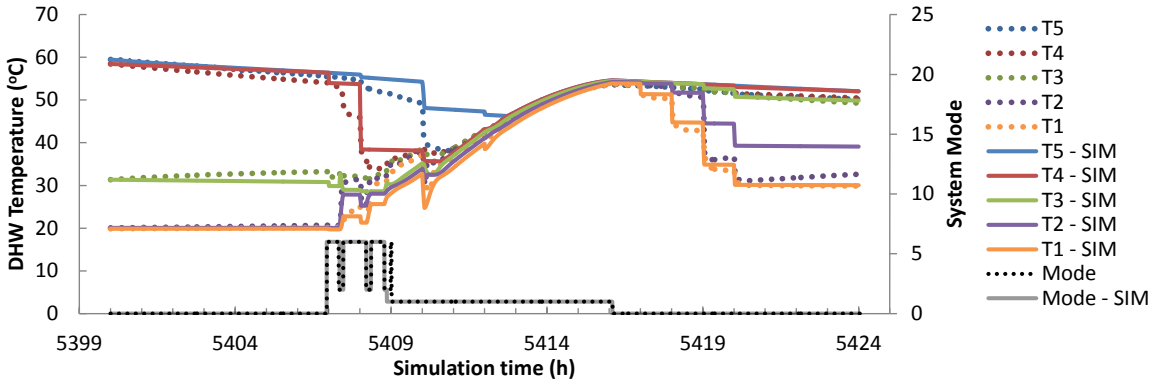

Figure 5.22 Comparison of ETU and TRNSYS model: DHW tank temperatures and system mode - disabled element - Aug. 13th

In this simulation, without the influence of the DHW element, there is a strong match between heat collected from solar energy in the experiment and the simulation. This match is highlighted in both Figure 5.23, and Figure 5.24 which depict a match between instantaneous, and cumulative heat collection, respectively.

Instead of solar collection being terminated by a bottom tank temperature limit, in this test the theoretical solar heat input dropped below the $\dot{Q}'_u HX = 500\ W$ heat collection limit. The controller

then attempted to run the system in HP mode, but was restricted since the bottom tank temperature exceeded $40℃$. Just like the test with an energized DHW element, the bottom tank temperature strayed from the experimental test; however, the bottom temperature corrected itself near hour 5413, see Figure 5.22. The TRNSYS simulation closely predicts the bottom tank temperature near hour 5416. As a result, the simulation and experimental unit reached the theoretical collector heat input limit, $\dot{Q}'_u HX = 500\ W$, at approximately the same time. Consequently, the solar collection period was nearly identical between the TRNSYS model and experimental results; see Figure 5.23 and Figure 5.24. The resulting cumulative solar heat input and total heat addition by fluid to the DHW tank were sufficiently matched to consider the simulation successful.

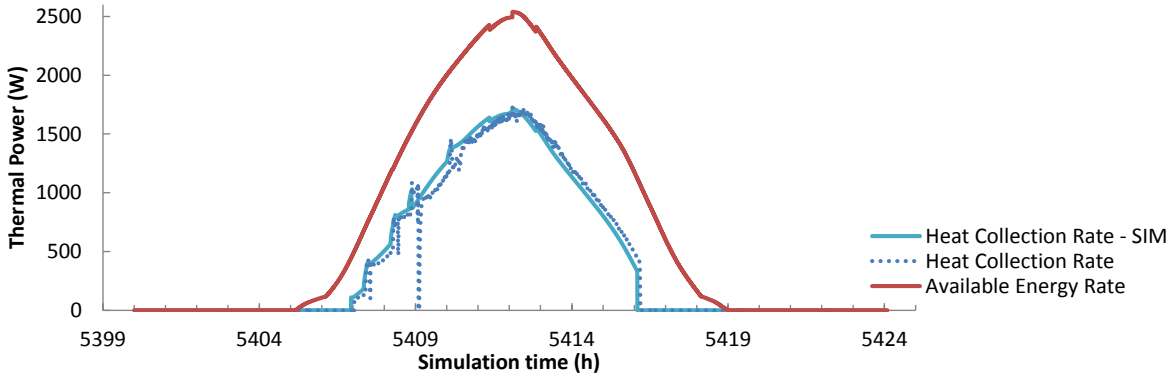

Figure 5.23 Comparison of ETU and TRNSYS model: available energy rate and simulated solar heat input - disabled element - Aug. 13th

It may be noted that in Figure 5.24, there was substantial deviation in actual and simulated heat removal. Unlike tests where the DHW electrical element was energized, in this test, the DHW tank's top temperature was allowed to dip below the desired delivery temperature. In this condition, the tempering valve ceased to mix incoming and outgoing flows; rather it prevented mixing and delivered hot water directly from the top of the DHW tank to the load. With this being the case, in order for experimental and simulated heat removal to match closely, there must first be a close match for the temperature at the top of the DHW tank. Due to the approximations in stratification and mixing effects of the DHW tank, it was shown that the top tank temperature deviates between simulation and experiment resulting in a poor match in heat removal, see Figure 5.22.

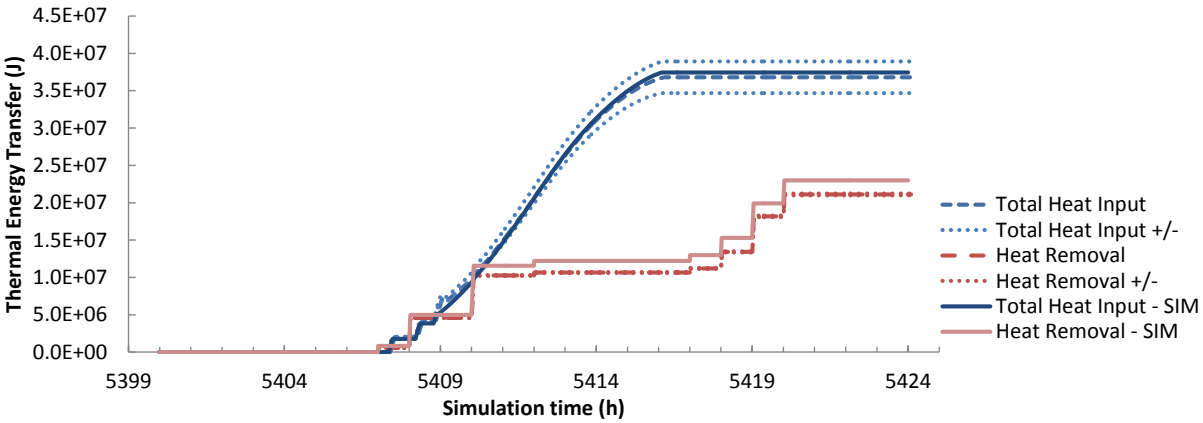

Figure 5.24 Comparison of ETU and TRNSYS model: cumulative DHW total heat addition and removal - disabled element - Aug. 13th

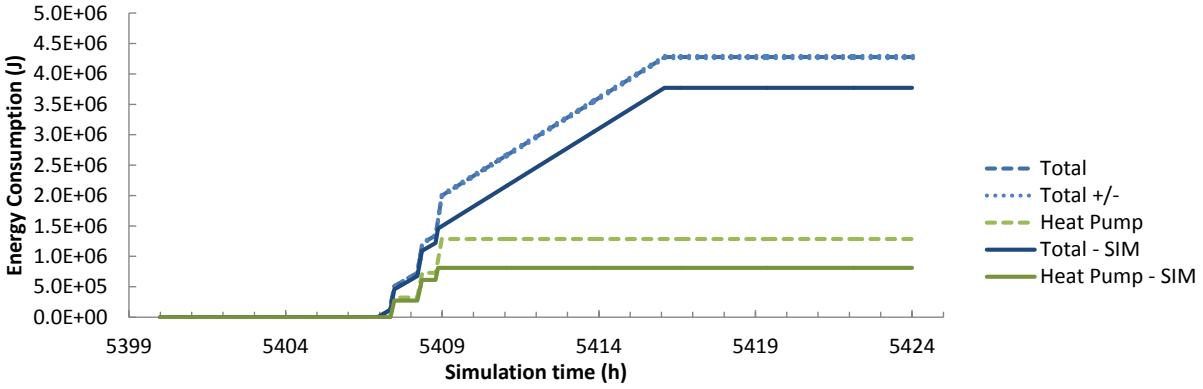

Figure 5.25 Comparison of ETU and TRNSYS model: cumulative electrical energy consumption - disabled element - Aug. 13th

Figure 5.25 presents a deviation between the experiment and TRNSYS model with respect to electrical energy consumption. The deviation is explained by observing the heat pump run time near hour 5409. Note that the simulated bottom tank temperature remained colder in the morning, see Figure 5.22. This meant that the TRNSYS ETU Controller would predict an increased solar energy collection in HX mode, and would therefore switch to HX mode sooner than in the experiment. As a result, the heat pump had a shorter total run time, accounting for the substantial deviation in electrical consumption. Again, deviation between the experiment and the model stemmed from deviation in tank temperatures. The difference in energy consumption in this case may seem large; however, the timing error in switching from HP mode use to HX mode differed by less than 10 minutes. It may be noted that for this comparison, the electrical energy consumption of the circulation pumps used in HX mode accounted for over half of the total energy consumption. Pump energy consumption became substantial when the DHW heating element consumption was suppressed.

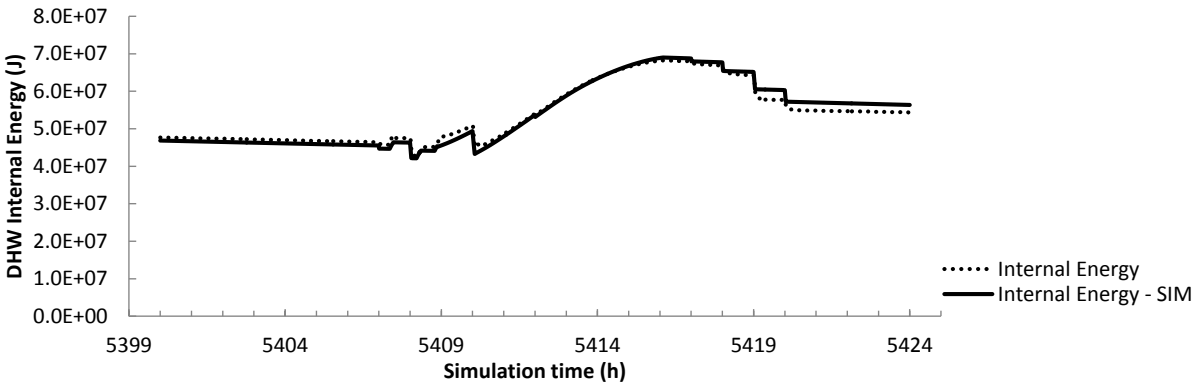

Figure 5.26 Comparison of ETU and TRNSYS model: DHW tank internal energy - disabled element - Aug. 13th

Throughout the course of the test, the internal energy of the DHW tank demonstrated a very close match in the trend of stored energy. Substantial differences towards the end of the day may be explained by a lack of resolution in temperature readings for the ETU DHW tank.

5.2 ETU - TRNSYS Comparison - October 28th - Ottawa

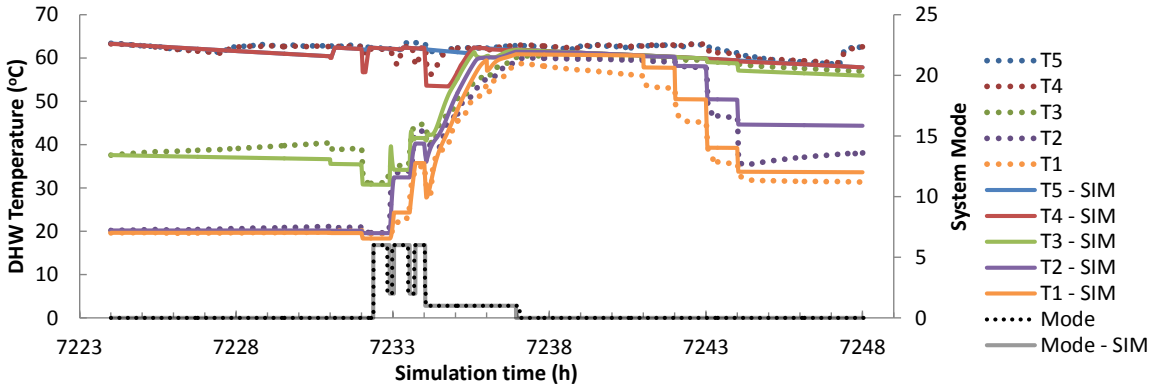

Figure 5.27 Comparison of ETU and TRNSYS model: DHW tank temperatures and system mode - Oct. 28th

The October 28th experimental test and simulation was run with an energized DHW heating element. Just like the August 13th comparison with an enabled DHW element, in this test, simulated DHW temperatures in the bottom half of the tank strayed from the experiment when the system switched to HX mode, see Figure 5.27. This reinforced earlier suggestions that in HX mode the reduced mixing, compared to HP mode, was not taken into consideration by the DHW tank model. As a result, the TRNSYS tank model over-predicted the use of the heating element within this period.

With the knowledge that the DHW tank model is an approximation of the true DHW tank, the October 28th test revealed the importance of the solar collection termination criteria. For the August

13th test with an enabled element, the collection termination criteria was the bottom tank temperature reaching a cut-out condition of 65℃. The result was the TRNSYS model halting solar collection much too early which caused significant error with respect to experimental results. In contrast, for the October 28th test, collection was terminated by a theoretical solar heat collection limit of $\dot{Q}'_u HX = 500\ W$. Though this theoretical heat collection limit had some temperature dependence, this termination criteria was much less sensitive to the bottom tank temperature. Once again, due to the simulation's elevated bottom tank temperature, solar collection in the simulation was terminated slightly early when compared to the experimental test; see simulation hour 7237 in Figure 5.28. However, the less sensitive termination meant the simulation matched the experimental results within experimental uncertainty. Simulations in which the bottom tank temperature reaches the high temperature cut-out of 65℃ will have some inherent inaccuracy. Simulations that are affected only by other cut-out conditions, such as solar heat collection limits, will provide a successful match to experiments.

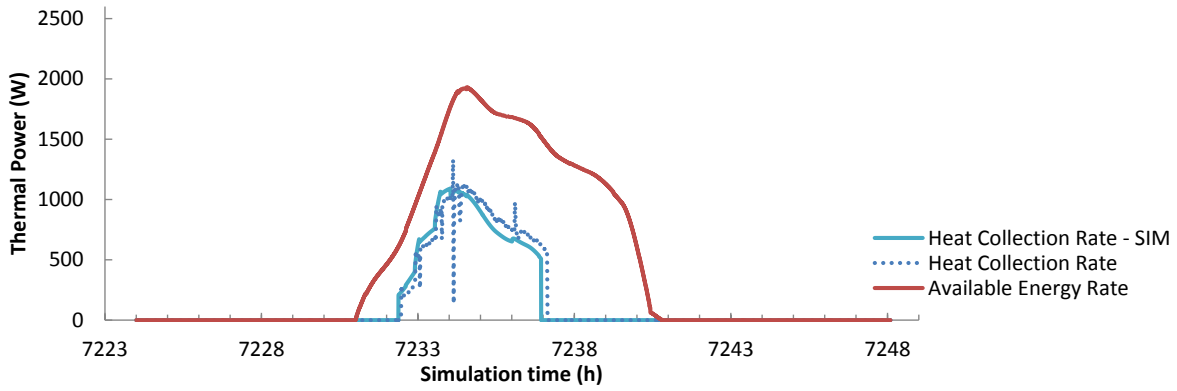

Figure 5.28 Comparison of ETU and TRNSYS model: available energy rate and simulated solar heat input - Oct. 28th

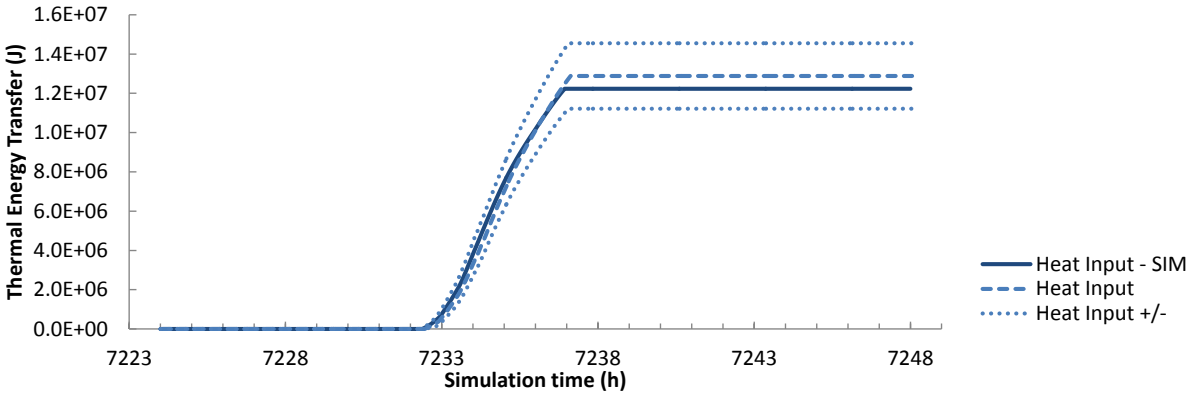

Figure 5.29 Comparison of ETU and TRNSYS model: cumulative simulated solar heat input - Oct. 28th

The simulated solar heat input to the system, Figure 5.29, demonstrated a very reasonable match between simulation and experiment. Although the TRNSYS heat addition by fluid, Figure 5.30, was a match within experimental uncertainty, it deviated further than might be expected after observing the match in cumulative solar heat input. The timing of heat pump cycling and the controlled switching to HX mode was responsible for this discrepancy. In the experiment, the HP briefly cycled on, (Mode 2), before switching to HX mode, (Mode 1). In the simulation, the system switched directly from the heat pump warm-up cycle, (Mode 6), to HX mode, (Mode 1). This meant that in the simulation, heat had been collected by the warm-up cycle in a similar fashion as the experiment; however, less of this heat was delivered to the DHW tank since the simulated TRNSYS HP did not run at hour 7234. Had the HP run time been matched more precisely, this discrepancy may have been averted. However, the switch to HX mode was once again influenced by the bottom tank temperature, and therefore, the timing had limited accuracy. The difference in timing for the switch to HX mode between the simulation and experiment was approximately 1 minute.

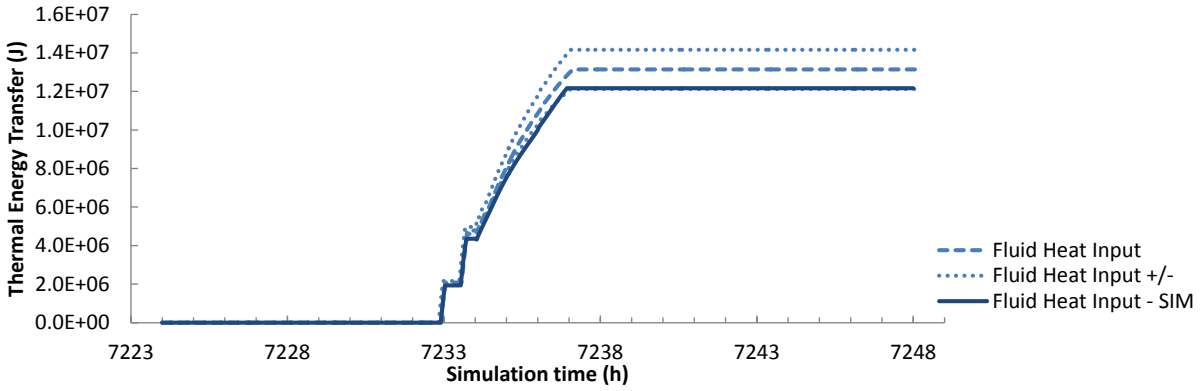

Figure 5.30 Comparison of ETU and TRNSYS model: cumulative DHW heat addition by fluid - Oct. 28th

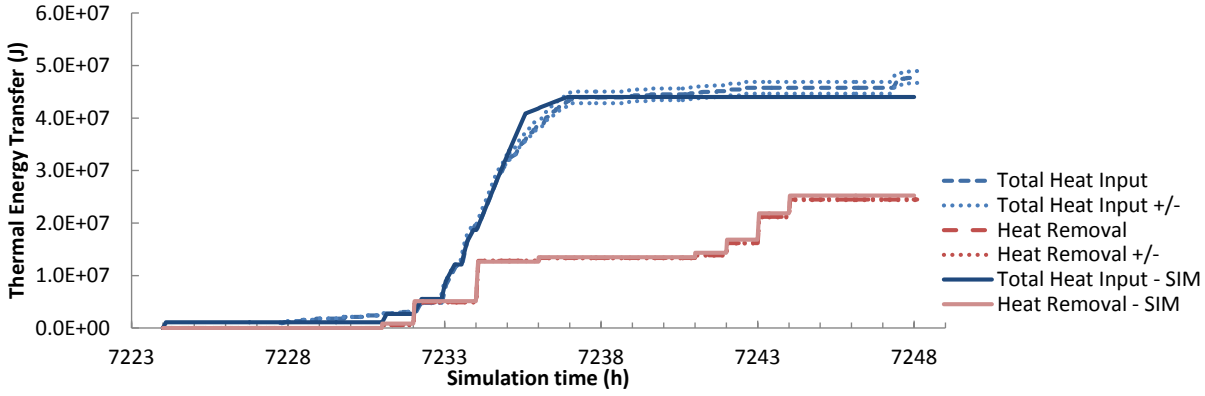

Figure 5.31 Comparison of ETU and TRNSYS model: cumulative DHW total heat addition and removal - Oct. 28th

The total heat addition to the DHW tank for the October 28th test showed a strong correlation between simulation and experiment, see Figure 5.31. Again, the excess heat addition by the DHW heating element was visible between simulation hours 5234 and 5237, and its impact is visible in both Figure 5.31 and Figure 5.32. By the time the solar collection period ended around hour 5237, the simulation and experimental tests matched up in terms of total heat addition to the DHW tank. After hour 5237 in the experiment, the DHW heating element began to add heat to the tank, while in the simulation, no heat was added. This is likely due to a slight difference in temperature near the center of the tank, where in the simulation no element heating was required since the temperature remained sufficiently high.

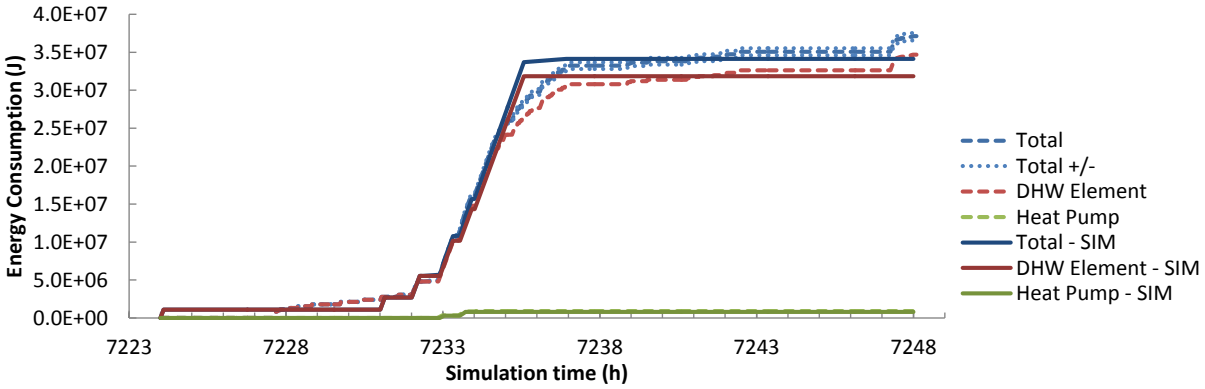

Figure 5.32 Comparison of ETU and TRNSYS model: cumulative electrical energy consumption - Oct. 28th

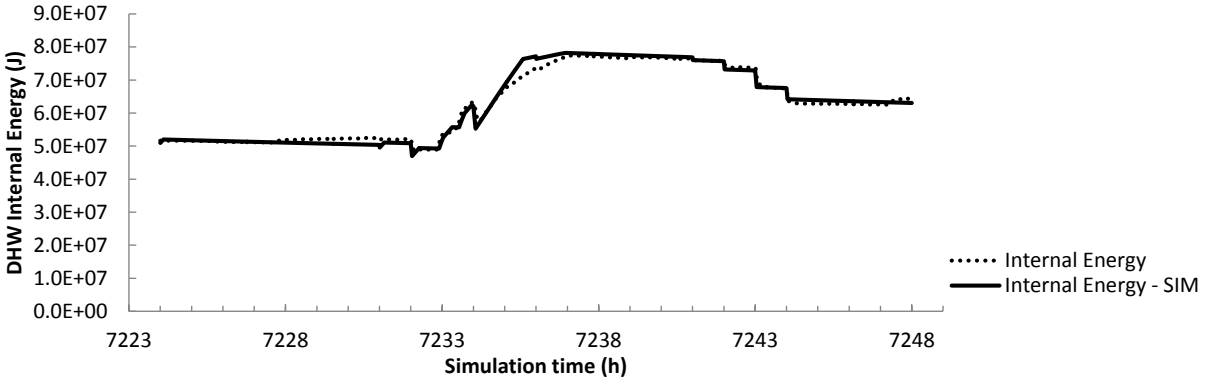

Figure 5.33 Comparison of ETU and TRNSYS model: DHW tank internal energy - Oct. 28th

Throughout the course of the October 28th test, in general the internal energy of the DHW tank once again demonstrated a very close match in energy storage trend. In this case, substantial deviation was visible between simulation hours 5234 and 5237, and corresponds to the simulation's excess use of the DHW heating element.

5.3 ETU - TRNSYS Comparison - January 12th - Ottawa

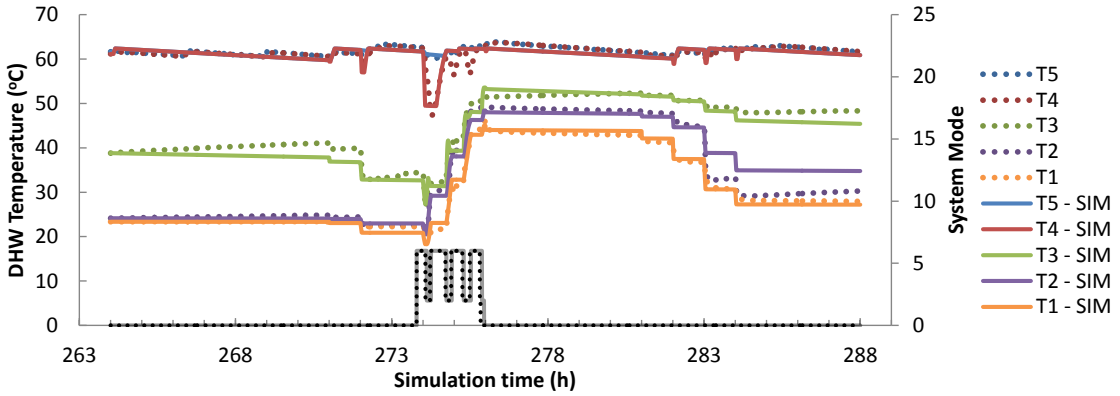

Figure 5.34 Comparison of ETU and TRNSYS model: DHW tank temperatures and system mode - Jan. 12th

The January 12th test represented the most accurate comparison between an ETU experiment and a TRNSYS simulation. Due to the lower levels of available radiation, in the January 12th test, the system was never allowed to switch to HX mode. In Sections 5.1 and 5.2, the simulation was shown to deviate from experimental results when in HX mode. Since the January 12th test avoided the use of the heat exchanger, the simulation was able to provide a much closer match. In Figure 5.34, particularly throughout the solar collection period, a substantial improvement in DHW tank temperature prediction is visible.

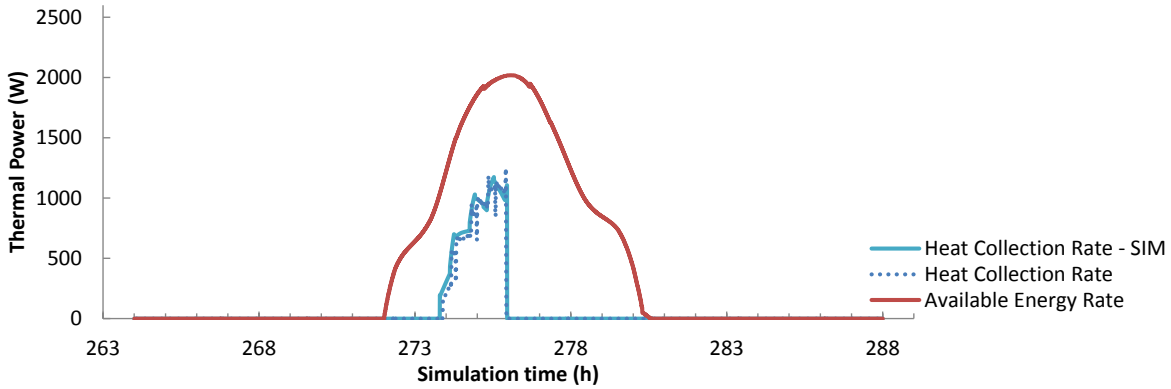

Figure 5.35 Comparison of ETU and TRNSYS model: available energy rate and simulated solar heat input - Jan. 12th

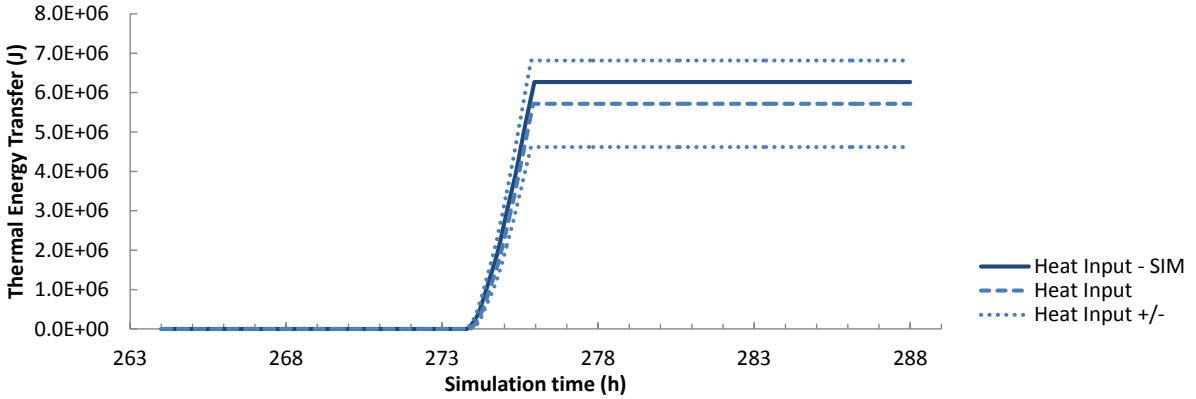

Figure 5.36 Comparison of ETU and TRNSYS model: cumulative simulated solar heat input - Jan. 12th

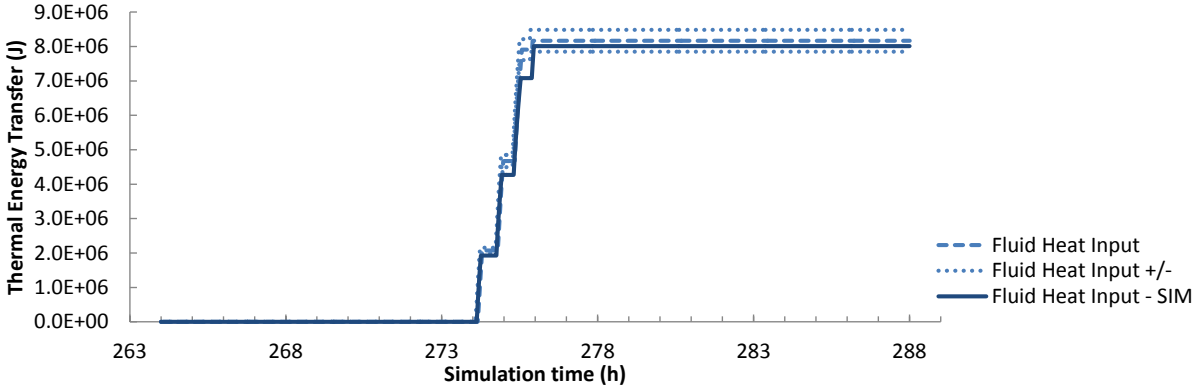

Figure 5.37 Comparison of ETU and TRNSYS model: cumulative DHW heat addition by fluid - Jan. 12th

Again, like the October 28th test, there was a slight discrepancy in HP cycling time. With the heat exchanger restricted, in this case, the bottom tank temperature was responsible for the termination of the solar collection period. In other tests, the bottom tank temperature had been a significant source of error; however, in this case, without the influence of HX mode, the bottom tank temperature was modelled very accurately. As a result, the TRNSYS simulated solar heat input, as well as the DHW heat addition by fluid, converged within experimental uncertainty. Factors affecting the HP cycling time include but are not limited to; the starting temperature, heat loss coefficient, and precise volume of the hot water buffering tank. Although the volume of a tank would ordinarily be a simple parameter to consider in a TRNSYS model, the buffering tank consists of an expansion tank with a largely deflated air bladder. The exact volume of this tank is unknown, and is subject to slight variation depending on the contained water temperature.

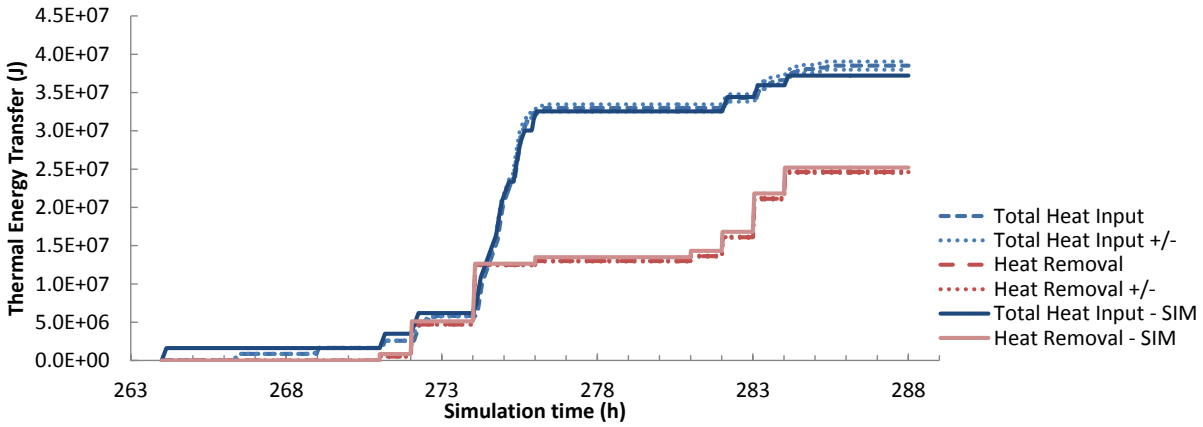

Figure 5.38 Comparison of ETU and TRNSYS model: cumulative DHW total heat addition and removal - Jan. 12th

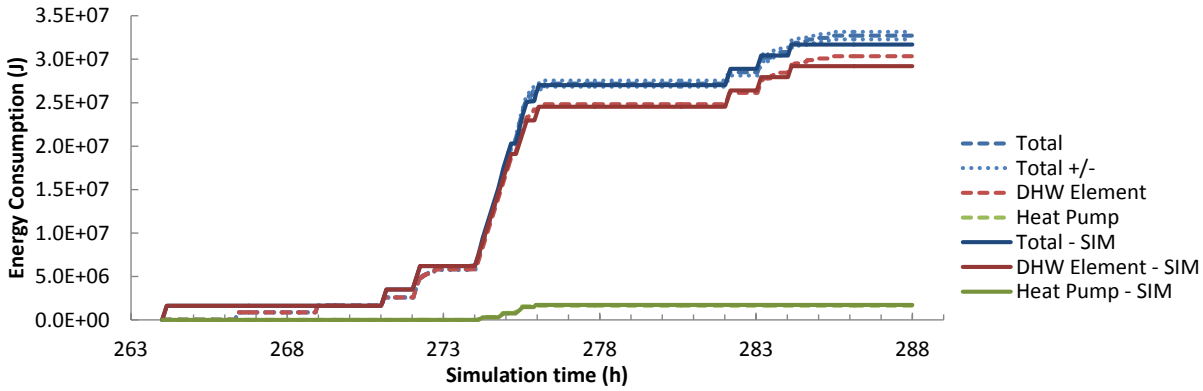

Figure 5.39 Comparison of ETU and TRNSYS model: cumulative electrical energy consumption - Jan. 12th

Without heat exchanger operation, there was no excess DHW heating element usage in the TRNSYS model. In the absence of excess DHW use, the temperatures in the lower portion of the DHW tank were more accurately predicted. With a better match in tank temperatures, the DHW element behaviour later in the day was better predicted by the January 12th TRNSYS model, see hour $282 - 284$ in Figure 5.39. Despite the slight deviation in DHW heating element use at the end of the day, both Figure 5.38 and Figure 5.39 present a strong qualitative match between the simulation and experimental results.

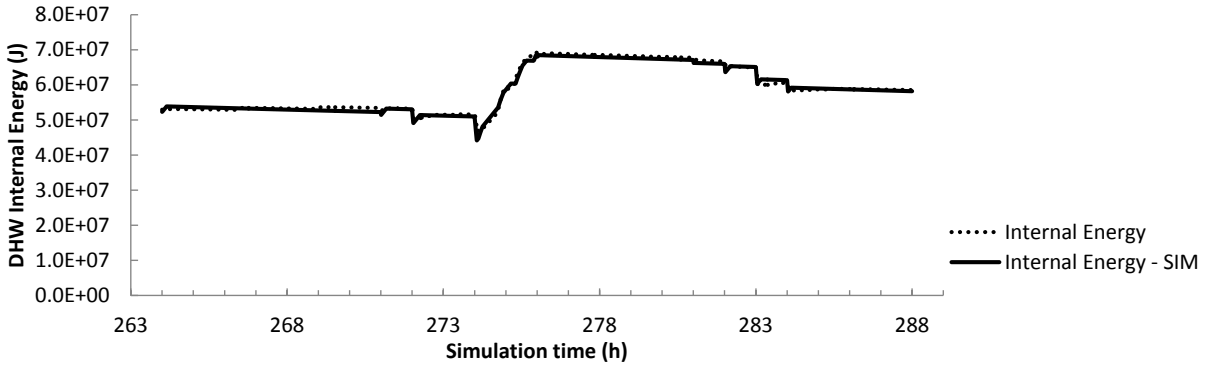

Figure 5.40 Comparison of ETU and TRNSYS model: DHW tank internal energy - Jan. 12th

Out of all of the TRNSYS simulations, the January 12th test provided the most accurate match to experimental results. Both strong qualitative and quantitative correlations were found between the simulation and experiment. Matching daily simulations both qualitatively and quantitatively is important for building confidence towards a successful annual simulation. The TRNSYS simulation of the Experimental Test Unit was sufficiently accurate so long as the solar collection period was not terminated by a DHW bottom tank temperature cut-out when the system had previously been running in HX mode. This reinforces the fact that simulating both moderate-flow HX and high-flow HP operation with the same TRNSYS tank model is challenging. This type of simulation has limited accuracy due to differences in mixing effects at the solar return port for significantly differing circulation flow rates.

Chapter 6 Conclusions and Recommendations

6.1 Conclusions

6.1.1 TRNSYS Model Validation

When attempting to match the performance of an experimental version of the Dual Side indirect heat pump assisted solar domestic hot water (I-HPASDHW) system with a TRNSYS simulation, the simulation performs with mixed results. Throughout the simulation process, a correlation was discovered between simulation error and the time spent collecting solar energy directly through the heat exchanger (HX). Days exhibiting lower levels of solar irradiation resulted in high quality experimental and simulation matches within experimental uncertainty. Higher levels of solar irradiation resulted in a poorer match between simulated and experimental results. Mixed results in simulation accuracy were largely attributed to matching domestic hot water (DHW) tank temperatures and electrical heating element operation using a built-in TRNSYS tank model. These effects often impacted control decisions, producing far-reaching consequences. Two major factors affected the quality of the system simulation; namely, the accuracy of modelled tank temperatures, and the controller's criteria used to terminate solar collection on a given day.

Throughout the experimental tests and corresponding TRNSYS simulations, deviation always occurred in DHW tank temperature approximations. Although all temperatures were approximations, the approximation of the bottom tank temperature had a particularly strong impact since this temperature was used in a number of control decisions. The temperatures in the lower part of the tank strayed more significantly when the system operated in heat exchanger mode. This was found to be due to a complex interaction between hot water circulation and the DHW electrical heating element, where solar return water mixing depended on circulation flow rate and was not replicated by the TRNSYS model.

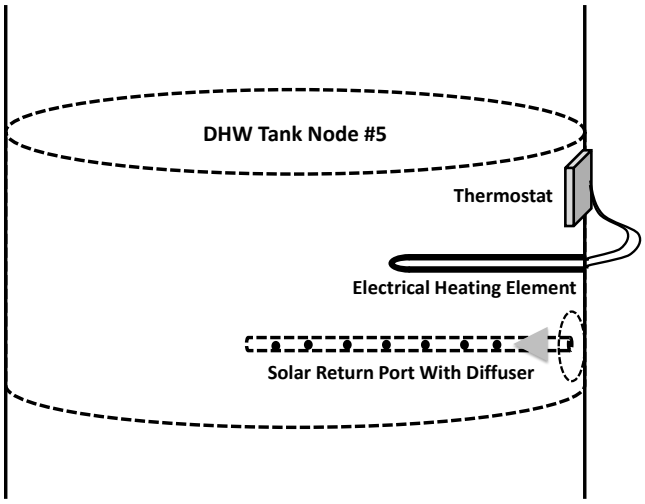

Figure 6.1 DHW Node Containing Solar Return, Thermostat, and Electrical Heating Element

The second major factor impacting the quality of match provided by the TRNSYS model was the Experimental Test Unit (ETU) Controller's criteria for the termination of solar collection. Inaccuracy was introduced any time a tank temperature was used to make a control decision, for example a change in modes. This was particularly true when a tank temperature was used to terminate the collection of solar energy, and especially when collection was terminated from HX mode. When the bottom tank temperature was used as a termination criterion for solar collection from HX mode, this temperature approximation became a significant source of error. This occurred only during the summer test since a sufficient quantity of heat was added to the tank to require termination of solar collection by the bottom tank temperature from HX mode. When less solar irradiation was available, the bottom tank temperature either remained low enough such that the termination criterion became the useful heat collection rate, or the heat exchanger was never operated. The most significant levels of simulation error found while matching summer tests are summarized in Table 6.1.

Table 6.1 Error involved with ETU and TRNSYS comparison for Aug. 13th

Cumulative Evaluation Metric	Simulation Error [%]
Simulated Solar Heat Input	14.3
DHW Heat Addition by Fluid	10.3
DHW Total Heat Input	1.14
Total Energy Consumption	8.71

It should be noted that certain limiting conditions programmed into the ETU Controller were intended to allow for safe operation of the ETU. For example, bottom tank temperature limits were used to avoid boiling conditions throughout the ETU. For a real system, such limitations are likely to be

relaxed, more often avoiding the bottom tank temperature termination criteria, allowing for improved simulations. Further, the sizing of the heat pump (HP) impacts the flow rate at which the system must operate in HP mode. Had the HP been small enough to match the flow rate of HX mode, a better fit between experiment and simulation may be found. Nevertheless, in the absence of a tank model which is capable of directing a specified fraction of electrically supplied heat to mix with circulating flow, simulation accuracy of the ETU's tank configuration is limited. Until such a tank model is developed, the positioning of components in the ETU's DHW tank will cause the TRNSYS model to predict excess electricity consumption during HX mode. The TRNSYS model may underestimate the benefits of operating in HX mode.

6.1.2 Dual Side I-HPASDHW System Design and Controls

6.1.2.1 DHW Tank and Electrical Heating Element Conclusions

In Section 5.1.1, the ETU's performance during a summer test is presented. Over the course of this 24 hour test, approximately 50% of the heat addition to the DHW tank was introduced by the electrical heating element. Although the tank started from a relatively uncharged condition, on a summer day one would expect a more substantial fraction of heat to be added by solar collection. The heating element was triggered by the circulation of fluid. From a design standpoint, this indicates the tendency of the ETU, and therefore the Dual Side I-HPASDHW system, to over-use the electrical backup element.

6.1.2.2 Heat Pump Conclusions

In the operation of a piece of equipment like a heat pump, it is important to closely manage equipment cycling. For a single tank HPASDHW system using an antifreeze-filled solar energy collection loop, the source side of the system has limited thermal mass. Further, the HP is intended to be operated under less than ideal solar heating conditions. Therefore, to avoid excessive cycling, the HP should be sized such that the source side heat transfer rate is matched to the capacity of the solar thermal array under moderate solar heating conditions. For the Dual Side I-HPASDHW system configuration of the ETU, the addition of thermal mass to the HP branch of the source loop was necessary. This allowed the heat pump to run for sufficiently long periods of time to avoid excessive cycling. Source side storage volume was integrated into the ETU using a dual port expansion tank. Adding a more substantial volume to the source side of the system comes at a significant cost and would lead to the system being classified as a dual tank system.

According to Sterling [17], adding a heat pump to a solar water heating system allows for improved solar collection when little solar radiation is available. This suggests improved collection in the morning, and later into the evening. However, the tests conducted with the ETU revealed a practical concern with respect to extending collection times. As is the case with the GX-W2W36, heat pump operating range is limited by source and load temperatures. In the operation of the ETU, the entering load temperature was found to be a significant limitation. Throughout testing of the ETU, the heat pump was not able to extend solar collection into the evening. The GX-W2W36 was not able to operate with inlet load temperatures in excess of $45℃$. Late into the afternoon, the bottom tank temperature was always in excess of $45℃$. Therefore, the heat pump was restricted from operating in the evening, limiting its solar collection benefits to the morning.

6.1.2.3 ETU Controller Conclusions

The ETU Controller was not optimized to maximize solar energy collection, instead favoring stability and predictability for validation. The impact associated with excluding control of the DHW electrical heating element from the ETU Controller is discussed in Section 6.1.2.1. Throughout the course of testing, control decisions detrimental to energy collection were noted. For example, for $\dot{Q}'_u HX < 500\ W$, heat exchanger operation was restricted even when the heat pump was not operational due to temperature limits. The $500\ W$ heat exchanger restriction meant that at times, both HX and HP were restricted while significant solar energy was available for collection. Whenever the DHW bottom tank temperature reached a sufficient temperature to restrict HP operation, no solar energy could be collected if the theoretical heat collection rate was less than $500\ W$. Over the course of full-day testing this restriction was not especially evident; however, for an annual simulation with the specified collector sizing, this restriction would have substantial consequences in terms of energy use.

6.2 Recommendations

6.2.1 Using the TRNSYS Model

The TRNSYS model of the Dual Side I-HPASDHW system should be used with care, but may be a very effective tool for comparative energy analysis for the optimization of the system. Adjustments to the Dual Side system may be applied through the model, using the ETU tests as baseline performance cases. In any future analyses, a number of simulation inaccuracies should be considered.

In simulations, the use of DHW tank temperatures to make sensitive control decisions should be limited wherever possible. The impact of the solar return port must be considered with the express

understanding that mixing effects in the built-in TRNSYS tank model cannot be accurately predicted for two substantially different flow rates in the current tank configuration. It has been shown that mixing effects are not always accurately predicted and that flow from the solar return port triggers the operation of the DHW electrical heating element. In annual simulations, it should be understood that there are inaccuracies in the activation of the DHW electrical heating element, and these inaccuracies may lead indirectly to early termination of solar collection due to excess electrical heating. In the current configuration, the TRNSYS model will over predict the use of the DHW heating element while the system is in HX mode; however, this may change drastically when modelling different tank configurations. Changes in behaviour should be expected particularly when the solar return port, DHW thermostat and electrical heating element positioning is significantly altered. Although small qualitative differences were found between ETU operation and the TRNSYS simulation, the simulation error was minimized through the use of common set-points, where the simulation often recovered from small deviations.

The most substantial factor affecting simulation accuracy is the criteria used to terminate solar energy collection for a given day. Compared to the validation study, for an annual performance simulation the high temperature cut-out limits used in controls could be relaxed. Further, cut-out limits could be applied to the top tank temperature only, a temperature which is generally modelled more accurately in TRNSYS simulations. Limiting the number of times solar collection is terminated by a high temperature cut-out condition and eliminating the dependence on bottom tank temperature will improve the quality of the simulation. Lastly, for annual simulations, a counter should be added to the controller such that the number of high temperature cut-outs occurring over the course of an annual simulation is tracked. This counter would provide an indication of the potential error associated with a given annual performance simulation.

A high level of confidence in each model has been established with the exception of the Type 4: Stratified Fluid Storage Tank. Custom models produced for the heat exchanger and heat pump have been validated only for the actual equipment size and the pre-set flow rates used in testing. Any changes such as scaling of these pieces of equipment, though useful for system optimization studies, have not been validated. Note that the use of a constant effectiveness heat exchanger may be sufficient for altered systems, but will introduce error associated with changes in fluid density when operating at constant mass flow rates. Note that the TRNSYS simulation is very sensitive to different tank configurations, where minor changes in key aspects may provide very different simulation results. Some changes to the control scheme such as altering the high temperature cut-out are likely to improve the

accuracy of simulations, while other control changes may be to the detriment of simulation accuracy. Lastly, model entries used for the validation of TRNSYS simulations against the ETU provide realistic baseline values to be used in future simulations.

6.2.2 Dual Side I-HPASDHW System Design and Controls

6.2.2.1 DHW Tank and Electrical Heating Element Recommendations

In order to improve the performance of the Dual Side I-HPASDHW system, several adjustments are recommended with respect to the DHW tank. The DHW thermostat was found to be triggered by water circulation through the solar return port, causing excess consumption of electricity. In order to reduce the activity of the electrical heating element, a more substantial diffuser should be added to the tank to further reduce the entrance plume. Plume reduction can also be encouraged by reducing the flow rate at which water is circulated. For example, a smaller heat pump may allow a lower flow rate to be used in HP mode. To separate the mutual influence between hot water circulation and DHW element activity, an adjusted DHW tank design would be beneficial. The vertical distance should be increased between the solar return port, and the electrical heating components. Note that increasing the ratio of solar collector area to volume of storage will increase tank charging, and is therefore likely to reduce electrical element use.

6.2.2.2 Heat Pump Recommendations

The heat pump installed on the ETU required both cycling and the addition of thermal mass to the source loop in order to operate effectively with a collector area of $2.494\ m^2$. A smaller heat pump is recommended to increase the cycle time also allowing a lower flow rate to be used and pump energy to be reduced. For improved control over the source loop temperature, a variable capacity heat pump using digital scroll or variable frequency drive technology may be useful. The use of such a device would avoid equipment cycling, and allow the heat pump to match the heat input of the solar collector. However, this is likely prohibitive until the cost of such technologies are reduced. Section 6.1.2.2, discusses the ETU's restriction of heat pump operation late into the afternoon. In order to take full advantage of a heat pump installed within the Dual Side I-HPASDHW system, the heat pump should be flexible in terms of source and load temperature limits. The heat pump should be able to operate with high inlet load temperatures, ideally in excess of $55℃$.

6.2.2.3 ETU Controller Recommendations

Since the ETU Controller was not optimized to maximize the collection of solar energy, a number of recommendations follow that are intended to improve system performance. Control over the DHW electrical heating element is strongly recommended to regulate the heating element's operation more closely and reduce electrical energy consumption. With the supply of solar energy and the load's hot water demand not always forming a match, the set level of daily tank charging is an important factor for energy performance. The desired level of daily DHW tank charging is controlled by high temperature cut-outs built into the ETU Controller. In order to improve electrical energy consumption, the high temperature cut-out should be set as high as possible while maintaining operational safety.

A number of ETU Controller settings should also be optimized for improved system performance. The set-points and dead bands for theoretical heat collection rates used to make a number of control decisions, $\dot{Q}'_u HX$ and $\dot{Q}'_u HP$, should be investigated. If desired, these collection rates could be calculated per unit of solar collector area to draw a relation between heat collection set-points and the level of solar irradiation. As discussed in Section 6.1.2.3, the current version of the ETU controller restricts the use of HX mode for a condition of $\dot{Q}'_u HX < 500W$. Instead of completely restricting HX operation, the $\dot{Q}'_u HX$ limit should be used in conjunction with supplementary conditions to give priority to the heat pump under low radiation conditions. When the $\dot{Q}'_u HP$ limit is satisfied, but HP operation is restricted by DHW temperatures, HX mode should be allowed to operate. Supplementary conditions that could be used to encourage HP operation might include factors like time of day and the amount of heat stored in the DHW tank. For example, it may be beneficial to eliminate morning heat pump operation if the DHW tank has reached certain threshold temperatures indicating that significant thermal energy has been stored. The current controls would substantially limit the collection of solar energy.

6.2.3 Future Work

When conducting investigations of energy systems combining multiple mechanical components, advanced controls, and external influences, a virtually inexhaustible number of studies are possible. In this section, specific factors that may impact the viability and performance of HPASDHW systems are presented. With respect to the Dual Side I-HPASDHW system, a variety of parameters are available for a future multi-dimensional system optimization studies:

- Sizing of the solar array, heat pump, heat exchanger, DHW tank, and electrical heating element
- Equipment and operational changes
    - Set pumping speeds and possibly variable speed pumping
    - Different heat pump selections with capacity modulation and flexible temperature limits
    - Increased spacing between solar return port and thermostat with heating element
- Altered and additional function of the ETU Controller
    - Theoretical heat collection rate settings and dead bands
    - High temperature cut-out limits and dead bands
    - Reducing restrictions on heat exchanger operation
    - Control over the DHW thermostat

If the performance of the Dual Side I-HPASDHW system were improved, a number of advanced studies may be useful for outlining the best possible system and controller, as well as re-evaluating the viability of such systems:

- Household hot water load prediction strategies for control decisions
- Outdoor temperature and solar radiation prediction strategies for control decisions
- The use of genetic algorithms for adaptive control strategies
- System performance evaluation for several geographic locations
- The impact of time of day energy billing
- Economic analysis of the Dual Side I-HPASDHW system and competitive technologies

Taking inspiration from the Dual Side I-HPASDHW system and the systems outlined in Sterling [17], a number of substantially altered systems may be worth investigating:

- A 2-tank HPASDHW system with a solar energy buffering tank allowed to float in temperature
    - Allowing simultaneous collection of solar energy and Float-to-DHW tank heat transfer
- Adding an air-source heat exchanger possibly incorporating an unglazed collector
    - Using the unglazed collector as both air-source and optional solar pre-heat collector
- A system simultaneously using the heat pump and heat exchanger in series, where heat transfer first occurs in the heat exchanger and is later boosted using the heat pump
- Community scale systems

References

[1] International Energy Agency (IEA), "Key World Energy Statistics 2010," 2010. [Online]. [Accessed 19 January 2011].

[2] R. Bentley, "Global oil & gas depletion: an overview," *Energy Policy,* vol. 30, pp. 189-205, 2002.

[3] The White House: Office of the Press Secretary, "Remarks by the President to the Nation on the BP Oil Spill," 15 June 2010. [Online]. Available: http://www.whitehouse.gov/the-press-office/remarks-president-nation-bp-oil-spill. [Accessed 24 July 2011].

[4] Intergovernmental Panel on Climate Change (IPCC), "Climate Change 2007: Synthesis Report," [Online]. Available: http://www.ipcc.ch/publications_and_data/publications_ipcc_fourth_assessment_report_synthesis_report.htm. [Accessed 19 January 2011].

[5] Natural Resources Canada, "Adapting to Climate Change: An Introduction for Canadian Municipalities," 2010. [Online]. Available: http://adaptation.nrcan.gc.ca/mun/index_e.php. [Accessed 20 January 2011].

[6] A. . M. Omer, "Energy, environment and sustainable development," *Renewable and Sustainable Energy Reviews,* vol. 12, p. 2265–2300, 2008.

[7] Natural Resources Canada: Office of Energy Efficiency, "Energy Use Data Handbook 1990 to 2007," 2010. [Online]. Available: http://oee.nrcan.gc.ca/publications/statistics/handbook09/pdf/handbook09.pdf. [Accessed 22 July 2011].

[8] U.S. Energy Information Administration, "2009 Annual Energy Review," [Online]. Available: http://www.eia.gov/totalenergy/data/annual/. [Accessed 22 July 2011].

[9] U.S. Department of Energy: Energy Efficiency and Renewable Energy, "Buildings Energy Databook 2010," [Online]. Available: http://buildingsdatabook.eren.doe.gov/DataBooks.aspx. [Accessed 22 July 2011].

[10] Natural Resources Canada: Office of Energy Efficiency, "Types of Water Heaters," [Online]. Available: http://oee.nrcan.gc.ca/residential/personal/water-heater-types.cfm?attr=4. [Accessed 28 January 2011].

[11] Natural Resources Canada: Office of Energy Efficiency, "Water Heaters: Energy Considerations," [Online]. Available: http://oee.nrcan.gc.ca/residential/personal/water-heater-oil-electric.cfm?attr=4#electric. [Accessed 27 July 2011].

[12] Natural Resources Canada: Office of Energy Efficiency, "Survey of Household Energy Use 2007: Summary Report," [Online]. Available: http://oee.nrcan.gc.ca/publications/statistics/sheu-summary07/pdf/sheu-summary07.pdf. [Accessed 27 July 2011].

[13] Natural Resources Canada: Office of Energy Efficiency, "Heating With Gas," [Online]. Available: http://oee.nrcan.gc.ca/publications/infosource/pub/home/Heating_With_Gas_Chapter8.cfm?attr=4. [Accessed 27 July 2011].

[14] U.S. National Aeronautics and Space Administration, "The Earth Radiation Budget Experiment (ERBE)," 2005. [Online]. Available: http://asd-www.larc.nasa.gov/erbe/components2.gif. [Accessed 16 August 2011].

[15] U.S. National Aeronautics and Space Administration, "Climate and Earth's Energy Budget," 2009. [Online]. Available: http://earthobservatory.nasa.gov/Features/EnergyBalance/. [Accessed 18 August 2011].

[16] M. Chandrashekar, N. Le, H. Sullivan and K. Hollands, "A comparative study of solar assisted heat pump systems for Canadian locations," *Solar Energy,* vol. 28, pp. 217-226, 1982.

[17] S. Sterling, "Feasibility analysis of two indirect heat pump assisted solar domestic hot water systems," 2011.

[18] Y. Kuang, R. Wang and L. Yu, "Experimental study on solar assisted heat pump systems for heat supply," *Energy Conversion and Management,* vol. 44, pp. 1089-1098, 2003.

[19] A. Shahed and S. Harrison, "Preliminary Review of Geothermal Solar Assisted Heat Pumps," in *4th Annual Canadian Solar Buildings Conference*, Toronto, June 25-27, 2009.

[20] J. Duffie and W. Beckman, Solar Engineering of Thermal Processes, 3rd Edition ed., New York: Wiley, 2006.

[21] U.S. Department of Energy: Energy Efficiency and Renewable Energy, "Energy Savers," [Online]. Available: http://www.energysavers.gov/your_home/water_heating/index.cfm/mytopic=12850. [Accessed 4 August 2011].

[22] Z. Lavan and J. Thompson, "Experimental study of thermally stratified hot water storage tanks," *Solar Energy,* vol. 19, pp. 519-524, 1977.

[23] K. Hollands and M. Lightstone, "A review of low-flow, stratified-tank solar water heating systems," vol. 43, no. 2, pp. 97-105, 1989.

[24] A. Fanney and S. Klein, "Thermal performance comparisons for solar hot water systems subjected to various collector and heat exchanger flow rates," vol. 40, no. 1, pp. 1-11, 1988.

[25] B. Huang and C. Lee, "Long-term performance of solar-assisted heat pump water heater," *Renewable Energy,* vol. 29, pp. 633-639, 2003.

[26] A. Nuntaphan, C. Chansena and T. Kiatsiriroat, "Performance analysis of solar water heater combined with heat pump using refrigerant mixture," *Applied Energy,* vol. 86, pp. 748-756, 2009.

[27] J. Kreider, P. Curtiss and A. Rabl, Heating and Cooling of Buildings: Design for Efficiency, 2 ed., Boca Raton: CRC/Taylor & Francis, 2010.

[28] H. Jin and J. Spitler, "Parameter estimation based model of water-to-water heat pumps with scroll compressors and water/glycol solutions," *Building Services Engineering Research and Technology,* vol. 24, pp. 203-219.

[29] Emerson Climate Technologies, "Digital Scroll Heating Technology," [Online]. Available: http://www.digitalscroll.com/sb300/portal/home/normal/41. [Accessed 31 January 2011].

[30] Y. Kuang, K. Sumathy and R. Wang, "Study on a direct-expansion solar-assisted heat pump water heating system," *International Journal of Energy Research,* vol. 27, pp. 531-548, 2003.

[31] S. Chaturvedi, D. Chen and A. Kheireddine, "Thermal performance of a variable capacity direct expansion solar-assisted heat pump," *Energy Conversion and Management,* vol. 39, pp. 181-191, 1998.

[32] A. Bridgeman and S. Harrison, "Preliminary experimental evaluations of indirect solar assisted heat pump systems," in *3rd Canadian Solar Buildings Conference*, Fredericton, August 20-22, 2008.

[33] T. Anderson and G. Morrison, "Effect of load pattern on solar-boosted heat pump water heater performance," *Solar Energy,* vol. 81, pp. 1386-1395, 2007.

[34] G. Freeman and S. Harrison, "Solar Assisted Heat Pump Hot Water Heaters for the Canadian Environment," in *Proceedings of the SESCI Conference*, Vancouver, 1997.

[35] R. Lazzarin and M. Noro, "District heating and gas engine heat pump: Economic analysis based on a case study," *Applied Thermal Engineering,* vol. 26, pp. 193-199, 2006.

[36] A. Hepbasli and Y. Kalinci, "A review of heat pump water heating systems," *Renewable and Sustainable Energy Reviews,* vol. 13, pp. 1211-1229, 2009.

[37] A.O. Smith, "Cirrex® SUN Direct Solar Booster Tanks," February 2011. [Online]. Available: http://www.hotwater.com/water-heaters/residential/solar/cirrex-sun-direct-solar-booster-tanks/sun-80-and-120/. [Accessed 2011].

[38] Canadian Standards Association, "Packaged solar domestic hot water (liquid-to-liquid heat transfer)," CSA, 2009.

[39] University of Wisconsin - Solar Energy Laboratory, "TRNSYS 16: a TRaNsient SYstem Simulation program, Volume 1: Getting Started," 2006.

[40] University of Wisconsin - Solar Energy Laboratory, "TRNSYS 16: a TRaNsient SYstem Simulation program, Volume 5: Mathematical Reference," 2006.

[41] Solar Rating & Certification Corporation, "OG-100 Operating Guidelines for Certifying Solar Collectors," 2012. [Online]. Available: http://www.solar-rating.org/standards_guidelines/OG100_document.pdf.

[42] Solar Rating & Certification Corporation, "Solar Collector Certification and Rating: Model 100-F, SV1/SH1," 2010. [Online]. Available: http://www.viessmann.ca/etc/medialib/internet-ca/pdfs/doc/vitosol.Par.47173.File.tmp/Vitosol_100-F_SRCC_Cert.pdf. [Accessed 2012].

[43] Y. A. Çengel, HEAT AND MASS TRANSFER A Practical Approach, New York: McGraw-Hill, 2007.

[44] "Online Curve And Surface Fitting," [Online]. Available: http://zunzun.com/. [Accessed 2012].

[45] R. J. Moffat, "Describing the Uncertainties in Experimental Results," *Experimental Thermal and Fluid Science,* vol. 1, pp. 3-17, 1988.

Appendix

Appendix A Characterization Data

A.1 Equipment Characterization

In order to match simulations in TRNSYS with the performance of the Experimental Test Unit (ETU), a characterization of each major component is necessary. To facilitate the collection of data, several virtual instruments have been constructed which generate and populate Microsoft Excel worksheets. Characterization VIs are started and stopped manually, but have been programmed to include several features. For example, the characterization virtual instruments (VIs) allow for data to be collected in time increments selected by the user. Further, several characterization VIs are programmed to collect data in selected nominal temperature increments and within windows of temperature. For example; the heat pump (HP) characterization VI was programmed to collect data at every $10℃$ nominal increment, and within a specified window $\pm\ 0.5℃$ of the increment.

A.2 Storage Tank Tests

The TRNSYS simulation of the domestic hot water (DHW) tank provides a number of parameters with which the tank model may be tuned. In order to determine the appropriate settings, simulations have been matched to simplified tests designed to investigate DHW tank behaviour.

In a standby-loss test, the DHW tank installed on the ETU had been heated to an elevated temperature and was left to cool from a stratified condition. In Figure A.1, the standby-loss test demonstrated a successful match between measured and simulated temperatures over an extended period of time. This test depicts results observed once the DHW tank had time to settle and reach its maximum level of stratification. If fluid flows enter or leave the tank, mixing effects may be observed, where the impact of these effects may take a number of hours to cause maximum stratification. Note that the numbering order for DHW tank temperatures starts from T1 representing the bottom of the tank, to T5 representing the top of the tank.

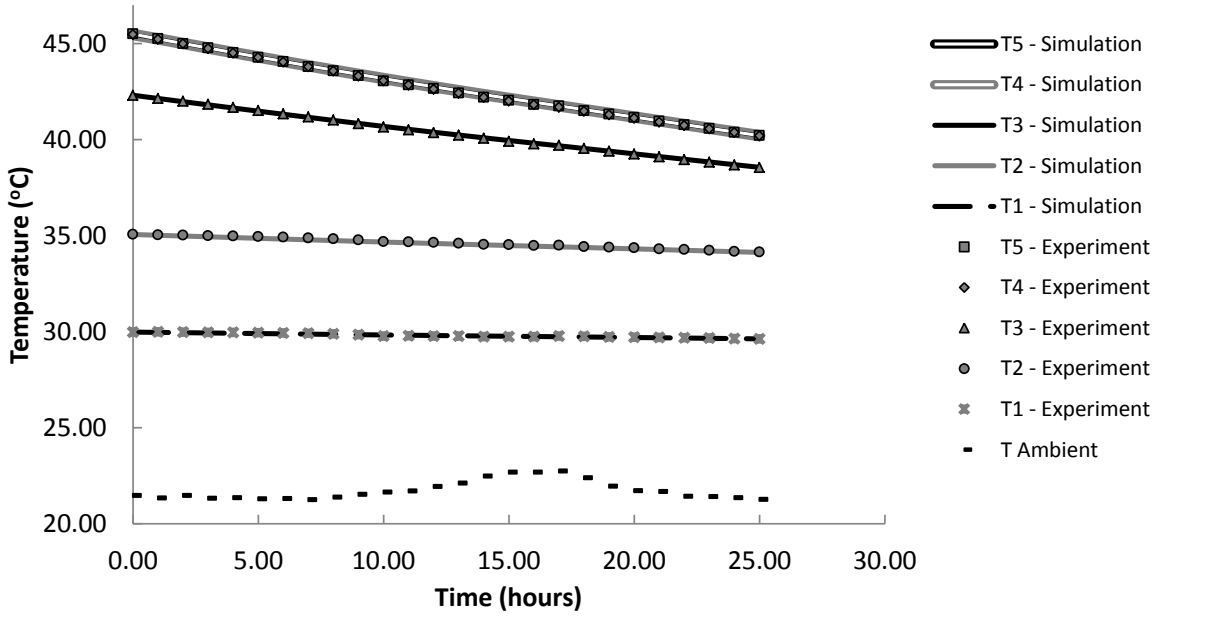

Figure A.1 Experimental and simulation results for DHW standby loss

In Figure A.2, a DHW tank charging test is shown where the ETU was run in heat exchanger (HX) mode at full circulation heater capacity. The results shown in Figure A.2 demonstrated that the DHW tank model's predicted temperatures significantly deviate from experimental results. This deviation is mainly due to a number of mixing effects which are either approximated or completely missed by the tank model.

Despite its placement significantly above the inlet solar return port, temperature sensor T4 of the ETU is influenced by incoming water flow. This effect is difficult to simulate using the stratified storage tank model. In the lower half of the tank, the simulated temperatures appear to be averaged over time, not reflecting the temperature swings shown in experimental results. This averaging effect is logical given the uniform node temperature assumption in place in the DHW tank model. The deviations between the experimental results and the TRNSYS simulation are not unique to the tuned tank model. A number of other modelled tank configurations demonstrated similar deviations with modest improvements in some cases. These improvements shown in charging tests came at the expense of increased deviations when full-day tests are simulated.

Over the course of full-day tests, where hot water draws occur and the system runs in HP mode, the observed mixing effects taking place in the real DHW tank are a better match to the TRNSYS simulation. It may also be noted that despite significant deviations between simulation and

experiments, there was a recovery as the DHW tank became increasingly charged. Approximately 90 minutes into the charging test, the model and experimental results began to synchronize. The tuned 10-node DHW tank model is an acceptable approximation for the ETU DHW tank, where it should be noted that deviations in stratification effects will impact other components within the system simulation.

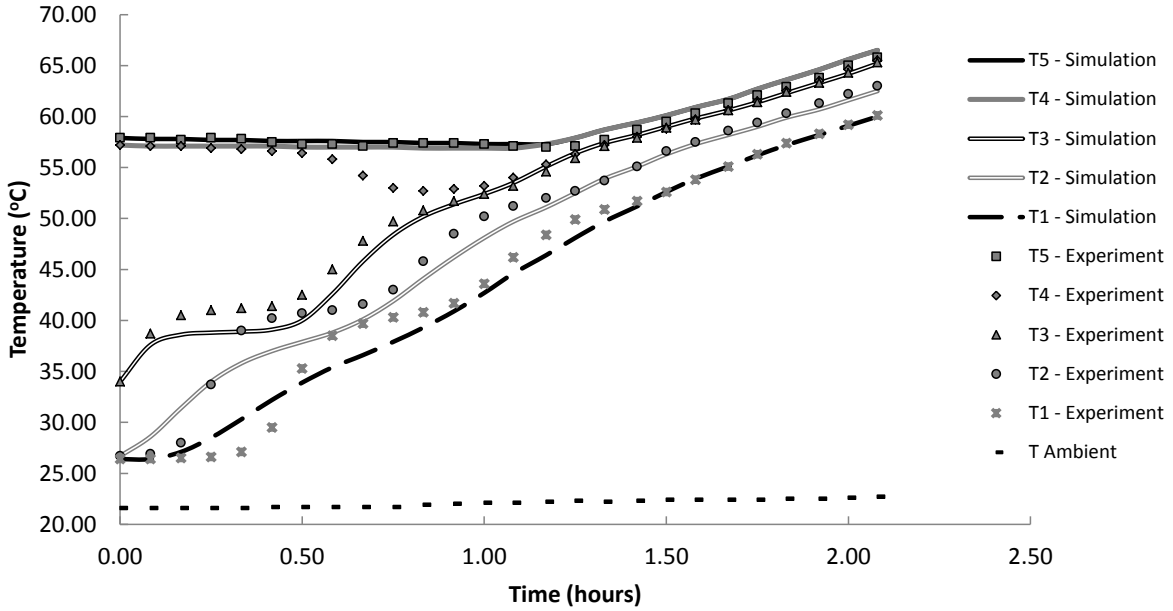

Figure A.2 Experimental and simulation results for DHW charging test with constant power heat source

The final stage in producing a successful DHW tank model is to calibrate the DHW thermostat and electrical heating element. Based upon over 700 measured data points, the average power of the DHW element was $3.1\ kW$. The DHW thermostat has also been observed switching on and off, where an additional temperature sensor was temporarily installed adjacent to the thermostat's temperature measurement surface. These observations revealed a consistent thermostat set-point of $62.4℃$ with a thermostat dead band of $5.9℃$.

A.3 Performance Mapping: Heat Exchanger

The performance of the heat exchanger was characterized through the use of heat exchanger effectiveness. When in heat exchanger mode, the ETU attempts to run at a constant mass flow rate of $5\ kg/min$ on both source and load sides. With a constant flow rate, the heat exchanger effectiveness was mapped over a variety of inlet source and load temperatures.

In Figure A.3, the planned mapping lines are shown. This figure represents the numerous points at which data might be collected to produce a heat exchanger performance map. The zero heat transfer line occurs when source and load fluids enter the heat exchanger at the same temperature. Producing the mapping lines parallel to the zero heat transfer line provide useful data and are simple to generate experimentally. For the full power test, the DHW tank was first flushed to the lowest temperature possible, in the range of $10 - 20℃$. The heater was then set to maximum power, transferring heat to the DHW tank through the heat exchanger. As the DHW tank temperature rose over the course of hours, heat exchanger data was collected at specified increments of inlet load temperature.

During actual heat exchanger tests, a 25-point average, completely refreshing approximately every 12.5 seconds, was applied to the source and load heat transfer rates. The desired data points were acquired within a window of $\pm\ 0.5℃$ of the desired inlet load temperature and were taken every 15 seconds. Depending on the desired condition, this resulted in a set of data of approximately 15 readings which could then be averaged to produce a single point of performance.

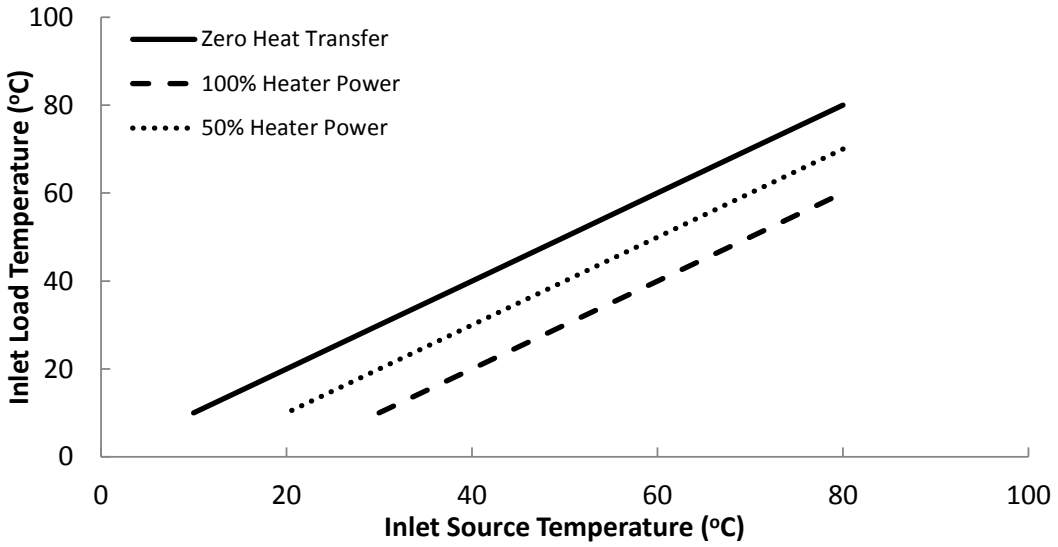

Figure A.3 Heat exchanger mapping plan

The effectiveness of a heat exchanger can be defined through Equations (A.1)-(A.3), where the values measured in the experiment were: $\dot{m}_h$, $\dot{m}_c$, $T_{h,i}$, $T_{c,i}$, and $\dot{Q}$. These equations are fundamental to any heat transfer text book covering heat exchanger analysis, such as Çengel [43].

$$C_h = C_{p,h} \cdot \dot{m}_h$$
$$C_c = C_{p,c} \cdot \dot{m}_c \quad \text{(A.1)}$$

$$C_{min} = \min(C_h, C_c) \quad \text{(A.2)}$$

$$\varepsilon = \frac{\dot{Q}}{\dot{Q}_{max}} = \frac{\dot{Q}}{C_{min}(T_{h,i} - T_{c,i})} \quad \text{(A.3)}$$

In TRNSYS, counter flow heat exchanger models are available which use either constant effectiveness or constant heat transfer coefficients. Experimentally determined performance of the SL15-25 heat exchanger showed that neither the effectiveness nor the overall heat transfer coefficient was constant. With variation in ε, a map of performance based upon inlet source and load temperatures was required. Upon investigation, a correlation was found between heat exchanger effectiveness and the average of inlet source and inlet load temperatures. The equation describing heat exchanger effectiveness in terms of average inlet temperature is presented below. The correlation between effectiveness and average inlet temperature was significant and worth accounting for. However, the coefficient of determination, $R^2 = 0.736$, demonstrated that this trend-line was far from a perfect fit. For a graphical representation of the correlation between averaged heat exchanger effectiveness readings and the average of inlet temperatures, see Figure A.4. Although deviations in the trend-line are statistically significant, Figure A.4 demonstrates that the absolute error of each data point is small.

$$\varepsilon = 1.01x10^{-3}(T_{avg}) + 0.579 \quad \text{(A.4)}$$

Where T_{avg} [℃] is the average of inlet source and inlet load temperatures

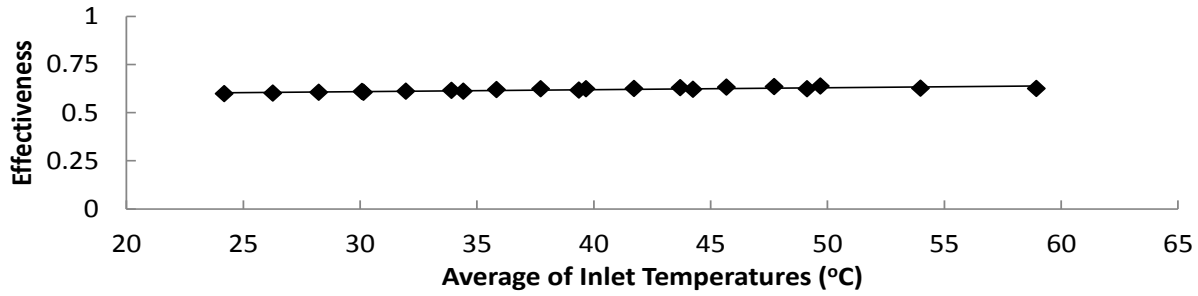

Figure A.4 Effectiveness correlation for SL15-25 heat exchanger

Table A.1 Data table of averaged values used for heat exchanger characterization

T_{source} [℃]	T_{load} [℃]	$\dot{Q}HX$ [W]	εHX
39.9	**20.4**	4090	0.605
43.9	**24.9**	4030	0.611
48.8	**29.9**	4039	0.617
53.5	**35.0**	3964	0.620
58.2	**40.0**	3957	0.624
62.9	**45.0**	3907	0.627
67.9	**50.0**	3800	0.626
28.6	**19.8**	1834	0.599
30.5	**22.0**	1787	0.601
32.4	**24.0**	1767	0.606
34.2	**26.0**	1743	0.609
35.9	**28.0**	1685	0.611
37.8	**30.0**	1659	0.616
39.7	**32.0**	1637	0.619
41.4	**34.0**	1610	0.624
43.4	**36.0**	1606	0.624
45.4	**38.0**	1617	0.625
47.4	**40.0**	1615	0.629
49.4	**42.0**	1624	0.632
51.4	**44.0**	1626	0.635
53.4	**46.0**	1635	0.638

A.4 Performance Mapping: Heat Pump

The performance of the heat pump was characterized through the measurement of three energy transfer rates describing equipment performance, namely, source heat removal, load heat addition, and compressor power consumption. When in heat pump mode, the ETU attempts to run at a constant flow rate of $10.75\ kg/min$ on both source and load sides. With a constant flow rate, the heat pump was mapped over a variety of inlet source and load temperature conditions.

Heat pump testing was executed in a similar fashion to heat exchanger testing. The DHW tank was first flushed to the lowest temperature possible, approximately 15℃. For heat pump testing, the circulation heater was set to maintain a set source temperature, transferring heat to the source side of the heat pump. As the DHW tank temperature rose over the course of hours, heat pump data was collected at specified increments of inlet load temperature. This process was repeated for a number of set source temperatures to produce a map as complete as possible.

Table A.2 Data table of averaged values used for heat pump characterization

T_{source} [°C]	T_{load} [°C]	$\dot{Q}_{source}$ [W]	$\dot{Q}_{load}$ [W]	$\dot{W}_c$ [W]	COP
9.6	**15.3**	3090	3526	564	6.3
9.6	**20.0**	2930	3420	624	5.5
9.5	**24.9**	2815	3290	685	4.8
9.6	**30.1**	2681	3178	760	4.2
9.6	**35.0**	2545	3020	840	3.6
9.6	**40.0**	2382	2938	941	3.1
9.7	**45.1**	2245	2859	1058	2.7
9.7	**50.0**	2088	2771	1189	2.3
14.4	**15.3**	3627	3912	550	7.1
14.5	**19.9**	3470	3864	611	6.3
14.5	**24.9**	3363	3769	677	5.6
14.5	**29.9**	3197	3624	750	4.8
14.6	**35.0**	3026	3456	836	4.2
14.7	**40.0**	2868	3423	937	3.7
14.7	**45.0**	2731	3281	1054	3.1
14.6	**50.0**	2519	3164	1188	2.7
19.3	**19.9**	3907	4529	607	7.4
19.3	**25.0**	3814	4341	671	6.5
19.3	**29.9**	3647	4161	744	5.6
19.4	**35.0**	3503	3979	833	4.8
19.4	**40.0**	3312	3882	936	4.1
19.4	**45.0**	3164	3714	1057	3.5
26.9	**30.1**	4547	4981	751	6.7
27.3	**34.9**	4400	4752	840	5.7
28.8	**40.0**	4405	4854	947	5.1
29.4	**44.9**	4181	4690	1071	4.4
29.4	**49.8**	3932	4690	1223	3.8

The performance maps resulting from heat pump testing are shown in Figure A.5 through to Figure A.8. These maps were generated by processing data from Table A.2 with the assistance of an online curve and surface fitting software [44]. The trends observed in mapped performance were consistent with the results presented in Anderson and Morrison [33]. Trends within the observed performance of the GX-W2W36 heat pump are described below:

- Source and load heat transfer rates increased strongly with increases in source temperature
- Source and load heat transfer rates increased moderately with decreases in load temperature
- Compressor power was almost entirely governed by the load temperature
- COP was improved for low load temperatures, where the influence of compressor power is evident

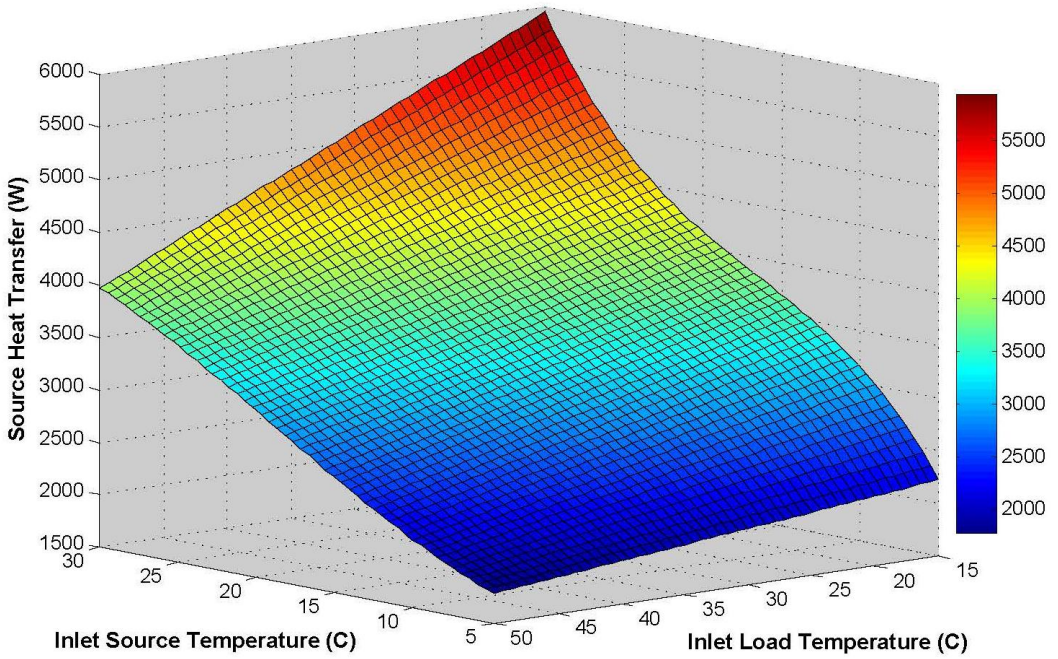

Figure A.5 Source heat transfer map for the GX-W2W36 heat pump

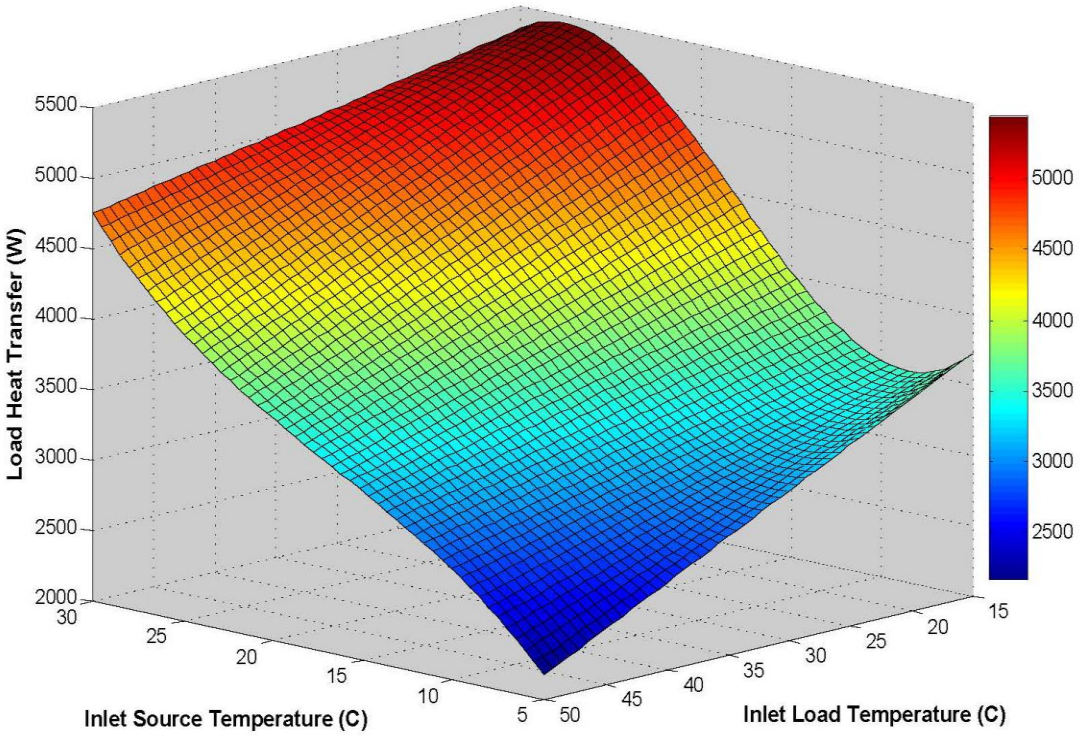

Figure A.6 Load heat transfer map for the GX-W2W36 heat pump

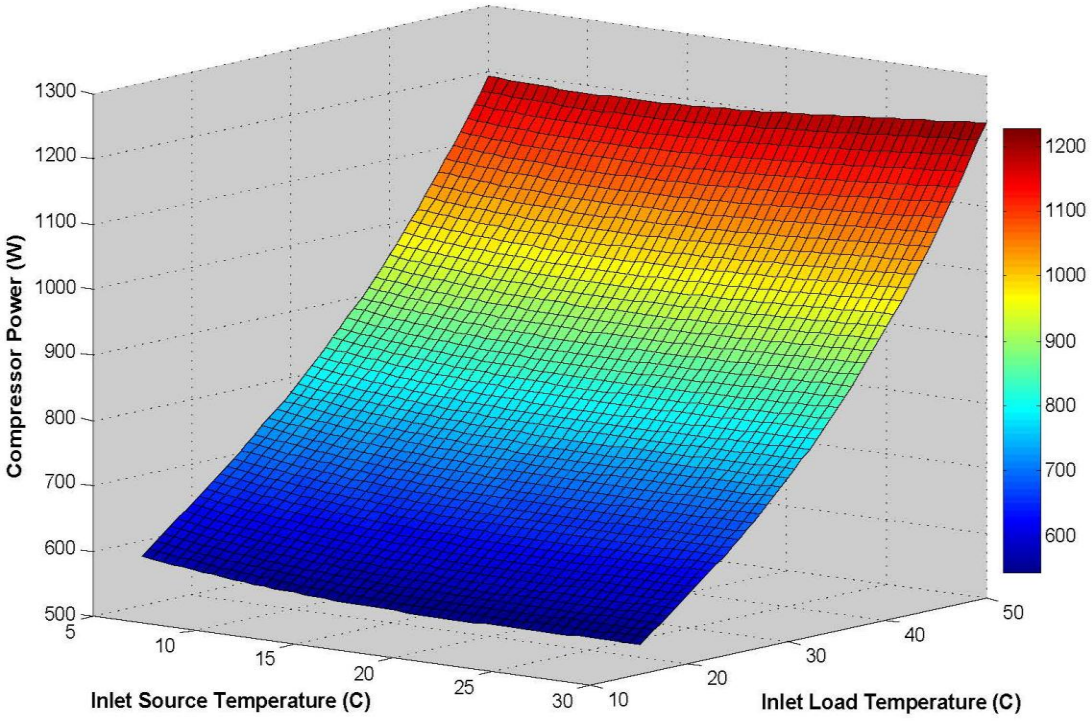

Figure A.7 Compressor power map for the GX-W2W36 heat pump

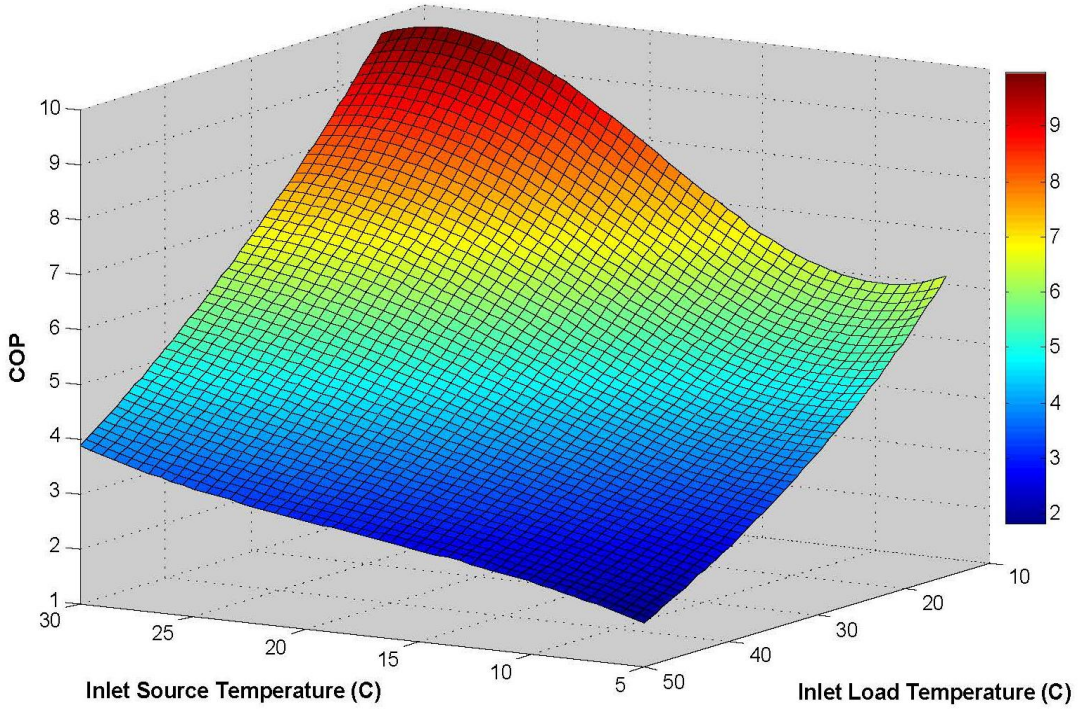

Figure A.8 COP map for the GX-W2W36 heat pump

The three dimensional curve equations generated using Online Curve and Surface Fitting [44] are presented in Equation (A.5). Equation (A.5) consists of a number of high order three dimensional equations. Within each equation, a number of coefficients were required to fit data from a generic form of each equation, see Table A.3. The COP was then calculated using Equation (A.6), from values determined from Equation (A.5).

Table A.3 Heat pump performance coefficients determined from online curve fitting software [44]

$\dot{W}_{comp}$ Coefficients		$\dot{Q}_{source}$ Coefficients		$\dot{Q}_{load}$ Coefficients	
a	3.979085866996637E+02	a_S	2.2792422799816873E+02	a_L	6.6387779902539087E+03
b	-5.5334702242327545E+00	b_S	2.7089521676786966E+01	b_L	-1.0777549071025348E+02
c	1.5933153236699374E+01	c_S	5.6909204208573010E+02	c_L	-6.6531594240976426E+02
d	2.5389274937948403E-01	d_S	-1.0980819858415735E+01	d_L	1.7794980114293022E+01
f	-2.0850956315706226E-01	f_S	-2.9092386404767815E+01	f_L	4.7622518320339196E+01
g	-3.0062593306920261E-03	g_S	6.6651413998470577E-01	g_L	-1.1335033919170665E+00
h	4.2934663209162971E-03	h_S	5.8121232503911524E-01	h_L	-8.8722168639507348E-01
i	-1.3560045271329768E-01	i_S	-1.3124628397107709E-02	i_L	2.1386903667490804E-02
j	9.2726503781772164E-05	-	-	-	-
k	3.1463637147147051E-03	-	-	-	-

$$\dot{W}_{comp} = a + bx + cy + dx^2 + fy^2 + gx^3 + hy^3 + ixy + jx^2y + kxy^2$$

$$\dot{Q}_{source} = a_S + b_S y + c_S x + d_S xy + f_S x^2 + g_S x^2 y + h_S x^3 + i_S x^3 y \quad \text{(A.5)}$$

$$\dot{Q}_{load} = a_L + b_L y + c_L x + d_L xy + f_L x^2 + g_L x^2 y + h_L x^3 + i_L x^3 y$$

Where:

x is the inlet source temperature supplied to the heat pump
y is a the inlet load temperature supplied to the heat pump

$$COP = \dot{Q}_{load}/\dot{W}_{compressor} \quad \text{(A.6)}$$

The statistical errors associated with three dimensional curve fitting were found to be very small, meaning that the heat pump correlations should provide a high degree of accuracy. The statistical errors for each of the three mapped parameters are shown in Table A.4.

Table A.4 Three dimensional curve fitting statistics - used for heat pump performance mapping

Curve Fitting Statistics	$\dot{Q}_{source}$	$\dot{Q}_{load}$	$\dot{W}_{comp}$
Maximum Relative Error [%]	1.07	1.59	0.62
Coefficient of Determination	0.9992	0.9975	0.9999

Appendix B Uncertainty Analysis

B.1 Heat Transfer Uncertainty

Experimental results in Chapter 5 are presented along with experimental uncertainty curves. Engineering uncertainty was calculated using the method described in Moffat [45]. The experimental uncertainty provides a method of expressing the uncertainty in a given calculation based upon the uncertainty of measurements used in the experiment. Equation (A.7) provides calculation procedures used to obtain heat and mass transfer rates, while Equations (A.8)and (A.9) are used to determine the uncertainty involved in heat transfer rate calculations. Table A.5 provides input uncertainty values for several parameters required for the calculation of heat transfer rate uncertainty.

Table A.5 Input uncertainty values for experimental heat transfer rate uncertainty calculation

Parameter	Uncertainty δ
Specific heat capacity	$\delta C_p \approx 0 \left[\frac{kJ}{kgK}\right]$
Density	$\delta\rho \approx 0 \left[\frac{kg}{m^3}\right]$
Volume flow rate	$\delta\dot{\mathrm{V}} = \pm 0.015\dot{\mathrm{V}}\ [m^3/s]$
Temperature difference	$\delta\Delta\mathrm{T} = \pm 0.2\ [℃]$

$$\dot{Q} = \dot{m}C_p\Delta T, \qquad \dot{m} = \rho\dot{V} \tag{A.7}$$

$$\delta\dot{m} = \sqrt{\left(\rho \cdot \delta\dot{V}\right)^2 + \left(\dot{V} \cdot \delta\rho\right)^2} \tag{A.8}$$

$$\delta\dot{Q} = \sqrt{\left(C_p\Delta T\delta\dot{m}\right)^2 + \left(\dot{m}\Delta T\delta C_p\right)^2 + \left(\dot{m}C_p\delta\Delta T\right)^2} \tag{A.9}$$

Sample Calculation:

$\rho = 1000\ kg/m^3$

$C_p = 4.1825\ kJ/kgK$

$\dot{V} = 8.33333333x10^{-5}\frac{m^3}{s}$

$\Delta T = 12℃$

$$\dot{Q} = 5\frac{kg}{min}\left(\frac{1\,min}{60\,s}\right)x\left(4.1825\frac{kJ}{kgK}\right)x(12℃) = 4.1825\,kW$$

$$\delta\dot{V} = 0.015x\dot{V} = 1.25x10^{-6}\frac{m^3}{s}$$

$$\delta\dot{m} = \sqrt{\left(1000\frac{kg}{m^3}\left(1.25x10^{-6}\frac{m^3}{s}\right)\right)^2} = 1.25x10^{-3}\frac{kg}{s}$$

$$\delta\dot{Q} = \sqrt{(4.1825\cdot 12\cdot 1.25x10^{-3})^2 + \left(1000\cdot 8.333\dot{3}x10^{-5}\cdot 4.1825\cdot 0.2\right)^2}$$

$$\delta\dot{Q} = \pm 0.0938\,kW\ or\ 2.24\%\ uncertainty$$

B.2 Electrical Power Uncertainty

Engineering uncertainty was also calculated for electrical power measurements. In LabVIEW, voltage and current measurements were taken at a frequency much greater than $60\ Hz$ such that the sinusoidal nature of AC power is considered through the integration of individual measurements. As such, the RMS values need not be considered in the calculation of electrical power uncertainties. Equation (A.10) provides calculation procedures used to obtain electrical power consumption rates, while Equation (A.11) is used to determine the uncertainty involved in electrical power consumption rates. Table A.6 provides input uncertainty values for several parameters required for the calculation of electrical power consumption rate uncertainty.

Table A.6 Input uncertainty values for experimental electrical power consumption rate uncertainty calculation

Parameter	Uncertainty δ
Voltage	$\delta V = \pm 0.01V\ [V]$
Current	$\delta I = \pm 0.01I\ [A]$

$$\dot{W} = VI \tag{A.10}$$

$$\delta\dot{W} = \sqrt{(V\delta I)^2 + (I\delta V)^2} \tag{A.11}$$

Sample Calculation for DHW element:

$V = 203.7\ V$

$I = 14.5\ A$

$\dot{W} = VI = (203.7\ V) \cdot (14.5\ A) = 2953.65\ W$

$\delta V = 0.01(203.7\ V) = 2.037\ V$

$\delta I = 0.01(14.5\ A) = 0.145\ A$

$\delta \dot{W} = \sqrt{((203.7\ V) \cdot (0.145\ A))^2 + ((14.5\ A) \cdot (2.037\ V))^2}$

$\delta \dot{W} = \pm 41.8\ W\ or\ 1.41\%\ uncertainty$

Appendix C Fortran Code for Custom TRNSYS Components

C.1 Type 161 Heat Pump GX-W2W36

```
SUBROUTINE TYPE161 (TIME,XIN,OUT,T,DTDT,PAR,INFO,ICNTRL,*)
C************************************************************************
C Object: Heat Pump GX-W2W36
C Simulation Studio Model: Type161
C
C Author: William Wagar
C Editor:
C Date:     May 28, 2012 last modified: Nov 23, 2012
C
C
C ***
C *** Model Parameters
C ***
C                               ScaleHP  any [0;1]
C                               COPDerating         any [0;1]
C                               CpSourcekJ/kg.K [0;10]
C                               CpLoad   kJ/kg.K [0;10]

C ***
C *** Model Inputs
C ***
C                               SourceFlowRate     kg/hr [0;1000]
C                               LoadFlowRate       kg/hr [0;1000]
C                               TSourceIn          C [-50;100]
C                               TLoadIn  C [-50;100]
C                               ControlSignal      any [0;1]

C ***
C *** Model Outputs
C ***
C                               SourceFlowRate     kg/hr [0;1000]
C                               LoadFlowRate       kg/hr [0;1000]
C                               QSource  W [0;7500]
C                               QLoad    W [0;7500]
C                               Power    W [0;2000]
C                               COP      any [0;10]
C                               TSourceOut         C [-50;100]
C                               TLoadOutC [-50;100]
C                               EBE      W [-7500;7500]
C                               TSourceIn          C [-50;100]
C                               TLoadIn  C [-50;100]
C                               Fault    any [0;1]

C ***
C *** Model Derivatives
C ***

C (Comments and routine interface generated by TRNSYS Studio)
C************************************************************************

C    TRNSYS acess functions (allow to acess TIME etc.)
     USE TrnsysConstants
     USE TrnsysFunctions

C-------------------------------------------------------------------------------------------------------------
C    REQUIRED BY THE MULTI-DLL VERSION OF TRNSYS
     !DEC$ATTRIBUTES DLLEXPORT :: TYPE161                    !SET THE CORRECT TYPE NUMBER HERE
C-------------------------------------------------------------------------------------------------------------
C-------------------------------------------------------------------------------------------------------------
C    TRNSYS DECLARATIONS
     IMPLICIT NONE                          !REQUIRES THE USER TO DEFINE ALL VARIABLES BEFORE USING THEM

          DOUBLE PRECISION XIN      !THE ARRAY FROM WHICH THE INPUTS TO THIS TYPE WILL BE RETRIEVED
```

```
      DOUBLE PRECISION OUT    !THE ARRAY WHICH WILL BE USED TO STORE THE OUTPUTS FROM THIS TYPE
      DOUBLE PRECISION TIME   !THE CURRENT SIMULATION TIME - YOU MAY USE THIS VARIABLE BUT DO NOT
SET IT!
      DOUBLE PRECISION PAR    !THE ARRAY FROM WHICH THE PARAMETERS FOR THIS TYPE WILL BE RETRIEVED
      DOUBLE PRECISION STORED !THE STORAGE ARRAY FOR HOLDING VARIABLES FROM TIMESTEP TO
TIMESTEP
      DOUBLE PRECISION T              !AN ARRAY CONTAINING THE RESULTS FROM THE DIFFERENTIAL
EQUATION SOLVER
      DOUBLE PRECISION DTDT  !AN ARRAY CONTAINING THE DERIVATIVES TO BE PASSED TO THE DIFF.EQ.
SOLVER
      INTEGER*4 INFO(15)              !THE INFO ARRAY STORES AND PASSES VALUABLE INFORMATION TO
AND FROM THIS TYPE
      INTEGER*4 NP,NI,NOUT,ND !VARIABLES FOR THE MAXIMUM NUMBER OF PARAMETERS,INPUTS,OUTPUTS AND
DERIVATIVES
      INTEGER*4 NPAR,NIN,NDER         !VARIABLES FOR THE CORRECT NUMBER OF
PARAMETERS,INPUTS,OUTPUTS AND DERIVATIVES
      INTEGER*4 IUNIT,ITYPE   !THE UNIT NUMBER AND TYPE NUMBER FOR THIS COMPONENT
      INTEGER*4 ICNTRL                !AN ARRAY FOR HOLDING VALUES OF CONTROL FUNCTIONS WITH THE
NEW SOLVER
      INTEGER*4 NSTORED               !THE NUMBER OF VARIABLES THAT WILL BE PASSED INTO AND OUT OF
STORAGE
      CHARACTER*3 OCHECK              !AN ARRAY TO BE FILLED WITH THE CORRECT VARIABLE TYPES FOR
THE OUTPUTS
      CHARACTER*3 YCHECK              !AN ARRAY TO BE FILLED WITH THE CORRECT VARIABLE TYPES FOR
THE INPUTS
C-------------------------------------------------------------------------------------------------------

C-------------------------------------------------------------------------------------------------------
C   USER DECLARATIONS - SET THE MAXIMUM NUMBER OF PARAMETERS (NP), INPUTS (NI),
C   OUTPUTS (NOUT), AND DERIVATIVES (ND) THAT MAY BE SUPPLIED FOR THIS TYPE
    PARAMETER (NP=4,NI=5,NOUT=12,ND=0,NSTORED=2)
C-------------------------------------------------------------------------------------------------------

C-------------------------------------------------------------------------------------------------------
C   REQUIRED TRNSYS DIMENSIONS
    DIMENSION XIN(NI),OUT(NOUT),PAR(NP),YCHECK(NI),OCHECK(NOUT),
          1   STORED(NSTORED),T(ND),DTDT(ND)
    INTEGER NITEMS
C-------------------------------------------------------------------------------------------------------
C-------------------------------------------------------------------------------------------------------
C   ADD DECLARATIONS AND DEFINITIONS FOR THE USER-VARIABLES HERE


C   PARAMETERS
    DOUBLE PRECISION ScaleHP              !Scaling parameter for nominal heat pump size
    DOUBLE PRECISION COPDerating !Derating parameter for HP performance
    DOUBLE PRECISION CpSource             !Source side specific heat
    DOUBLE PRECISION CpLoad               !Load side specific heat

C   INPUTS
    DOUBLE PRECISION SourceFlowRate       !Source side mass flow rate
    DOUBLE PRECISION LoadFlowRate         !Load side mass flow rate
    DOUBLE PRECISION TSourceIn            !Source side inlet temperature
    DOUBLE PRECISION TLoadIn              !Load side inlet temperature
    DOUBLE PRECISION ControlSignal !Signal from controller

!       LOCAL VARIABLES
        DOUBLE PRECISION x                      !Corrected source side inlet temperature
        DOUBLE PRECISION y                      !Corrected load side inlet temperature
        DOUBLE PRECISION SourceFlow             !Converted source side flow rate
        DOUBLE PRECISION LoadFlow               !Converted load side flow rate
!       FAULT VARIABLES
        INTEGER RUN
!       POWER VARIABLES
        DOUBLE PRECISION Power                  !Heat pump compressor power
        DOUBLE PRECISION a                      !Curve fit constants:
        DOUBLE PRECISION b
        DOUBLE PRECISION c
        DOUBLE PRECISION d
        DOUBLE PRECISION f
```

```
            DOUBLE PRECISION g
            DOUBLE PRECISION h
            DOUBLE PRECISION i
            DOUBLE PRECISION j
            DOUBLE PRECISION k
!           SOURCE Q VARIABLES
            DOUBLE PRECISION QSource            !Heat pump source side heat transfer rate
            DOUBLE PRECISION aS                 !Curve fit constants:
            DOUBLE PRECISION bS
            DOUBLE PRECISION cS
            DOUBLE PRECISION dS
            DOUBLE PRECISION fS
            DOUBLE PRECISION gS
            DOUBLE PRECISION hS
            DOUBLE PRECISION iS
!           LOAD Q VARIABLES
            DOUBLE PRECISION QLoad              !Heat pump load side heat transfer rate
            DOUBLE PRECISION aL                 !Curve fit constants:
            DOUBLE PRECISION bL
            DOUBLE PRECISION cL
            DOUBLE PRECISION dL
            DOUBLE PRECISION fL
            DOUBLE PRECISION gL
            DOUBLE PRECISION hL
            DOUBLE PRECISION iL
!           OUTPUT VARIABLES
            DOUBLE PRECISION COP                !Coefficient of performance
            DOUBLE PRECISION EBE                !Energy balance error between Power, QSource, and QLoad
            DOUBLE PRECISION TSourceOut         !Source side outlet temperature
            DOUBLE PRECISION TLoadOut           !Load side outlet temperature
            DOUBLE PRECISION Fault              !Indicator for restricted heat pump conditions

C-------------------------------------------------------------------------------------------------------------------
C     READ IN THE VALUES OF THE PARAMETERS IN SEQUENTIAL ORDER
      ScaleHP=PAR(1)
      COPDerating=PAR(2)
      CpSource=PAR(3)
      CpLoad=PAR(4)

C-------------------------------------------------------------------------------------------------------------------
C    RETRIEVE THE CURRENT VALUES OF THE INPUTS TO THIS MODEL FROM THE XIN ARRAY IN SEQUENTIAL ORDER

      SourceFlowRate=XIN(1)
      LoadFlowRate=XIN(2)
      TSourceIn=XIN(3)
      TLoadIn=XIN(4)
      ControlSignal=XIN(5)
            IUNIT=INFO(1)
            ITYPE=INFO(2)

C-------------------------------------------------------------------------------------------------------------------
C    SET THE VERSION INFORMATION FOR TRNSYS
      IF(INFO(7).EQ.-2) THEN
            INFO(12)=16
            RETURN 1
          ENDIF
C-------------------------------------------------------------------------------------------------------------------

C-------------------------------------------------------------------------------------------------------------------
C    DO ALL THE VERY LAST CALL OF THE SIMULATION MANIPULATIONS HERE
      IF (INFO(8).EQ.-1) THEN
            RETURN 1
          ENDIF
C-------------------------------------------------------------------------------------------------------------------

C-------------------------------------------------------------------------------------------------------------------
C    PERFORM ANY 'AFTER-ITERATION' MANIPULATIONS THAT ARE REQUIRED HERE
C    e.g. save variables to storage array for the next timestep
      IF (INFO(13).GT.0) THEN
                  NITEMS=2
```

```
                        !SETTING AND STORING HEAT PUMP ANTI SHORT-CYCLE TIMER
                        IF ((RUN .EQ. 0) .AND. (STORED(2).EQ.1)) THEN !HEAT PUMP HAS TURNED OFF
                              STORED(1)=TIME ! RESET THE TIMER
                        ENDIF
                        !STORING CURRENT HP OPERATING CONDITION
                 STORED(2)= RUN ! ENTER OPERATING CONDITION
                CALL setStorageVars(STORED,NITEMS,INFO)
                RETURN 1
              ENDIF
C
C-------------------------------------------------------------------------------------------------------------

C-------------------------------------------------------------------------------------------------------------
C    DO ALL THE VERY FIRST CALL OF THE SIMULATION MANIPULATIONS HERE
     IF (INFO(7).EQ.-1) THEN

C       SET SOME INFO ARRAY VARIABLES TO TELL THE TRNSYS ENGINE HOW THIS TYPE IS TO WORK
        INFO(6)=NOUT
        INFO(9)=1
              INFO(10)=0        !STORAGE FOR VERSION 16 HAS BEEN CHANGED

C       SET THE REQUIRED NUMBER OF INPUTS, PARAMETERS AND DERIVATIVES THAT THE USER SHOULD SUPPLY IN
THE INPUT FILE
C       IN SOME CASES, THE NUMBER OF VARIABLES MAY DEPEND ON THE VALUE OF PARAMETERS TO THIS MODEL....
        NIN=NI
              NPAR=NP
              NDER=ND

C       CALL THE TYPE CHECK SUBROUTINE TO COMPARE WHAT THIS COMPONENT REQUIRES TO WHAT IS SUPPLIED
IN
C       THE TRNSYS INPUT FILE
              CALL TYPECK(1,INFO,NIN,NPAR,NDER)

C       SET THE NUMBER OF STORAGE SPOTS NEEDED FOR THIS COMPONENT
        NITEMS=2
              CALL setStorageSize(NITEMS,INFO)

C       RETURN TO THE CALLING PROGRAM
        RETURN 1

     ENDIF
C-------------------------------------------------------------------------------------------------------------

C-------------------------------------------------------------------------------------------------------------
C    DO ALL OF THE INITIAL TIMESTEP MANIPULATIONS HERE - THERE ARE NO ITERATIONS AT THE INTIAL TIME
     IF (TIME .LT. (getSimulationStartTime() +
    . getSimulationTimeStep()/2.D0)) THEN

C       SET THE UNIT NUMBER FOR FUTURE CALLS
        IUNIT=INFO(1)
        ITYPE=INFO(2)

C       CHECK THE PARAMETERS FOR PROBLEMS AND RETURN FROM THE SUBROUTINE IF AN ERROR IS FOUND
C         IF(...) CALL TYPECK(-4,INFO,0,"BAD PARAMETER #",0)

C       PERFORM ANY REQUIRED CALCULATIONS TO SET THE INITIAL VALUES OF THE OUTPUTS HERE
C                       SourceFlowRate
                              OUT(1)=0
C                       LoadFlowRate
                              OUT(2)=0
C                       QSource
                              OUT(3)=0
C                       QLoad
                              OUT(4)=0
C                       Power
                              OUT(5)=0
C                       COP
                              OUT(6)=0
C                       TSourceOut
                              OUT(7)=0
```

```
C                       TLoadOut
                                OUT(8)=0
C                       EBE
                                OUT(9)=0
C                       TSourceIn
                                OUT(10)=0
C                       TLoadIn
                                OUT(11)=0
C                       Fault
                                OUT(12)=0

C       PERFORM ANY REQUIRED CALCULATIONS TO SET THE INITIAL STORAGE VARIABLES HERE
        NITEMS=2
                STORED(1)= 0
                STORED(2)= 0

C       PUT THE STORED ARRAY IN THE GLOBAL STORED ARRAY
        CALL setStorageVars(STORED,NITEMS,INFO)

C       RETURN TO THE CALLING PROGRAM
        RETURN 1

      ENDIF
C-------------------------------------------------------------------------------------------------------------------

C-------------------------------------------------------------------------------------------------------------------
C     *** ITS AN ITERATIVE CALL TO THIS COMPONENT ***
C-------------------------------------------------------------------------------------------------------------------


C-------------------------------------------------------------------------------------------------------------------
C     RETRIEVE THE VALUES IN THE STORAGE ARRAY FOR THIS ITERATION
C      NITEMS=
C             CALL getStorageVars(STORED,NITEMS,INFO)
C     STORED(1)=
C-------------------------------------------------------------------------------------------------------------------
C-------------------------------------------------------------------------------------------------------------------
C     CHECK THE INPUTS FOR PROBLEMS
C       IF(...) CALL TYPECK(-3,INFO,'BAD INPUT #',0,0)
C             IF(IERROR.GT.0) RETURN 1
C-------------------------------------------------------------------------------------------------------------------
C-------------------------------------------------------------------------------------------------------------------
C     *** PERFORM ALL THE CALCULATION HERE FOR THIS MODEL. ***
C-------------------------------------------------------------------------------------------------------------------

!             COMPONENT EQUATIONS

!             CHECKING FOR A CONTROL SIGNAL
              IF (ControlSignal .LE. 0.5D0) THEN
                      Power = 0.0D0
                      QSource = 0.0D0
                      QLoad = 0.0D0
                      COP = 0.0D0
                      EBE = 0.0D0
                      TSourceOut = TSourceIn
                      TLoadOut = TLoadIn
                      Fault = 0.2
                      RUN = 0 !HEAT PUMP DOES NOT RUN
                      GOTO 100
              ENDIF

!             CHECKING FOR SHORT-CYCLE TIMER EXPIRY
              IF ((TIME - STORED(1)) .LE. (5.D0/60.D0)) THEN
                      Power = 0.0D0
                      QSource = 0.0D0
                      QLoad = 0.0D0
                      COP = 0.0D0
                      EBE = 0.0D0
                      TSourceOut = TSourceIn
                      TLoadOut = TLoadIn
```

```
                Fault = 0.4
                RUN = 0
                GOTO 100
        ENDIF

!       CHECKING LOWER LIMIT FOR INLET FLOW
        IF ((SourceFlowRate .LE. 0.0D0) .OR.
     & (LoadFlowRate .LE. 0.0D0)) THEN
                Power = 0.0D0
                QSource = 0.0D0
                QLoad = 0.0D0
                COP = 0.0D0
                EBE = 0.0D0
                TSourceOut = TSourceIn
                TLoadOut = TLoadIn
                Fault = 0.6
                RUN = 0
                GOTO 100
        ENDIF

!       CHECKING UPPER LIMITS FOR INLET TEMPERATURES
        IF ((TSourceIn .GT. 30.0D0) .OR.
     & (TLoadIn .GT. 50.0D0)) THEN
                Power = 0.0D0
                QSource = 0.0D0
                QLoad = 0.0D0
                COP = 0.0D0
                EBE = 0.0D0
                TSourceOut = TSourceIn
                TLoadOut = TLoadIn
                Fault = 0.8
                RUN = 0
                GOTO 100
        ENDIF

!       DEFINING VARIABLES x AND y FOR CURVE FITTING
!       SETTING x AND y
        x = TSourceIn
        y = TLoadIn

!       SOURCE-LOAD TEMPERATURE CROSS-OVER RESTRICTION
        IF (x .GT. y) THEN
                x = y
        ENDIF

!       PERFORMING FLOW RATE UNIT CONVERSION
        SourceFlow = SourceFlowRate/3600.D0
        LoadFlow = LoadFlowRate/3600.D0

!       Power CALCULATION
        a = 3.9790858669966377E+02
        b = -5.5334702242327545E+00
        c = 1.5933153236699374E+01
        d = 2.5389274937948403E-01
        f = -2.0850956315706226E-01
        g = -3.0062593306920261E-03
        h = 4.2934663209162971E-03
        i = -1.3560045271329768E-01
        j = 9.2726503781772164E-05
        k = 3.1463637147147051E-03

        Power = (ScaleHP/COPDerating)*(a + b*x + c*y + d*(x**2) + f*(y**2) +
     & g*(x**3) + h*(y**3) + i*x*y + j*(x**2)*y + k*x*(y**2))

!       QSource CALCULATION
        aS = 2.2792422799816873E+02
        bS = 2.7089521676786966E+01
        cS = 5.6909204208573010E+02
        dS = -1.0980819858415735E+01
        fS = -2.9092386404767815E+01
```

```
            gS = 6.6651413998470577E-01
            hS = 5.8121232503911524E-01
            iS = -1.3124628397107709E-02

            QSource = ScaleHP*(aS + bS*y + cS*x + dS*x*y + fS*(x**2) +
     & gS*(x**2)*y + hS*(x**3) + iS*(x**3)*y)

!           QLoad CALCULATION
            aL = 6.6387779902539087E+03
            bL = -1.0777549071025348E+02
            cL = -6.6531594240976426E+02
            dL = 1.7794980114293022E+01
            fL = 4.7622518320339196E+01
            gL = -1.1335033919170665E+00
            hL = -8.8722168639507348E-01
            iL = 2.1386903667490804E-02

            QLoad = ScaleHP*(aL + bL*y + cL*x + dL*x*y + fL*(x**2) +
     & gL*(x**2)*y + hL*(x**3) + iL*(x**3)*y)

!           OUTPUT CALCULATIONS
            COP = QLoad/Power
            EBE = QSource + Power - QLoad
            TSourceOut = TSourceIn - QSource/(SourceFlow*CpSource*1000.D0)
            TLoadOut = QLoad/(LoadFlow*CpLoad*1000.D0) + TLoadIn

!           CHECKING OUTLET TEMPERATURE LIMITS
            IF ((TSourceOut .LE. 5.0D0) .OR.
     & (TLoadOut .LE. 0.0D0)) THEN
                        Power = 0.0D0
                        QSource = 0.0D0
                        QLoad = 0.0D0
                        COP = 0.0D0
                        EBE = 0.0D0
                        TSourceOut = TSourceIn
                        TLoadOut = TLoadIn
                        Fault = 1
                        RUN = 0
                        GOTO 100
            ELSE
                        RUN = 1
            ENDIF

C-------------------------------------------------------------------------------------------------------------------

C-------------------------------------------------------------------------------------------------------------------
C-------------------------------------------------------------------------------------------------------------------
C   SET THE STORAGE ARRAY AT THE END OF THIS ITERATION IF NECESSARY
C     NITEMS=
C     STORED(1)=
C           CALL setStorageVars(STORED,NITEMS,INFO)
C-------------------------------------------------------------------------------------------------------------------
C-------------------------------------------------------------------------------------------------------------------
C   REPORT ANY PROBLEMS THAT HAVE BEEN FOUND USING CALLS LIKE THIS:
C     CALL MESSAGES(-1,'put your message here','MESSAGE',IUNIT,ITYPE)
C     CALL MESSAGES(-1,'put your message here','WARNING',IUNIT,ITYPE)
C     CALL MESSAGES(-1,'put your message here','SEVERE',IUNIT,ITYPE)
C     CALL MESSAGES(-1,'put your message here','FATAL',IUNIT,ITYPE)
C-------------------------------------------------------------------------------------------------------------------
C-------------------------------------------------------------------------------------------------------------------
C   SET THE OUTPUTS FROM THIS MODEL IN SEQUENTIAL ORDER AND GET OUT
C                       SourceFlowRate
100                             OUT(1)=SourceFlowRate
C                       LoadFlowRate
                                OUT(2)=LoadFlowRate
C                       QSource
                                OUT(3)=QSource
C                       QLoad
                                OUT(4)=QLoad
C                       Power
```

```
                        OUT(5)=Power
C                   COP
                        OUT(6)=COP
C                   TSourceOut
                        OUT(7)=TSourceOut
C                   TLoadOut
                        OUT(8)=TLoadOut
C                   EBE
                        OUT(9)=EBE
C                   TSourceIn
                        OUT(10)=TSourceIn
C                   TLoadIn
                        OUT(11)=TLoadIn
C                   Fault
                        OUT(12)=Fault

C-------------------------------------------------------------------------------------------------------------------
C    EVERYTHING IS DONE - RETURN FROM THIS SUBROUTINE AND MOVE ON
     RETURN 1
     END
C-------------------------------------------------------------------------------------------------------------------
```

C.2 Type 162 Heat Exchanger SL15-25

```
SUBROUTINE TYPE162 (TIME,XIN,OUT,T,DTDT,PAR,INFO,ICNTRL,*)
C************************************************************************
C Object: Heat Exchanger SL15-25
C Simulation Studio Model: Type162
C
C Author: William Wagar
C Editor:
C Date:     June 21, 2012 last modified: Nov 23, 2012
C
C
C ***
C *** Model Parameters
C ***
C                               ScaleHX  any [0;1]
C                               CpSourcekJ/kg.K [0;10]
C                               CpLoad   kJ/kg.K [0;10]

C ***
C *** Model Inputs
C ***
C                               SourceFlowRate     kg/hr [0;1000]
C                               LoadFlowRate       kg/hr [0;1000]
C                               TSourceIn          C [-50;100]
C                               TLoadIn   C [-50;100]

C ***
C *** Model Outputs
C ***
C                               SourceFlowRate     kg/hr [0;1000]
C                               LoadFlowRate       kg/hr [0;1000]
C                               Q          W [0;7500]
C                               TSourceOut         C [-50;100]
C                               TLoadOutC [-50;100]
C                               TSourceIn          C [-50;100]
C                               TLoadIn   C [-50;100]
C                               Effectiveness      any [0;1]

C ***
C *** Model Derivatives
C ***

C (Comments and routine interface generated by TRNSYS Studio)
C************************************************************************
```

```
C    TRNSYS acess functions (allow to acess TIME etc.)
     USE TrnsysConstants
     USE TrnsysFunctions

C-------------------------------------------------------------------------------------------------------------
C    REQUIRED BY THE MULTI-DLL VERSION OF TRNSYS
     !DEC$ATTRIBUTES DLLEXPORT :: TYPE162                              !SET THE CORRECT TYPE NUMBER HERE
C-------------------------------------------------------------------------------------------------------------
C-------------------------------------------------------------------------------------------------------------
C    TRNSYS DECLARATIONS
     IMPLICIT NONE                              !REQUIRES THE USER TO DEFINE ALL VARIABLES BEFORE USING THEM

          DOUBLE PRECISION XIN     !THE ARRAY FROM WHICH THE INPUTS TO THIS TYPE WILL BE RETRIEVED
          DOUBLE PRECISION OUT     !THE ARRAY WHICH WILL BE USED TO STORE THE OUTPUTS FROM THIS TYPE
          DOUBLE PRECISION TIME    !THE CURRENT SIMULATION TIME - YOU MAY USE THIS VARIABLE BUT DO NOT
SET IT!
          DOUBLE PRECISION PAR     !THE ARRAY FROM WHICH THE PARAMETERS FOR THIS TYPE WILL BE RETRIEVED
          DOUBLE PRECISION STORED !THE STORAGE ARRAY FOR HOLDING VARIABLES FROM TIMESTEP TO
TIMESTEP
          DOUBLE PRECISION T               !AN ARRAY CONTAINING THE RESULTS FROM THE DIFFERENTIAL
EQUATION SOLVER
          DOUBLE PRECISION DTDT  !AN ARRAY CONTAINING THE DERIVATIVES TO BE PASSED TO THE DIFF.EQ.
SOLVER
          INTEGER*4 INFO(15)               !THE INFO ARRAY STORES AND PASSES VALUABLE INFORMATION TO
AND FROM THIS TYPE
          INTEGER*4 NP,NI,NOUT,ND !VARIABLES FOR THE MAXIMUM NUMBER OF PARAMETERS,INPUTS,OUTPUTS AND
DERIVATIVES
          INTEGER*4 NPAR,NIN,NDER          !VARIABLES FOR THE CORRECT NUMBER OF
PARAMETERS,INPUTS,OUTPUTS AND DERIVATIVES
          INTEGER*4 IUNIT,ITYPE      !THE UNIT NUMBER AND TYPE NUMBER FOR THIS COMPONENT
          INTEGER*4 ICNTRL                 !AN ARRAY FOR HOLDING VALUES OF CONTROL FUNCTIONS WITH THE
NEW SOLVER
          INTEGER*4 NSTORED                !THE NUMBER OF VARIABLES THAT WILL BE PASSED INTO AND OUT OF
STORAGE
          CHARACTER*3 OCHECK               !AN ARRAY TO BE FILLED WITH THE CORRECT VARIABLE TYPES FOR
THE OUTPUTS
          CHARACTER*3 YCHECK               !AN ARRAY TO BE FILLED WITH THE CORRECT VARIABLE TYPES FOR
THE INPUTS
C-------------------------------------------------------------------------------------------------------------

C-------------------------------------------------------------------------------------------------------------
C    USER DECLARATIONS - SET THE MAXIMUM NUMBER OF PARAMETERS (NP), INPUTS (NI),
C    OUTPUTS (NOUT), AND DERIVATIVES (ND) THAT MAY BE SUPPLIED FOR THIS TYPE
     PARAMETER (NP=3,NI=4,NOUT=8,ND=0,NSTORED=0)
C-------------------------------------------------------------------------------------------------------------

C-------------------------------------------------------------------------------------------------------------
C    REQUIRED TRNSYS DIMENSIONS
     DIMENSION XIN(NI),OUT(NOUT),PAR(NP),YCHECK(NI),OCHECK(NOUT),
          1   STORED(NSTORED),T(ND),DTDT(ND)
     INTEGER NITEMS
C-------------------------------------------------------------------------------------------------------------
C-------------------------------------------------------------------------------------------------------------
C    ADD DECLARATIONS AND DEFINITIONS FOR THE USER-VARIABLES HERE


C    PARAMETERS
     DOUBLE PRECISION ScaleHX                 !Scaling parameter for nominal heat exchanger size
     DOUBLE PRECISION CpSource                !Source side specific heat
     DOUBLE PRECISION CpLoad                  !Load side specific heat

C    INPUTS
     DOUBLE PRECISION SourceFlowRate          !Source side mass flow rate
     DOUBLE PRECISION LoadFlowRate            !Load side mass flow rate
     DOUBLE PRECISION TSourceIn               !Source side inlet temperature
     DOUBLE PRECISION TLoadIn                 !Load side inlet temperature

!         LOCAL VARIABLES
          DOUBLE PRECISION SourceFlow              !Converted source side flow rate
          DOUBLE PRECISION LoadFlow                !Converted load side flow rate
```

```
!           EFFECTIVENESS VARIABLES
            DOUBLE PRECISION Cs                     !Source side heat capacity rate
            DOUBLE PRECISION Cl                     !Load side heat capacity rate
            DOUBLE PRECISION Cmin                   !Minimum heat capacity rate
            DOUBLE PRECISION a                      !Correlation constant for effectiveness calculation
            DOUBLE PRECISION b                      !Correlation constant for effectiveness calculation
            DOUBLE PRECISION z                      !Placeholder for average of inlet source and load temperatures
            DOUBLE PRECISION Effectiveness      !Calculated heat exchanger effectiveness

!           OUTPUT VARIABLES
            DOUBLE PRECISION Q                      !Heat transfer rate
            DOUBLE PRECISION TSourceOut             !Source side outlet temperature
            DOUBLE PRECISION TLoadOut               !Load side outlet temperature


C-------------------------------------------------------------------------------------------------------------------
C     READ IN THE VALUES OF THE PARAMETERS IN SEQUENTIAL ORDER
    ScaleHX=PAR(1)
    CpSource=PAR(2)
    CpLoad=PAR(3)

C-------------------------------------------------------------------------------------------------------------------
C    RETRIEVE THE CURRENT VALUES OF THE INPUTS TO THIS MODEL FROM THE XIN ARRAY IN SEQUENTIAL ORDER

    SourceFlowRate=XIN(1)
    LoadFlowRate=XIN(2)
    TSourceIn=XIN(3)
    TLoadIn=XIN(4)
            IUNIT=INFO(1)
            ITYPE=INFO(2)

C-------------------------------------------------------------------------------------------------------------------
C    SET THE VERSION INFORMATION FOR TRNSYS
    IF(INFO(7).EQ.-2) THEN
            INFO(12)=16
            RETURN 1
           ENDIF
C-------------------------------------------------------------------------------------------------------------------

C-------------------------------------------------------------------------------------------------------------------
C    DO ALL THE VERY LAST CALL OF THE SIMULATION MANIPULATIONS HERE
    IF (INFO(8).EQ.-1) THEN
            RETURN 1
           ENDIF
C-------------------------------------------------------------------------------------------------------------------

C-------------------------------------------------------------------------------------------------------------------
C    PERFORM ANY 'AFTER-ITERATION' MANIPULATIONS THAT ARE REQUIRED HERE
C    e.g. save variables to storage array for the next timestep
    IF (INFO(13).GT.0) THEN
            NITEMS=0
C           STORED(1)=... (if NITEMS > 0)
C      CALL setStorageVars(STORED,NITEMS,INFO)
            RETURN 1
           ENDIF
C
C-------------------------------------------------------------------------------------------------------------------

C-------------------------------------------------------------------------------------------------------------------
C    DO ALL THE VERY FIRST CALL OF THE SIMULATION MANIPULATIONS HERE
    IF (INFO(7).EQ.-1) THEN

C     SET SOME INFO ARRAY VARIABLES TO TELL THE TRNSYS ENGINE HOW THIS TYPE IS TO WORK
      INFO(6)=NOUT
      INFO(9)=1
            INFO(10)=0        !STORAGE FOR VERSION 16 HAS BEEN CHANGED

C     SET THE REQUIRED NUMBER OF INPUTS, PARAMETERS AND DERIVATIVES THAT THE USER SHOULD SUPPLY IN
THE INPUT FILE
C     IN SOME CASES, THE NUMBER OF VARIABLES MAY DEPEND ON THE VALUE OF PARAMETERS TO THIS MODEL....
```

```
      NIN=NI
            NPAR=NP
            NDER=ND

C     CALL THE TYPE CHECK SUBROUTINE TO COMPARE WHAT THIS COMPONENT REQUIRES TO WHAT IS SUPPLIED
IN
C     THE TRNSYS INPUT FILE
            CALL TYPECK(1,INFO,NIN,NPAR,NDER)

C     SET THE NUMBER OF STORAGE SPOTS NEEDED FOR THIS COMPONENT
      NITEMS=0
C           CALL setStorageSize(NITEMS,INFO)

C     RETURN TO THE CALLING PROGRAM
      RETURN 1

    ENDIF
C-----------------------------------------------------------------------------------------------------------

C-----------------------------------------------------------------------------------------------------------
C   DO ALL OF THE INITIAL TIMESTEP MANIPULATIONS HERE - THERE ARE NO ITERATIONS AT THE INTIAL TIME
    IF (TIME .LT. (getSimulationStartTime() +
   . getSimulationTimeStep()/2.D0)) THEN

C     SET THE UNIT NUMBER FOR FUTURE CALLS
      IUNIT=INFO(1)
      ITYPE=INFO(2)

C     CHECK THE PARAMETERS FOR PROBLEMS AND RETURN FROM THE SUBROUTINE IF AN ERROR IS FOUND
C       IF(...) CALL TYPECK(-4,INFO,0,"BAD PARAMETER #",0)

C     PERFORM ANY REQUIRED CALCULATIONS TO SET THE INITIAL VALUES OF THE OUTPUTS HERE
C                     SourceFlowRate
                            OUT(1)=0
C                     LoadFlowRate
                            OUT(2)=0
C                     Q
                            OUT(3)=0
C                     TSourceOut
                            OUT(4)=0
C                     TLoadOut
                            OUT(5)=0
C                     TSourceIn
                            OUT(6)=0
C                     TLoadIn
                            OUT(7)=0
C                     Effectiveness
                            OUT(8)=0


C     PERFORM ANY REQUIRED CALCULATIONS TO SET THE INITIAL STORAGE VARIABLES HERE
      NITEMS=0
C           STORED(1)=...

C     PUT THE STORED ARRAY IN THE GLOBAL STORED ARRAY
C       CALL setStorageVars(STORED,NITEMS,INFO)

C     RETURN TO THE CALLING PROGRAM
      RETURN 1

    ENDIF
C-----------------------------------------------------------------------------------------------------------

C-----------------------------------------------------------------------------------------------------------
C   *** ITS AN ITERATIVE CALL TO THIS COMPONENT ***
C-----------------------------------------------------------------------------------------------------------


C-----------------------------------------------------------------------------------------------------------
C   RETRIEVE THE VALUES IN THE STORAGE ARRAY FOR THIS ITERATION
```

```
C     NITEMS=
C           CALL getStorageVars(STORED,NITEMS,INFO)
C     STORED(1)=
C-----------------------------------------------------------------------------------------------------------------------
C-----------------------------------------------------------------------------------------------------------------------
C    CHECK THE INPUTS FOR PROBLEMS
C      IF(...) CALL TYPECK(-3,INFO,'BAD INPUT #',0,0)
C           IF(IERROR.GT.0) RETURN 1
C-----------------------------------------------------------------------------------------------------------------------
C-----------------------------------------------------------------------------------------------------------------------
C    *** PERFORM ALL THE CALCULATION HERE FOR THIS MODEL. ***
C-----------------------------------------------------------------------------------------------------------------------

!           COMPONENT EQUATIONS

!           CHECKING LOWER LIMIT FOR INLET FLOW
            IF ((SourceFlowRate .LE. 0.0D0) .OR.
     & (LoadFlowRate .LE. 0.0D0)) THEN ! NO HEAT TRANSFER
                        Q = 0.0D0
                        TSourceOut = TSourceIn
                        TLoadOut = TLoadIn
                        Effectiveness = 0.0D0
                        GOTO 100

                        ELSE !CALCULATE HEAT TRANSFER RATE

            !           PERFORMING FLOW RATE UNIT CONVERSION
                        SourceFlow = SourceFlowRate/3600.D0
                        LoadFlow = LoadFlowRate/3600.D0

            !           EFFECTIVENESS CALCULATION
                        a = 1.01234E-3
                        b = 5.79105E-1
                        z = (TSourceIn + TLoadIn)/2.D0
                        Effectiveness = ScaleHX*(a*z + b)

            !           COOERCE CALCULATED EFFECTIVENESS BETWEEN 0 AND 1
                        IF (Effectiveness .LE. 0.D0) THEN
                                    Effectiveness = 0.D0
                                    ELSEIF (Effectiveness .GE. 1.D0) THEN
                                    Effectiveness = 1.D0
                                    ELSE
                                    Effectiveness = Effectiveness
                        ENDIF

            !           CALCULATING HEAT CAPACITY RATES TO INTERPRET EFFECTIVENESS
                        Cs = 1000.D0*SourceFlow*CpSource
                        Cl = 1000.D0*LoadFlow*CpLoad
                        Cmin = MIN(Cs,Cl)

            !           CALCULATING HEAT TRANSFER RATE
                        Q = Effectiveness*Cmin*(TSourceIn - TLoadIn)

            !           CALCULATING OUTPUT TEMPERATURES
                        TSourceOut = TSourceIn - Q/Cs
                        TLoadOut = Q/Cl + TLoadIn

                        GOTO 100
            ENDIF

C-----------------------------------------------------------------------------------------------------------------------

C-----------------------------------------------------------------------------------------------------------------------
C-----------------------------------------------------------------------------------------------------------------------
C    SET THE STORAGE ARRAY AT THE END OF THIS ITERATION IF NECESSARY
C      NITEMS=
C      STORED(1)=
C           CALL setStorageVars(STORED,NITEMS,INFO)
C-----------------------------------------------------------------------------------------------------------------------
C-----------------------------------------------------------------------------------------------------------------------
```

```
C   REPORT ANY PROBLEMS THAT HAVE BEEN FOUND USING CALLS LIKE THIS:
C     CALL MESSAGES(-1,'put your message here','MESSAGE',IUNIT,ITYPE)
C     CALL MESSAGES(-1,'put your message here','WARNING',IUNIT,ITYPE)
C     CALL MESSAGES(-1,'put your message here','SEVERE',IUNIT,ITYPE)
C     CALL MESSAGES(-1,'put your message here','FATAL',IUNIT,ITYPE)
C-----------------------------------------------------------------------------------------------------------------
C-----------------------------------------------------------------------------------------------------------------
C           SET THE OUTPUTS FROM THIS MODEL IN SEQUENTIAL ORDER AND GET OUT

C                       SourceFlowRate
100                             OUT(1)= SourceFlowRate
C                       LoadFlowRate
                                OUT(2)=LoadFlowRate
C                       Q
                                OUT(3)=Q
C                       TSourceOut
                                OUT(4)=TSourceOut
C                       TLoadOut
                                OUT(5)=TLoadOut
C                       TSourceIn
                                OUT(6)=TSourceIn
C                       TLoadIn
                                OUT(7)=TLoadIn
C                       Effectiveness
                                OUT(8)=Effectiveness

C-----------------------------------------------------------------------------------------------------------------
C    EVERYTHING IS DONE - RETURN FROM THIS SUBROUTINE AND MOVE ON
     RETURN 1
     END
C-----------------------------------------------------------------------------------------------------------------
```

C.3 Type 163 ETU Controller

```
SUBROUTINE TYPE163 (TIME,XIN,OUT,T,DTDT,PAR,INFO,ICNTRL,*)
C**************************************************************************
C Object: ETU Controller
C Simulation Studio Model: Type163
C
C Author: William Wagar
C Editor:
C Date:     October 29, 2012 last modified: Nov 23, 2012
C
C
C ***
C *** Model Parameters
C ***
C                               Area        m^2 [0;10]
C                               EtaInt      any [0;1]
C                               EtaSlope    any [0;10]
C                               EtaCurve    any [0;10]

C ***
C *** Model Inputs
C ***
C                               GT          kJ/hr.m^2 [-100000;10000]
C                               HPPower W [-10000;10000]
C                               TTopDHW             C [-100;100]
C                               TBotDHW             C [-100;100]
C                               THPSIn    C [-100;100]
C                               THPSOut C [-100;100]
C                               THPLIn    C [-100;100]
C                               TAMB      C [-100;100]

C ***
C *** Model Outputs
C ***
C                               SystemMode          any [0;10]
```

```
C                               CSigDiv1 any [0;1]
C                               CSigDiv2 any [0;1]
C                               CSigP1   any [0;1]
C                               CSigP2   any [0;1]
C                               CSigHP   any [0;1]
C                               RadLimit  any [0;1]
C                               TTopLimitany [0;1]
C                               TBotLimit any [0;1]
C                               TimerLimit          any [0;1]

C ***
C *** Model Derivatives
C ***

C (Comments and routine interface generated by TRNSYS Studio)
C*************************************************************************

C   TRNSYS acess functions (allow to acess TIME etc.)
    USE TrnsysConstants
    USE TrnsysFunctions

C-------------------------------------------------------------------------------------------------------------
C   REQUIRED BY THE MULTI-DLL VERSION OF TRNSYS
    !DEC$ATTRIBUTES DLLEXPORT :: TYPE163                                !SET THE CORRECT TYPE NUMBER HERE
C-------------------------------------------------------------------------------------------------------------
C-------------------------------------------------------------------------------------------------------------
C   TRNSYS DECLARATIONS
    IMPLICIT NONE                               !REQUIRES THE USER TO DEFINE ALL VARIABLES BEFORE USING THEM

          DOUBLE PRECISION XIN     !THE ARRAY FROM WHICH THE INPUTS TO THIS TYPE WILL BE RETRIEVED
          DOUBLE PRECISION OUT     !THE ARRAY WHICH WILL BE USED TO STORE THE OUTPUTS FROM THIS TYPE
          DOUBLE PRECISION TIME    !THE CURRENT SIMULATION TIME - YOU MAY USE THIS VARIABLE BUT DO NOT
SET IT!
          DOUBLE PRECISION PAR     !THE ARRAY FROM WHICH THE PARAMETERS FOR THIS TYPE WILL BE RETRIEVED
          DOUBLE PRECISION STORED !THE STORAGE ARRAY FOR HOLDING VARIABLES FROM TIMESTEP TO
TIMESTEP
          DOUBLE PRECISION T                !AN ARRAY CONTAINING THE RESULTS FROM THE DIFFERENTIAL
EQUATION SOLVER
          DOUBLE PRECISION DTDT  !AN ARRAY CONTAINING THE DERIVATIVES TO BE PASSED TO THE DIFF.EQ.
SOLVER
          INTEGER*4 INFO(15)                !THE INFO ARRAY STORES AND PASSES VALUABLE INFORMATION TO
AND FROM THIS TYPE
          INTEGER*4 NP,NI,NOUT,ND !VARIABLES FOR THE MAXIMUM NUMBER OF PARAMETERS,INPUTS,OUTPUTS AND
DERIVATIVES
          INTEGER*4 NPAR,NIN,NDER           !VARIABLES FOR THE CORRECT NUMBER OF
PARAMETERS,INPUTS,OUTPUTS AND DERIVATIVES
          INTEGER*4 IUNIT,ITYPE     !THE UNIT NUMBER AND TYPE NUMBER FOR THIS COMPONENT
          INTEGER*4 ICNTRL                  !AN ARRAY FOR HOLDING VALUES OF CONTROL FUNCTIONS WITH THE
NEW SOLVER
          INTEGER*4 NSTORED                 !THE NUMBER OF VARIABLES THAT WILL BE PASSED INTO AND OUT OF
STORAGE
          CHARACTER*3 OCHECK                !AN ARRAY TO BE FILLED WITH THE CORRECT VARIABLE TYPES FOR
THE OUTPUTS
          CHARACTER*3 YCHECK                !AN ARRAY TO BE FILLED WITH THE CORRECT VARIABLE TYPES FOR
THE INPUTS
C-------------------------------------------------------------------------------------------------------------

C-------------------------------------------------------------------------------------------------------------
C   USER DECLARATIONS - SET THE MAXIMUM NUMBER OF PARAMETERS (NP), INPUTS (NI),
C   OUTPUTS (NOUT), AND DERIVATIVES (ND) THAT MAY BE SUPPLIED FOR THIS TYPE
    PARAMETER (NP=4,NI=8,NOUT=10,ND=0,NSTORED=3)
C-------------------------------------------------------------------------------------------------------------

C-------------------------------------------------------------------------------------------------------------
C   REQUIRED TRNSYS DIMENSIONS
    DIMENSION XIN(NI),OUT(NOUT),PAR(NP),YCHECK(NI),OCHECK(NOUT),
          1   STORED(NSTORED),T(ND),DTDT(ND)
    INTEGER NITEMS
C-------------------------------------------------------------------------------------------------------------
C-------------------------------------------------------------------------------------------------------------
```

```
C   ADD DECLARATIONS AND DEFINITIONS FOR THE USER-VARIABLES HERE


C   PARAMETERS
      DOUBLE PRECISION Area          !Solar collector area
      DOUBLE PRECISION EtaInt        !Solar collector intercept efficiency
      DOUBLE PRECISION EtaSlope      !Solar collector efficiency slope
      DOUBLE PRECISION EtaCurve      !Solar collector efficiency curvature

C   INPUTS
      DOUBLE PRECISION GT            !Total radiation on the tilted solar collector surface
      DOUBLE PRECISION HPPower       !Heat pump compressor power
      DOUBLE PRECISION TTopDHW       !DHW tank top temperature
      DOUBLE PRECISION TBotDHW       !DHW tank bottom temperature
      DOUBLE PRECISION THPSIn        !Heat pump source side inlet temperature
      DOUBLE PRECISION THPSOut       !Heat pump source side outlet temperature
      DOUBLE PRECISION THPLIn        !Heat pumpload side inlet temperature
      DOUBLE PRECISION TAMB          !Ambient outdoor air temperature

!   LOCAL VARIABLES
      DOUBLE PRECISION GTConv        !Converted total radiation on the tilted solar collector surface
      DOUBLE PRECISION TimeSet       !Set time for heat pump anti short-cycle timer
      DOUBLE PRECISION Timer         !Elapsed time from onset of the heat pump anti short-cycle timer
      DOUBLE PRECISION TiPrimeHX     !Theoretical solar collector inlet temperature used for HX mode
      DOUBLE PRECISION TiPrimeHP     !Theoretical solar collector inlet temperature used for HP mode
      DOUBLE PRECISION EtaHX         !Theoretical solar collection efficiency from HX mode
      DOUBLE PRECISION EtaHP         !Theoretical solar collection efficiency from HP mode
      DOUBLE PRECISION QuPrimeHX     !Theoretical solar heat collection rate from HX mode
      DOUBLE PRECISION QuPrimeHP     !Theoretical solar heat collection rate from HP mode
      DOUBLE PRECISION SignHX        !(TiPrime - TAMB) sign placeholder for HX mode
      DOUBLE PRECISION SignHP        !(TiPrime - TAMB) sign placeholder for HP mode
      DOUBLE PRECISION CSigDiv1      !Control signal for source side diverter valve
      DOUBLE PRECISION CSigDiv2      !Control signal for load side diverter valve
      DOUBLE PRECISION CSigP1        !Control signal for source side pump
      DOUBLE PRECISION CSigP2        !Control signal for load side pump
      DOUBLE PRECISION CSigHP        !Control signal for heat pump
      INTEGER Mode                   !Control mode for system operation
      INTEGER RadLimit               !Integer indicator for incoming solar radiation limit
      INTEGER TTopLimit              !Integer indicator for DHW tank top temperature limit
      INTEGER TBotLimit              !Integer indicator for DHW tank bottom temperature limit
      INTEGER TimerLimit             !Integer indicator for heat pump anti short-cycle timer limit

 !   BOOLEAN VARIABLES
      INTEGER HXMODEB                !Boolean indicator indicating possible HX or HP operation
      INTEGER RadLimitB              !Boolean indicator for incoming solar radiation limit
      INTEGER TTopLimitB             !Boolean indicator for DHW tank top temperature limit
      INTEGER TBotLimitB             !Integer indicator for DHW tank bottom temperature limit
      INTEGER TimerLimitB            !Integer indicator for heat pump anti short-cycle timer limit

C-------------------------------------------------------------------------------------------------------------------
C     READ IN THE VALUES OF THE PARAMETERS IN SEQUENTIAL ORDER
      Area=PAR(1)
      EtaInt=PAR(2)
      EtaSlope=PAR(3)
      EtaCurve=PAR(4)

C-------------------------------------------------------------------------------------------------------------------
C   RETRIEVE THE CURRENT VALUES OF THE INPUTS TO THIS MODEL FROM THE XIN ARRAY IN SEQUENTIAL ORDER

      GT=XIN(1)
      HPPower=XIN(2)
      TTopDHW=XIN(3)
      TBotDHW=XIN(4)
      THPSIn=XIN(5)
      THPSOut=XIN(6)
      THPLIn=XIN(7)
      TAMB=XIN(8)
            IUNIT=INFO(1)
            ITYPE=INFO(2)
```

```
C-------------------------------------------------------------------------------------------------------------
C    SET THE VERSION INFORMATION FOR TRNSYS
     IF(INFO(7).EQ.-2) THEN
               INFO(12)=16
               RETURN 1
             ENDIF
C-------------------------------------------------------------------------------------------------------------

C-------------------------------------------------------------------------------------------------------------
C    DO ALL THE VERY LAST CALL OF THE SIMULATION MANIPULATIONS HERE
     IF (INFO(8).EQ.-1) THEN
               RETURN 1
             ENDIF
C-------------------------------------------------------------------------------------------------------------

C-------------------------------------------------------------------------------------------------------------
C    PERFORM ANY 'AFTER-ITERATION' MANIPULATIONS THAT ARE REQUIRED HERE
C    e.g. save variables to storage array for the next timestep
     IF (INFO(13).GT.0) THEN
               NITEMS=3
                    ! STORE VALUES UPON EXIT
                    STORED(1) = HPPower        !STORES THE CURRENT HEAT PUMP POWER FOR FUTURE TIMESTEPS
                    STORED(2) = TimeSet        !STORES THE SETTING TIME FOR THE ANTI SHORT-CYCLE TIMER
                    STORED(3) = Mode           !STORES THE CURRENT SYSTEM MODE FOR FUTURE TIMESTEPS
       CALL setStorageVars(STORED,NITEMS,INFO)
               RETURN 1
             ENDIF
C
C-------------------------------------------------------------------------------------------------------------

C-------------------------------------------------------------------------------------------------------------
C    DO ALL THE VERY FIRST CALL OF THE SIMULATION MANIPULATIONS HERE
     IF (INFO(7).EQ.-1) THEN

C      SET SOME INFO ARRAY VARIABLES TO TELL THE TRNSYS ENGINE HOW THIS TYPE IS TO WORK
       INFO(6)=NOUT
       INFO(9)=1
               INFO(10)=0         !STORAGE FOR VERSION 16 HAS BEEN CHANGED

C      SET THE REQUIRED NUMBER OF INPUTS, PARAMETERS AND DERIVATIVES THAT THE USER SHOULD SUPPLY IN
THE INPUT FILE
C      IN SOME CASES, THE NUMBER OF VARIABLES MAY DEPEND ON THE VALUE OF PARAMETERS TO THIS MODEL....
       NIN=NI
               NPAR=NP
               NDER=ND

C      CALL THE TYPE CHECK SUBROUTINE TO COMPARE WHAT THIS COMPONENT REQUIRES TO WHAT IS SUPPLIED
IN
C      THE TRNSYS INPUT FILE
               CALL TYPECK(1,INFO,NIN,NPAR,NDER)

C      SET THE NUMBER OF STORAGE SPOTS NEEDED FOR THIS COMPONENT
       NITEMS=3
               CALL setStorageSize(NITEMS,INFO)

C      RETURN TO THE CALLING PROGRAM
       RETURN 1

     ENDIF
C-------------------------------------------------------------------------------------------------------------

C-------------------------------------------------------------------------------------------------------------
C    DO ALL OF THE INITIAL TIMESTEP MANIPULATIONS HERE - THERE ARE NO ITERATIONS AT THE INTIAL TIME
     IF (TIME .LT. (getSimulationStartTime() +
    . getSimulationTimeStep()/2.D0)) THEN

C      SET THE UNIT NUMBER FOR FUTURE CALLS
       IUNIT=INFO(1)
       ITYPE=INFO(2)
```

```
C      CHECK THE PARAMETERS FOR PROBLEMS AND RETURN FROM THE SUBROUTINE IF AN ERROR IS FOUND
C        IF(...) CALL TYPECK(-4,INFO,0,"BAD PARAMETER #",0)

C      PERFORM ANY REQUIRED CALCULATIONS TO SET THE INITIAL VALUES OF THE OUTPUTS HERE
C                       SystemMode
                                OUT(1)=0
C                       CSigDiv1
                                OUT(2)=0
C                       CSigDiv2
                                OUT(3)=0
C                       CSigP1
                                OUT(4)=0
C                       CSigP2
                                OUT(5)=0
C                       CSigHP
                                OUT(6)=0
C                       RadLimit
                                OUT(7)=0
C                       TTopLimit
                                OUT(8)=0
C                       TBotLimit
                                OUT(9)=0
C                       TimerLimit
                                OUT(10)=0

C      PERFORM ANY REQUIRED CALCULATIONS TO SET THE INITIAL STORAGE VARIABLES HERE
       NITEMS=3
              STORED(1)=0
              STORED(2)=0
              STORED(3)=0

C      PUT THE STORED ARRAY IN THE GLOBAL STORED ARRAY
C        CALL setStorageVars(STORED,NITEMS,INFO)

C      RETURN TO THE CALLING PROGRAM
       RETURN 1

     ENDIF
C-------------------------------------------------------------------------------------------------------------------

C-------------------------------------------------------------------------------------------------------------------
C    *** ITS AN ITERATIVE CALL TO THIS COMPONENT ***
C-------------------------------------------------------------------------------------------------------------------


C-------------------------------------------------------------------------------------------------------------------
C    RETRIEVE THE VALUES IN THE STORAGE ARRAY FOR THIS ITERATION
     NITEMS=3
              CALL getStorageVars(STORED,NITEMS,INFO)
C      STORED(1)=
C-------------------------------------------------------------------------------------------------------------------
C-------------------------------------------------------------------------------------------------------------------
C    CHECK THE INPUTS FOR PROBLEMS
C      IF(...) CALL TYPECK(-3,INFO,'BAD INPUT #',0,0)
C              IF(IERROR.GT.0) RETURN 1
C-------------------------------------------------------------------------------------------------------------------
C-------------------------------------------------------------------------------------------------------------------
C    *** PERFORM ALL THE CALCULATION HERE FOR THIS MODEL. ***
C-------------------------------------------------------------------------------------------------------------------

!COMPONENT EQUATIONS

!CHECKING FOR INCIDENT RADIATION
!              PERFORMING UNIT CONVERSION FOR GT (W/m^2)
               GTConv = GT/(3.60D0)

!              CHECKING FOR SUFFICIENT RADIATION TO PROCEED
               IF (GT .LE. 10) THEN
               Mode = 0
               GOTO 100
```

```
        ENDIF

!CALCULATION SEQUENCES MATCH THE LabVIEW ETU CONTROLLER
!0 SEQUENCE
!       CALCULATE CURRENT TIMER VALUE
        Timer = TIME - STORED(2)

!       COERCE TIMER TO ACCEPTED RANGE
        IF (Timer .GE. 0.1) THEN
                Timer = 0.1D0
        ELSEIF (Timer .LE. 0) THEN
                Timer = 0.0D0
        ENDIF


!1 SEQUENCE
!       CALCULATE TiPrime TO BE USED FOR COLLECTOR EQUATIONS
        TiPrimeHX= TBotDHW + 10.0D0
        TiPrimeHP = 25.0D0


!2 SEQUENCE
!       CALCULATE QuPrime FOR HP AND HX
!       CALCULATE QuPrimeHX(TiPrimeHX):
        IF ((TiPrimeHX - TAMB) .GE. 0) THEN
                SignHX = 1.0D0
        ELSE
                SignHX = -1.0D0
        ENDIF

        EtaHX = EtaInt - EtaSlope*((TiPrimeHX - TAMB)/GTConv)
    & - EtaCurve*SignHX*(((TiPrimeHX- TAMB)**2)/GTConv)

        QuPrimeHX = EtaHX*GTConv*Area

!       CALCULATE QuPrimeHP(TiPrimeHP):
        IF ((TiPrimeHP - TAMB) .GE. 0) THEN
                SignHP = 1.0D0
        ELSE
                SignHP = -1.0D0
        ENDIF

        EtaHP = EtaInt - EtaSlope*((TiPrimeHP - TAMB)/GTConv)
    & - EtaCurve*SignHP*(((TiPrimeHP- TAMB)**2)/GTConv)

        QuPrimeHP = EtaHP*GTConv*Area


!3 SEQUENCE
!       CHECK RADIATION LEVELS TO DETERMINE HXMODE OR HPMODE FOR POSSIBLE OPERATION
        IF ((QuPrimeHX .GE. 1000.0D0) .OR. ((STORED(3) .EQ. 1) .AND.
    & (QuPrimeHX .GE. 500.0D0))) THEN
                HXMODEB = .TRUE.
        ELSE
                HXMODEB = .FALSE.
        ENDIF


!4 SEQUENCE
!       DETERMINE IF THE TIMER HAS EXPIRED AND SET THE BOOLEAN INDICATOR
        IF (Timer .LT. (6.0D0/60.0D0)) THEN
                TimerLimitB = .TRUE.
        ELSE
                TimerLimitB = .FALSE.
        ENDIF


!4.1 SEQUENCE - LIMIT CONDITIONS CASE STRUCTURE
!       IF SYSTEM WAS PREVIOUSLY OFF (NOTE THAT DEAD BANDS CHANGE B/T OFF/ON SYSTEM)
        IF (STORED(3) .EQ. 0) THEN
```

```
                ! CHECKING MAXIMUM TEMPERATURE LIMIT
                IF (TTopDHW .GE. 70.0D0) THEN
                        TTopLimitB = .TRUE.
                ELSE
                        TTopLimitB = .FALSE.
                ENDIF
                ! CHECKING CONDITIONS FOR HXMODE ELSE HPMODE (NOTE THAT LIMIT CONDITIONS CHANGE)
                IF (HXMODEB) THEN
                        !       RESTRICT OPERATION IF LOAD TEMPERATURE IS SUFFICIENTLY HIGH
                        IF (TBotDHW .GE. 60.0D0) THEN
                                TBotLimitB = .TRUE.
                        ELSE
                                TBotLimitB = .FALSE.
                        ENDIF
                        ! LIMIT FOR SUFFICIENT RADIATION IS UNNECESSARY
                        RadLimitB = .FALSE.
                ELSE
                        ! RESTRICT OPERATION IF LOAD TEMPERATURE IS SUFFICIENTLY HIGH
                        IF (TBotDHW .GE. 40.0D0) THEN
                                TBotLimitB = .TRUE.
                        ELSE
                                TBotLimitB = .FALSE.
                        ENDIF
                        ! CHECKING FOR SUFFICIENT INCIDENT RADIATION
                        IF (QuPrimeHP .GE. 250.0D0) THEN
                                RadLimitB = .FALSE.
                        ELSE
                                RadLimitB = .TRUE.
                        ENDIF
                ENDIF
        ! REPEAT FOR SYSTEM PREVIOUSLY ON (NOTE THAT DEAD BANDS HAVE CHANGED)
        ELSE
                ! CHECKING MAXIMUM TEMPERATURE LIMIT
                IF (TTopDHW .GE. 80.0D0) THEN
                        TTopLimitB = .TRUE.
                ELSE
                        TTopLimitB = .FALSE.
                ENDIF
                ! CHECKING CONDITIONS FOR HXMODE ELSE HPMODE (NOTE THAT LIMIT CONDITIONS CHANGE)
                IF (HXMODEB) THEN
                        ! RESTRICT OPERATION IF LOAD TEMPERATURE IS SUFFICIENTLY HIGH
                        IF (TBotDHW .GE. 65.0D0) THEN
                                TBotLimitB = .TRUE.
                        ELSE
                                TBotLimitB = .FALSE.
                        ENDIF
                        ! LIMIT FOR SUFFICIENT INCIDENT RADIATION IS UNNECESSARY
                        RadLimitB = .FALSE.
                ELSE
                        ! RESTRICT OPERATION IF LOAD TEMPERATURE IS SUFFICIENTLY HIGH
                        IF (TBotDHW .GE. 45.0D0) THEN
                                TBotLimitB = .TRUE.
                        ELSE
                                TBotLimitB = .FALSE.
                        ENDIF
                        ! CHECKING FOR SUFFICIENT INCIDENT RADIATION
                        IF (QuPrimeHP .GE. 200.0D0) THEN
                                RadLimitB = .FALSE.
                        ELSE
                                RadLimitB = .TRUE.
                        ENDIF
                ENDIF
        ENDIF


!5 SEQUENCE - MODE SETTING CASE STRUCTURE
        ! CHECKING CUTOUT CONDITIONS
        IF (TTopLimitB .OR. TBotLimitB .OR. RadLimitB) THEN
                ! CUTOUT IS ACTIVE
                Mode = 0
```

```
ELSE
        ! CUTOUT IS INACTIVE, CHECK FOR HX OR HP MODE
        IF (HXMODEB) THEN
                ! HX SHOULD RUN
                Mode = 1
        ELSE
                ! MUST CONTROL HEAT PUMP CYCLING
                ! STARTING FROM OFF CONDITION
                IF (STORED(3).EQ. 0) THEN
                        IF (TimerLimitB) THEN
                                ! TIMER LIMIT HAS NOT EXPIRED, SYSTEM REMAINS OFF
                                Mode = 0
                        ELSE
                                ! START HEAT PUMP WARM-UP CYCLE
                                Mode = 6
                        ENDIF
                ! STARTING FROM HX CONDITION
                ELSEIF (STORED(3) .EQ. 1) THEN
                        ! SWITCH TO OFF CONDITION
                        Mode = 0
                ! STARTING FROM HP CONDITION
                ELSEIF (STORED(3) .EQ. 2) THEN
                        ! CHECKING IF HP CAN CONTINUE TO RUN
                        IF ((THPSOut .LE . 5) .OR. ((HPPower .LE. 10) .AND.
&               (STORED(1) .GT. 10))) THEN
                                ! HEAT PUMP NEEDS TO CYCLE OFF FOR WARMUP CYCLE
                                Mode = 6
                        ELSE
                                ! HEAT PUMP MAY CONTINUE TO RUN
                                Mode = 2
                        ENDIF
                ! STARTING FROM SOLAR TO FLOAT CONDITION (FOR FUTURE USE)
                ELSEIF (STORED(3) .EQ. 3) THEN
                        Mode = 0
                ! STARTING FROM FLOAT TO HX CONDITION (FOR FUTURE USE)
                ELSEIF (STORED(3)  .EQ. 4) THEN
                        Mode = 0
                ! STARTING FROM FLOAT TO HP CONDITION (FOR FUTURE USE)
                ELSEIF (STORED(3)  .EQ. 5) THEN
                        Mode = 0
                ! STARTING FROM HP WARMUP CONDITION
                ELSEIF (STORED(3)  .EQ. 6) THEN
                        ! CHECK HP TIMER
                        IF (TimerLimitB) THEN
                                ! HEAT PUMP WARM-UP CYCLE OPERATES UP TO 25C
                                IF (THPSIn .GE. 25.0D0) THEN
                                        ! SHUT OFF AND WAIT FOR TIMER LIMIT TO EXPIRE
                                        Mode = 0
                                ELSE
                                        ! KEEP ADDING HEAT TO THE LOOP
                                        Mode = 6
                                ENDIF
                        ELSE
                        ! TIMEOUT HAS EXPIRED
                                IF (THPSIn .LE. 25.0D0) THEN
                                        ! KEEP ADDING HEAT TO THE LOOP
                                        Mode = 6
                                ELSE
                                        ! CYCLE THE HEAT PUMP BACK ON
                                        Mode = 2
                                ENDIF
                        ENDIF
                ! IN CASE OF ERROR
                ELSE
                        ! PUT THE SYSTEM IN OFF CONDITION
                        Mode = 0
                ENDIF
        ENDIF
ENDIF
```

```
!6 SEQUENCE - OUTPUT PREPARATION
        ! SET HP TIMER
        IF ((STORED(3)  .EQ. 2) .AND. (Mode .NE. 2)) THEN
                TimeSet = TIME
        ENDIF

        ! SET LIMITS
        IF (TimerLimitB) THEN
                TimerLimit = 1
        ELSE
                TimerLimit = 0
        ENDIF

        IF (RadLimitB) THEN
                RadLimit = 1
        ELSE
                RadLimit = 0
        ENDIF

        IF (TTopLimitB) THEN
                TTopLimit = 1
        ELSE
                TTopLimit = 0
        ENDIF

        IF (TBotLimitB) THEN
                TBotLimit = 1
        ELSE
                TBotLimit = 0
        ENDIF

        ! PROCEED TO SET CONTROL OUTPUTS
        GOTO 100

!       SET CONTROL OUTPUTS
100     IF (Mode .EQ. 0) THEN
                CSigDiv1 = 0.0D0
                CSigDiv2 = 0.0D0
                CSigP1 = 0.0D0
                CSigP2 = 0.0D0
                CSigHP = 0.0D0
        ELSEIF (Mode .EQ. 1) THEN
                CSigDiv1 = 0.0D0
                CSigDiv2 = 0.0D0
                CSigP1 = 0.46511D0
                CSigP2 = 0.46511D0
                CSigHP = 0.0D0
        ELSEIF (Mode .EQ. 2) THEN
                CSigDiv1 = 1.0D0
                CSigDiv2 = 1.0D0
                CSigP1 = 1.0D0
                CSigP2 = 1.0D0
                CSigHP = 1.0D0
        ELSEIF (Mode .EQ. 6) THEN
                CSigDiv1 = 1.0D0
                CSigDiv2 = 0.0D0
                CSigP1 = 1.0D0
                CSigP2 = 0.0D0
                CSigHP = 0.0D0
        ELSE
                CSigDiv1 = 0.0D0
                CSigDiv2 = 0.0D0
                CSigP1 = 0.0D0
                CSigP2 = 0.0D0
                CSigHP = 0.0D0
        ENDIF

C-------------------------------------------------------------------------------------------------------------------
```

```
C-------------------------------------------------------------------------------------------------------------------
C-------------------------------------------------------------------------------------------------------------------
C   SET THE STORAGE ARRAY AT THE END OF THIS ITERATION IF NECESSARY
C     NITEMS=
C     STORED(1)=
C           CALL setStorageVars(STORED,NITEMS,INFO)
C-------------------------------------------------------------------------------------------------------------------
C-------------------------------------------------------------------------------------------------------------------
C   REPORT ANY PROBLEMS THAT HAVE BEEN FOUND USING CALLS LIKE THIS:
C     CALL MESSAGES(-1,'put your message here','MESSAGE',IUNIT,ITYPE)
C     CALL MESSAGES(-1,'put your message here','WARNING',IUNIT,ITYPE)
C     CALL MESSAGES(-1,'put your message here','SEVERE',IUNIT,ITYPE)
C     CALL MESSAGES(-1,'put your message here','FATAL',IUNIT,ITYPE)
C-------------------------------------------------------------------------------------------------------------------
C-------------------------------------------------------------------------------------------------------------------
C   SET THE OUTPUTS FROM THIS MODEL IN SEQUENTIAL ORDER AND GET OUT

C                       SystemMode
                                OUT(1)=Mode
C                       CSigDiv1
                                OUT(2)=CSigDiv1
C                       CSigDiv2
                                OUT(3)=CSigDiv2
C                       CSigP1
                                OUT(4)=CSigP1
C                       CSigP2
                                OUT(5)=CSigP2
C                       CSigHP
                                OUT(6)=CSigHP
C                       RadLimit
                                OUT(7)=RadLimit
C                       TTopLimit
                                OUT(8)=TTopLimit
C                       TBotLimit
                                OUT(9)=TBotLimit
C                       TimerLimit
                                OUT(10)=TimerLimit

C-------------------------------------------------------------------------------------------------------------------
C   EVERYTHING IS DONE - RETURN FROM THIS SUBROUTINE AND MOVE ON
    RETURN 1
    END
C-------------------------------------------------------------------------------------------------------------------
```